Area

Value	Unit	Time	Object	Group	Index
485,4200134	um^2	1	Spot 87	Group 9	1365
876,539978	um^2	1	Spot 88	Group 9	419
2900,881104	um^2	1	Spot 89	Group 9	[illegible]
415,5700073	um^2	1	Spot 90	Group 9	[illegible]
2172,686035	um^2	1	Spot 91	Group 9	331
397,82901	um^2	1	Spot 92	Group 9	806
531,8809814	um^2	1	Spot 93	Group 9	435
1453,748047	um^2	1	Spot 94	Group 9	560
681,3839722	um^2	1	Spot 95	Group 9	924
319,5270081	um^2	1	Spot 96	Group 9	1123
687,2459717	um^2	1	Spot 97	Group 9	1379
[illegible]				Group 9	798
[illegible]			[illegible] 111	Group 9	820
			Spot 112	Group 9	930
			Spot 113	Group 9	188
1109,420044	um^2	1	Spot 121	Group 9	809
850,4500122	um^2	1	Spot 122	Group 9	1429
			Spot 123	Group 9	1321
			Spot 124	Group 9	506
			Spot 125	Group 9	1144
			Spot 126	Group 9	1414
			Spot 127	Group 9	1143
			Spot 128	Group 9	880
			Spot 129	Group 9	411
			Spot 130	Group 9	282

Advanced Live Cell Imaging

SPECIAL EDITION OF

Imaging & Microscopy
RESEARCH • DEVELOPMENT • PRODUCTION

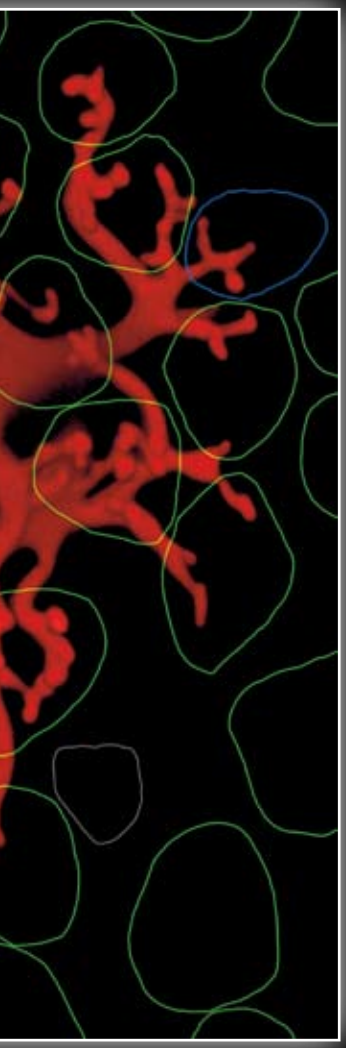

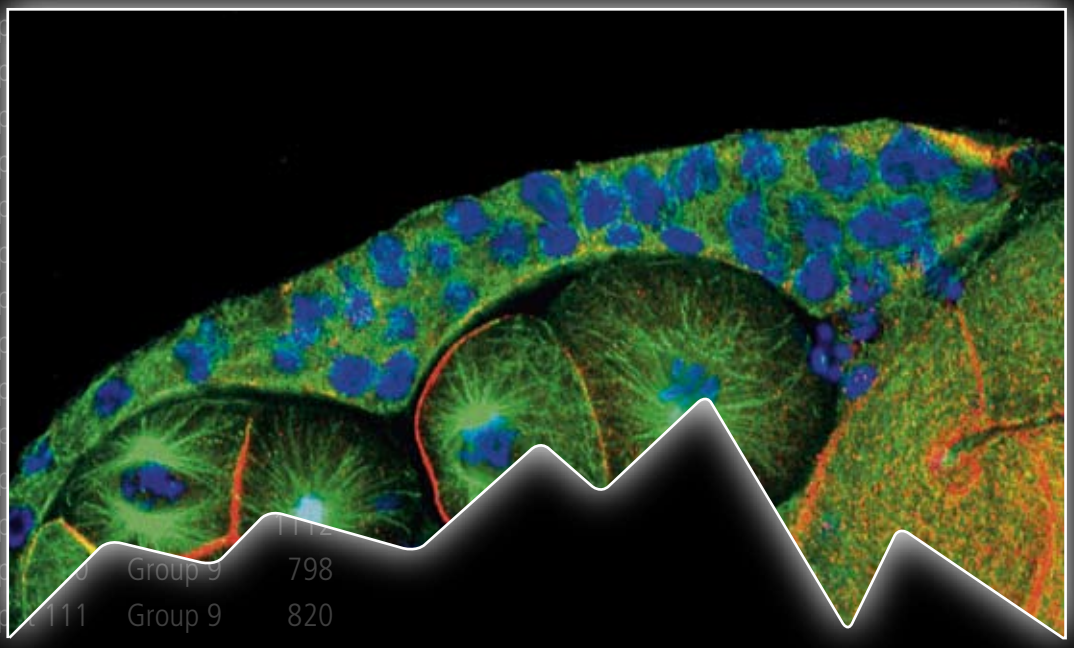

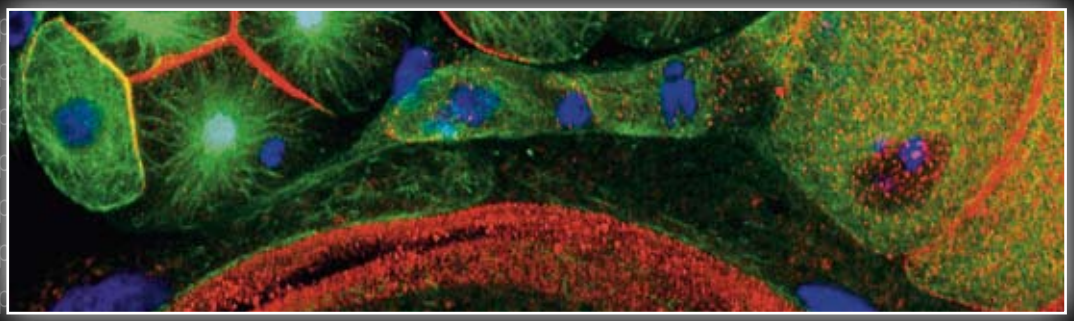

BICENTENNIAL 1807 WILEY 2007 BICENTENNIAL
GIT VERLAG
A Wiley Company
www.gitverlag.com

Male reproductive organ of a previously undescribed butterfly species of Carpatolechia. Dissected tissue was stained with EosinY and imaged using an LSM 510.
Dr S. Lee, Mississippi University, Mississippi State, USA

Group	Index
Group 9	1365
Group 9	419
Group 9	388
Group 9	486
Group 9	331
Group 9	806
Group 9	435
Group 9	560
Group 9	924
Group 9	1123
Group	
Group	
Group	
Group	
Group	
Group 9	792
Group 9	700
Group	
Group	
Group 9	1312
Group 9	1254
Group 9	251
Group 9	1112
Group 9	798
Group 9	820
Group 9	930
Group 9	188
Group 9	473
Group 9	875
Group 9	191
Group 9	304
Group 9	1122
Group 9	425
Group 9	317
Group 9	809
Group 9	1429
Group 9	1321
Group 9	506
Group 9	1144
Group 9	1414
Group 9	1143
Group 9	880

Advances in Microscopy

Dear Reader,

In the last twenty years, fluorescence light microscopy has steadily gained in importance and has become one of the key technologies in biomedical research. This impact on the modern life sciences is due to several developments. 1) Progresses in digital camera technology, computer hard- and software and sensor electronics allow us to record more data at higher speeds and with a much improved signal to noise ratio. 2) Genetically engineered cells and embryos allow us to label a relatively small number of molecules and thus work very specifically. 3) New methods that provide optical sectioning allow us to work with physiologically relevant „thick" specimens.

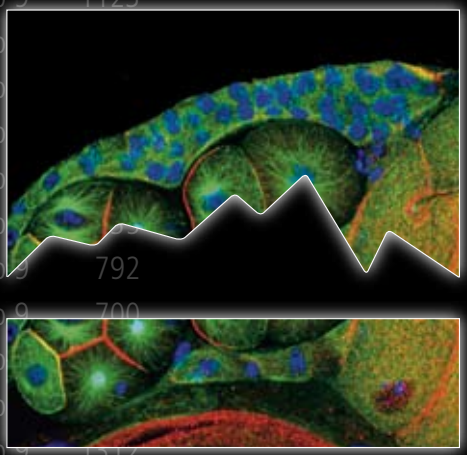

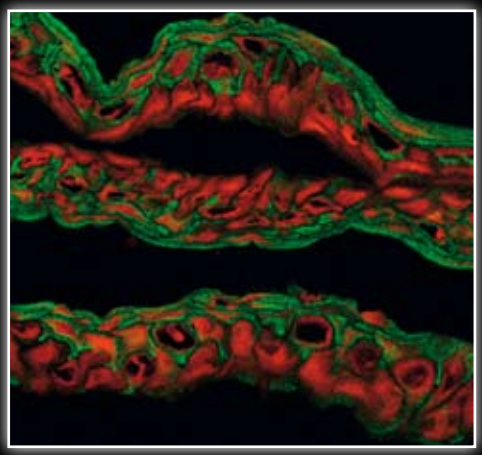

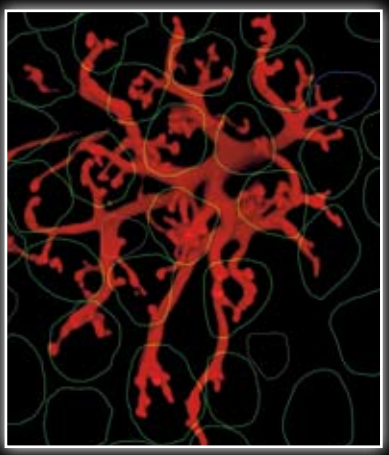

The development of the microscope itself, i.e. the improvements of the many optical elements, the way we interact with a complex device etc., has been tremendous and it is beyond the scope of this special edition to give a comprehensive overview of all recent achievements.

The invaluable advantage of modern microscopy results from its ability to image the complex and dynamic aspects of natural objects in a relatively well-controlled spectrally-resolved spatio-temporal context. Beyond the beautiful insights into structural details and the localization of molecules, it is the quantitative investigation of molecular interactions and dynamics that have recently contributed a lot to the unraveling of a variety of nature's facts.

It was our goal to collect a number of excellent applications in different areas of research, in which microscopy -or the development of a particular microscopy technique- was key to the understanding of biologically relevant details. We asked the researchers to present their results to an audience, which appreciate their fascination with the subjects and appreciates the subtle beauties of their approaches.

Confocal fluorescence microscopy produces optical sections by discrimination in the detection process and avoids physical sectioning and destruction of a sample. It is widely used and within the last decades has improved with respect to its spatial, spectral and the temporal resolution. The investigation of the development of the vertebrate heart, as detailed in the article by Mary Dickinson (page 48), requires confocal fluorescence imaging at a rate of hundreds of frames per second, which could only be achieved by the implementation of a parallel scanning process.

Only very recently, another optical sectioning technique, 'single plane illumination microscopy' has been developed in the team of Ernst Stelzer (page 7), in order to further increase speed, field of view and axial resolution with true optical sectioning capability. It us used with very small as well as relatively large objects and will have a dramatic impact on traditional cell biology.

Simultaneous with the improvement of optics, specific staining methods have become available through the development of antibody labeling, cell permeant dyes and fluorescent fusion proteins. The group of Atsushi Miyawaki has been very successful in modifying and improving fluorescent protein based probes and using them for the investigation of molecular interactions and as reporters for the dynamics of second messenger molecules. He gives some fascinating insides of their use on page 16. A variety of spectrally different subtypes of fluorescent proteins have complemented the initially identified fluorescent protein

Dr Ernst Stelzer

Dr Jens Rietdorf

Dr Patrick Schwarb

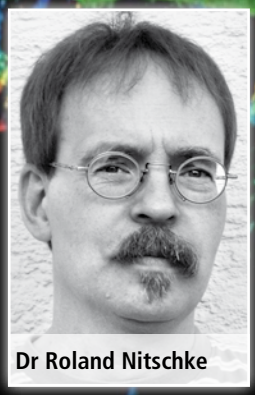

Dr Roland Nitschke

from an Aeqorea species, which for the first time provided the means to stain biological samples using molecular biology methods. The investigation of the vertebrate brain, as presented in the article of Frank Kirchhoff (page 36) has profited from both, fluorescent proteins and the use of multi-photon microscopy, another variant of microscopy producing optical sections. Sensors which drastically change their optical properties in response to changes of their environment are used as reporters. Michael Duchen presents the use of such sensors to investigate the (patho) physiology of mitochondria.

While a huge variety of microscopy methods is currently available, challenges for the future remain. The automation of spectrally resolved, spatio-temporal microscope imaging and the investigation of multiple samples in a single experiment vastly increase the amount of data obtained per experiment, but also the overall amount of data that has to be handled in a research department or an entire institute. Further, microscopy data derived from the use of the ever increasing number of different optical methods have to be integrated into models and represented in a way, that alows the human observer to make sense of it. Roger Wepf reports on recent findings from combining light and electron microscopy methods on page 28.

We hope the reader of this special edition enjoy the reading and watching of this little collection of 'microscopy pearls' presented here and looking forward to the new developments we can expect for the future.

We thank Carl Zeiss AG for the fruitful co-operation and the support of this little booklet and the continuous development of microscopy equipment, as well as the people from GIT Verlag for editorial support and remain,

Sincerely,
Ernst, Jens, Patrick & Roland

To access our digital version of this publication visit www.imaging-git.com

Imprint

Published by
Head Office:
GIT VERLAG GmbH & Co. KG
Roesslerstrasse 90 · 64293 Darmstadt, Germany
Tel.: +49 6151 80 90 0 · Fax: -144
E-mail: imaging@gitverlag.com

Managing Directors
Dr Michael Schön
Bijan Ghawami

Publishing Director
Dr Michael Klinge

Head of Sales & Marketing
Anna Seidinger

Editorial Board
Dr Ernst Stelzer
EMBL Heidelberg, Germany
stelzer@embl.de

Dr Jens Rietdorf
FMI, Basel Switzerland
jens.rietdorf@fmi.ch

Dr Patrick Schwarb
FMI, Basel Switzerland
patrick.schwarb@fmi.ch

Dr Roland Nitschke
University Freiburg, Germany
Roland.Nitschke@biologie.uni-freiburg.de

Dr Bernhard Zimmermann
Carl Zeiss MicroImaging, Jena, Germany
b.zimmermann@zeiss.de

Dr Carsten Hoyer
Carl Zeiss MicroImaging, Göttingen, Germany
hoyer@zeiss.de

Managing Editor
Dr Martin Friedrich
m.friedrich@gitverlag.com

In Cooperation with
Carl Zeiss MicroImaging GmbH
Carl-Zeiss-Promenade 10
07745 Jena, Germany
www.zeiss.com/micro

Editorial Assistance
Tina Weber
E-mail: t.weber@gitverlag.com

Angela Seibert-Weck
E-mail: a.weck@gitverlag.com

Production Managers
Dietmar Edhofer, Sandra Rauch
E-mail: production@gitverlag.com

Layout/Litho
Vassilios Ekoutsidis/Elke Palzer

Printed by
Frotscher Druck
Riedstrasse 8 · 64295 Darmstadt, Germany

Circulation
40,000 copies

Specially identified contributions are the responsibility of the author. Manuscripts should be addressed to the editorial office. We assume no liability for unsolicited, submitted manuscripts. Reproduction, including excerpts, is permitted only with the permission of the editorial office and with citation of the source.

The publishing house is granted the exclusive right, with regard to space, time and content to use the works/ editorial contributions in unchanged or edited form for any and all purposes any number of times itself, or to transfer the rights for the use of other organizations in which it holds partnership interests, as well as to third parties. This right of use relates to print as well as electronic media, including the Internet, as well as databases/ data carriers of any kind.

All names, designations or signs in this issue, whether referred to and/ or shown, could be trade names of the respective owner.

Printed in Germany

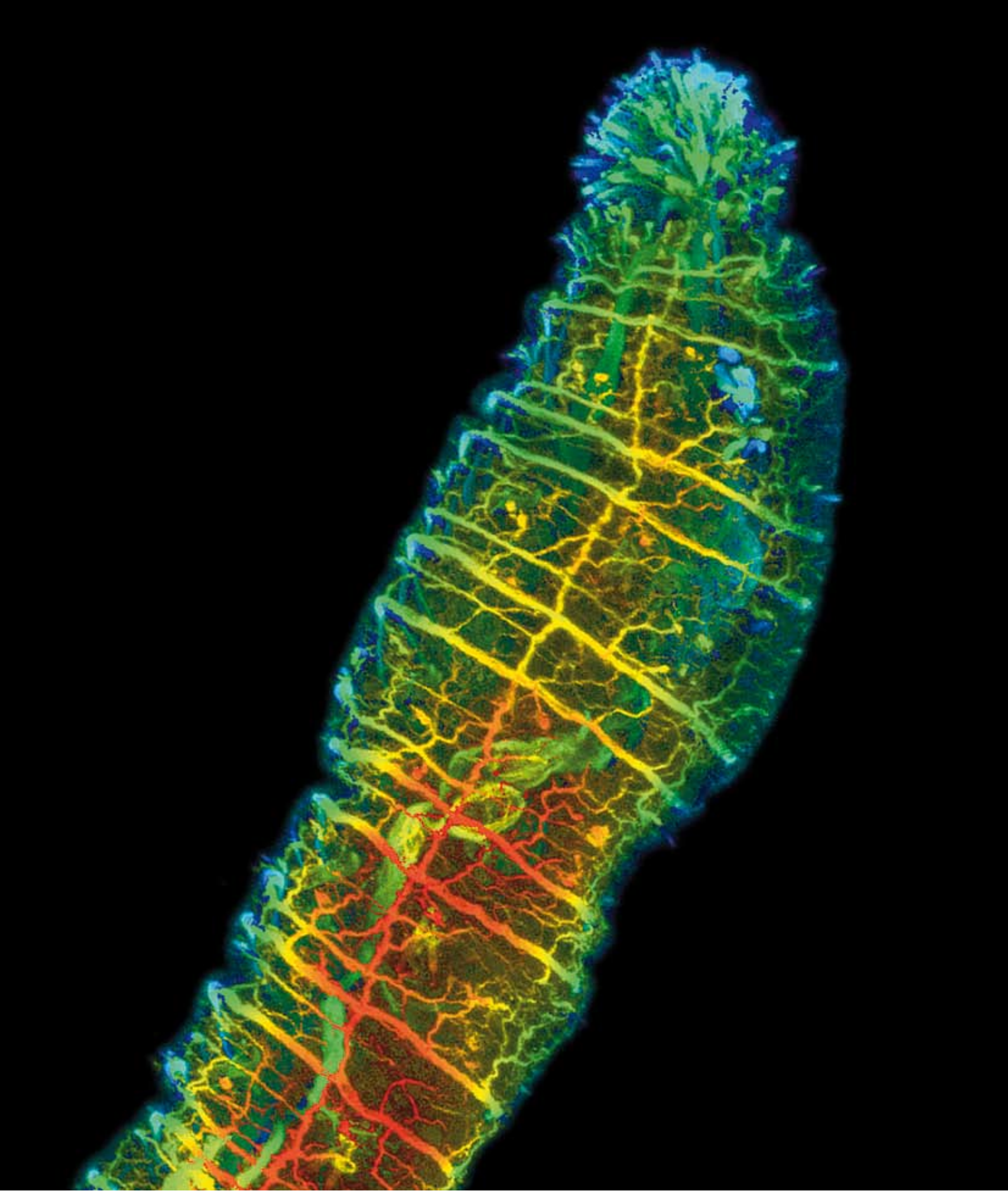

Nervous system in the head region of a young terrestrial earthworm. Depth coding projection of tubulin-stained axons, acquired with an LSM 410.
Dr H. Hessling, University of Osnabrück, Germany

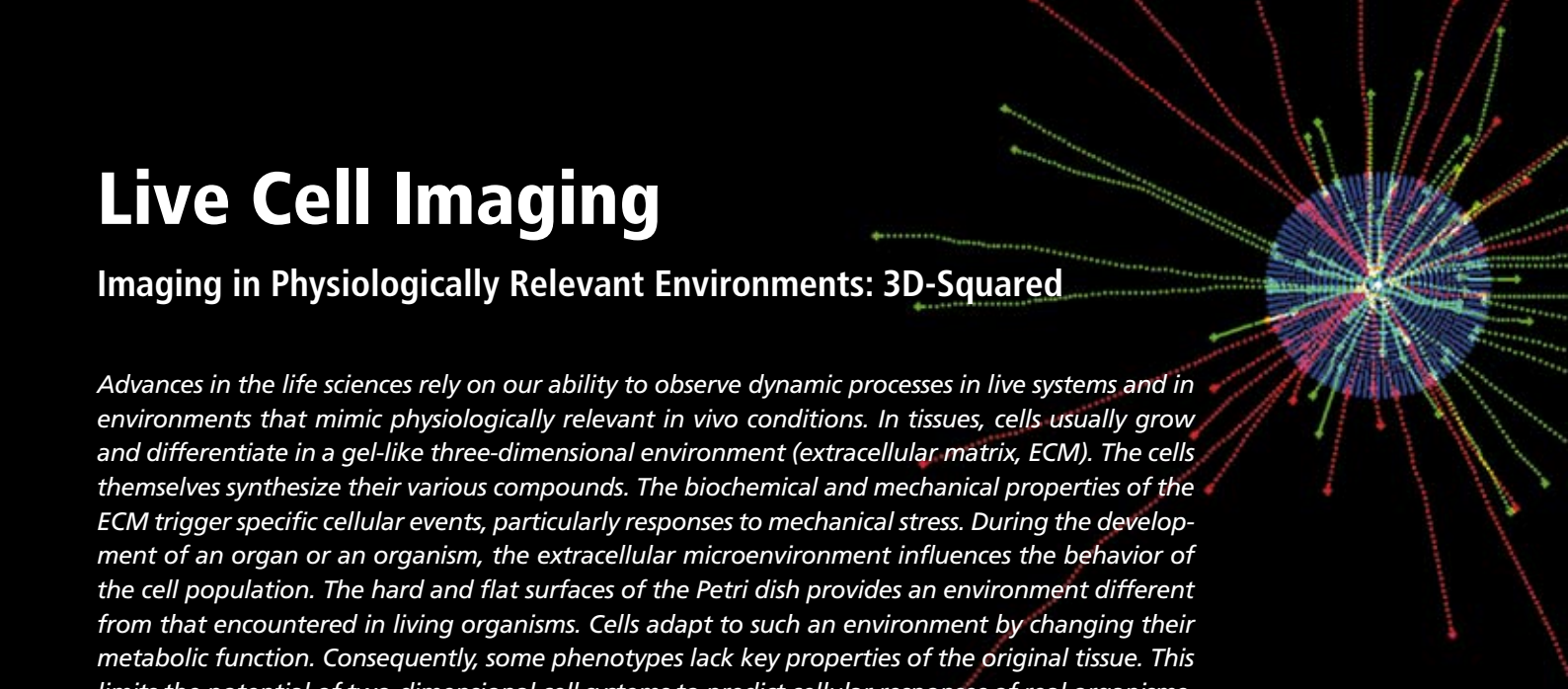

Live Cell Imaging

Imaging in Physiologically Relevant Environments: 3D-Squared

Advances in the life sciences rely on our ability to observe dynamic processes in live systems and in environments that mimic physiologically relevant in vivo conditions. In tissues, cells usually grow and differentiate in a gel-like three-dimensional environment (extracellular matrix, ECM). The cells themselves synthesize their various compounds. The biochemical and mechanical properties of the ECM trigger specific cellular events, particularly responses to mechanical stress. During the development of an organ or an organism, the extracellular microenvironment influences the behavior of the cell population. The hard and flat surfaces of the Petri dish provides an environment different from that encountered in living organisms. Cells adapt to such an environment by changing their metabolic function. Consequently, some phenotypes lack key properties of the original tissue. This limits the potential of two-dimensional cell systems to predict cellular responses of real organisms. Applying three-dimensional cultures is thus motivated by the necessity to work with cellular models that are „closer" to living tissues. Such cultures could have a strong impact on the efficiency of drug screening and contribute to a decrease in the use of laboratory animals, e.g. in the context of toxicity assays. The dichotomy between "two-dimensional" and "three-dimensional" approaches is found at multiple levels of experimental complexity ranging from highly simplified biophysical studies to entire developing organisms.
We describe three seemingly different sets of experiments. 1) We perform experiments in a three-dimensional environment using physiological microtubule extracts that provide a deeper insight into their nano-scale behavior. 2) We describe different approaches to cultivating cells in three-dimensional environments. 3) We point out the importance of model embryos. A common aspect is the combination of three-dimensional sample preparation with three-dimensional imaging light sheet based fluorescence microscopy (3D-squared, Stelzer & Keller 2007).

ライフサイエンスの進歩は、生きたままの生命システムや、生理的に意味のあるin vivoに近い条件下で起きているダイナミックな過程を観察する我々の能力に負っている。通常、組織内にある細胞はゲル状の三次元的な環境（ECM＝細胞外基質）のもとで増殖・分化を行う。細胞自身がこれらのさまざまな基質や化合物を合成する。ECMの生化学的、力学的な性状は細胞の特異的な反応を惹起し、特に機械刺激応答を引き起こす。器官や生命体そのものの発生過程を通じて細胞外部の微小環境は細胞集団の挙動に影響を与える。硬く平らなペトリ皿表層の環境は、細胞が実際の生命体の中で出会うものとは異なっている。こうした環境に細胞は代謝機能を調整することにより適応する。結果として、これまでに知られているフェノタイプは、もともとの組織内における形質を欠落させている、ということになる。実際の生命体における細胞応答を解析しようとしたときに、二次元的な細胞システムの性能には制約がある。
以上のことをふまえ、三次元細胞培養システムは、生きたままの生体組織により近い条件で細胞モデルを研究する必要性から導入されることになった。この培養システムは薬学におけるドラッグ・スクリーニングの効率に目覚しい影響を与え、たとえば毒性試験などで使われる実験動物の数を減少させるだろう。"二次元"的アプローチと、"三次元"的アプローチという二面性は、きわめて単純化された生物物理学的研究から、一個体の発生に渡るまでのさまざまな階層における実験系に見受けられる。
ここで我々は、三種類の実験系について説明したい。（1）微小管を含む細胞抽出液を使った三次元環境における実験を我々は行った。微小管のナノスケールレベルの挙動を明らかにした。（2）三次元環境での細胞培養系のさまざまなアプローチ。（3）さまざまなモデル胚の重要性を指摘する。共通する点は三次元環境を保持したサンプルの調整と、光シート型蛍光顕微鏡を利用した三次元イメージングの組み合わせである（(3D-squared, Stelzer & Keller 2007）。

Light Sheet Based Fluorescence Microscopy

Conventional and confocal epi-fluorescence microscopies employ the same lens for both fluorescence excitation and detection. Confocal theta fluorescence microscopy (Stelzer & Lindek 1994) introduced the use of separate lenses for illumination and detection. In such an azimuthal system, the optical axes are arranged at an angle between

Keywords:
microtubules, fluorescence microscopy, single plane illumination microscopy (SPIM), cell biology, developmental biology

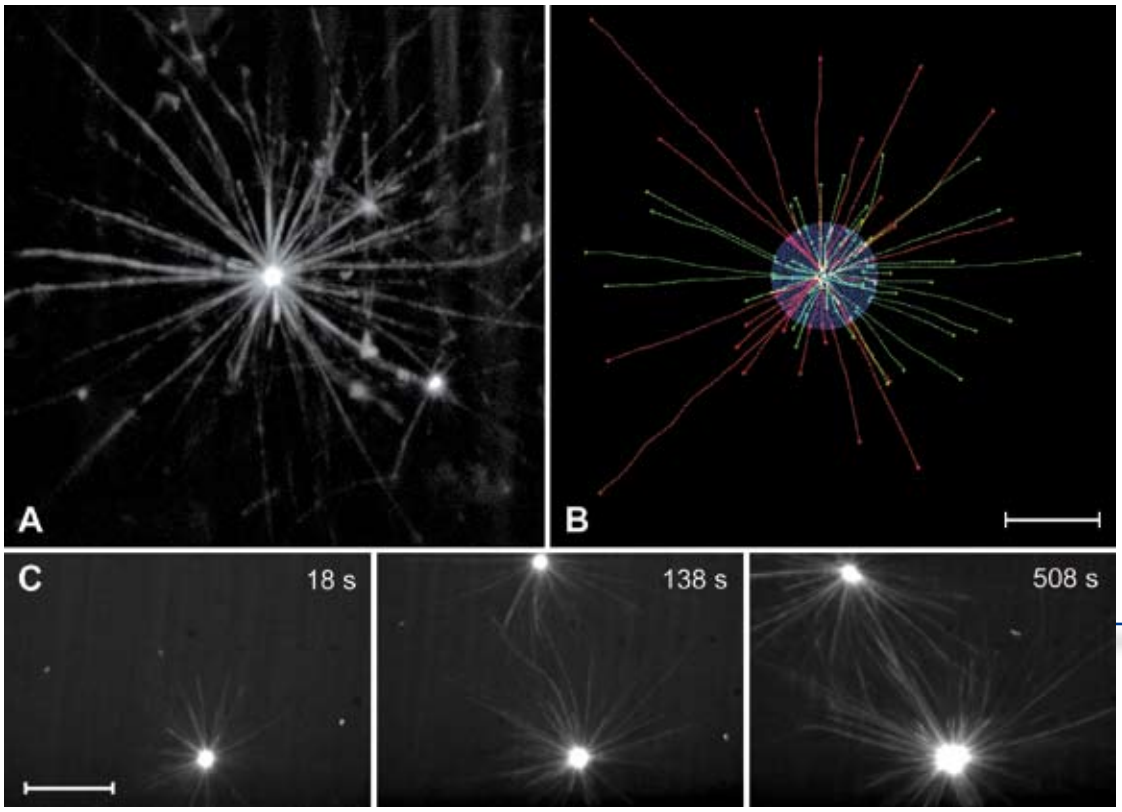

Fig. 1: Microtubule asters in interphase Xenopus laevis egg extract. A: Maximum-intensity projection of a three-dimensional LSFM data set of a microtubule aster polymerized in high-speed interphasic Xenopus laevis egg extract. The three-dimensional image stack contains 68 planes at 300 nm spacing. Tubulin was labeled with TAMRA. Detection via Carl Zeiss Achroplan W 100x/1.0 lens. Sample preparation by Annie Rousselet (Institut Curie), imaging by Philipp J. Keller. B: Three-dimensional reconstruction of the microtubule aster with custom automated image processing routines. Green traces indicate microtubules that were partly located outside the recording volume. For those traces, the last cross does not correspond to the plus-end, but rather to the position at which the tracing algorithm recognized an intersection of the microtubule's contour with the recording volume's boundaries. Red traces indicate MTs that were located fully inside the recording volume. Scale bar 10 µm. C: Maximum-intensity projections of a SPIM time-lapse 3D recording in interphase Xenopus laevis egg extract. Each projection is based on 28 planes recorded at a spacing of 700 nm. Tubulin was labeled at a low ratio with Alexa-488. Elapsed time is relative to the start time of imaging. Carl Zeiss Achroplan 100x/1.0 water objective. Scale bar 10 µm.

80° and 110°, which improves the axial resolution instrumentally by a factor between five and ten and results in an almost spherical point spread function.

The wide-field implementation of the theta principle illuminates the specimen along an entire plane with a light sheet. The use of light sheets for imaging purposes has been known for more than one hundred years (e.g. Siedentopf & Zsigmondy 1903). However, its applicability for high-resolution fluorescence light microscopy has not been realized until recently. One implementation of a light-sheet-based fluorescence microscope (LSFM) is EMBL's Single Plane Illumination Microscope (SPIM, Huisken et al. 2004, Greger et al. 2007). Such a system relies on two independent processes: excitation of a fluoropohore and observation of a fluorescence signal. Optical sectioning arises from the overlap between the focal plane of the fluorescence detection system and the central plane of the excitation light sheet.

Conventional as well as confocal fluorescence microscopes excite fluorophores along the entire illumination axis. Hence, when recording a single plane they cause damage almost everywhere in the object. The three-dimensional resolution of confocal fluorescence microscopes is achieved by discriminating against the light that is emitted outside the focal plane. In contrast, SPIM provides optical sectioning directly. It only excites the fluorophores in the illuminated plane and completely avoids photo-bleaching and other photo-induced damage outside the thin volume of interest. Thereby, it greatly reduces photo-toxic effects, which actually cause problems in all experiments that rely on imaging. Therefore, light sheet-based fluorescence microscopes are particularly well suited for imaging sensitive biological objects over long periods of time.

This implies that long working distance lenses, which usually have a lower numerical aperture (NA) and are therefore less efficient in light collection, can be applied. Since SPIM performs well with long working-distance lenses and has an excellent penetration depth, it allows the observation of millimeter-sized specimens in their entirety and as a function of time.

Since the NA of the illumination system is much smaller than that of the detection system, LSFM have a good penetration depth. The illumination NA is 1/6 to 1/10 of the detection NA. Importantly, LSFM takes advantage of state-of-the-art scientific cameras and easily records up to seven frames (4 mega pixels each) per second with a dynamic range of 12–14 bits.

In EMBL's LSFMs, a further increase in resolution and information content can be obtained by observing the same specimen multiple times, but along different directions. Parts of the sample that would otherwise be hidden or obscured along one direction now become visible. In a further step, researchers can combine stacks of typically 100–2000 images that were recorded along different directions in later image processing steps to yield very high-resolution images (Swoger et al. 2007).

In such data sets, the lateral resolution dominates the three-dimensional resolution and the resolution actually becomes identical (i.e. isotropic) along all directions (Swoger et al. 2007). When compared to conventional microscopy, this

results in an axial resolution improvement by a factor of five to ten. Since imaging with a SPIM provides an excellent signal-to-noise ratio, many image-processing procedures such as deconvolution work extremely well (Verveer et al. 2007).

Assuming one observes GFP, a lens with an NA of 0.16 will provide a lateral resolution of 2 µm and an axial resolution of 7 µm (about six and four times better than a conventional respectively a confocal microscope), while an NA of 1.0 will provide 0.3 µm and 0.9 µm respectively (Engelbrecht & Stelzer 2007). In a multiple view recording, the axial resolution can drop to 2 µm and 0.3 µm, respectively. This can result in isotropic resolutions of 1.4 µm and 0.2 µm for the two objective lenses mentioned above.

Current efforts in SPIM technology development aim at the integration of advanced light microscope methods (such as lifetime imaging, photo activation, etc.) and optical manipulation tools (such as optical tweezers and three-dimensional laser ablation). Additionally, we are investigating new approaches that improve essential technical parameters like sample depth penetration, image resolution, image homogeneity and imaging speed.

Microtubules

Microtubules are of particular interest in cell biology as well as in biophysics (Bray 2001). They are hollow cylindrical structures (app. 25 nm in diameter), which are found in the cytoplasm of a cell. Microtubules are involved in intracellular transport and cell shape regulation. Microtubules are very dynamic structures, i.e. they constantly switch between phases of growth, shrinkage and pausing. This behavior has been termed microtubule dynamic instability. Conventional 2D *in vitro* approaches study microtubule dynamic instability in artificial set-ups, which bias certain aspects of the microtubules' dynamic properties and introduce artifacts via the hard and flat surfaces, e.g. of the surrounding glass. The microtubules' proximity to hard glass surfaces accounts for a dynamic behavior of these protein polymers that seems different in a more physiological setting. Hence, overcoming the limitations of traditional microscopy is crucial to quantitatively access the microtubules' intrinsic properties.

We introduced a three-dimensional experimental approach to studies of microtubule dynamics, based on laser light-sheet fluorescence microscopy and a sample preparation in spacious transparent Teflon cylinders (Keller et al. 2006, Keller et al. 2007). Using these cylinders, microtubule asters (star-shaped microtubule structures nucleated from centrosomes) can form in a mechanically almost unconstrained environment (Fig. 1A, B). In such a three-dimensional situation, the surface-over-volume ratio is smaller by a factor of 50 than in a classical 2D sample preparation. The biopolymers encounter no hard artificial surfaces and tend to behave much more like in a natural environment (Fig. 1C). Moreover, in order to ensure a physiologically relevant context, the microtubule asters are polymerized in Xenopus laevis egg extracts rather than in a buffer-based system.

Our experiments show that microtubules behave quite differently in an unconstrained three-dimensional system. The most striking differences are a dramatically reduced probability of microtubule shrinkage (by a factor of twelve), an increase in microtubule pausing (by a factor of three) and a reduction of the polymers' growth speed (by a factor of two) in three dimensions. These differences of up to one order of magnitude illustrate the strong influence of the experimental approach on the measurements themselves as well as the need to explicitly consider the third dimension to obtain quantitatively meaningful data. In addition, the three-dimensional system allows for the analysis of almost all of a microtubule aster's filaments and thereby gives experimental access to microtubule population statistics. This is particularly helpful in case rare dynamic events are to be analyzed quantitatively. We demonstrate the potential of this technique by deriving evidence for a stochastic character of microtubule pausing.

In summary, our results support previous studies that have found microtubule growth rates and frequencies of catastrophe (i.e. the rate of switching from the polymerizing/growing to the depolymerizing/shrinking state) to be force-depend-

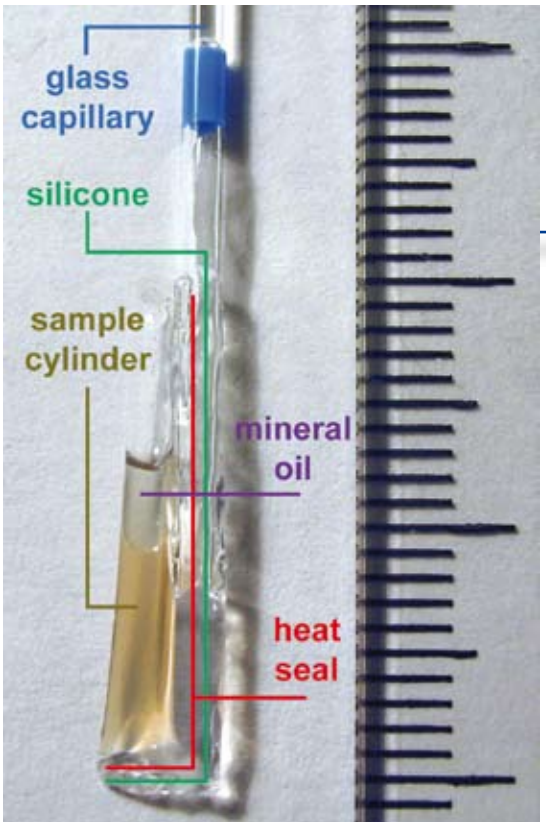

Fig. 2: Three-dimensional preparation of Xenopus laevis egg extracts in transparent Teflon-based cylinders. A polytetrafluorethylen (PTFE) cylinder loaded with egg extract as employed in the 3D experiments of microtubule dynamic instability. The cylinder is formed using a 25 µm thin PTFE foil. By application of heat, the bottom part and the seam of the cylinder are sealed. A glass capillary is glued to the cylinder with silicone. While the heat seal prevents contact of the silicone with the inside of the PTFE cylinder, the mineral oil protects the egg extract from degradation caused by oxygen in the air.

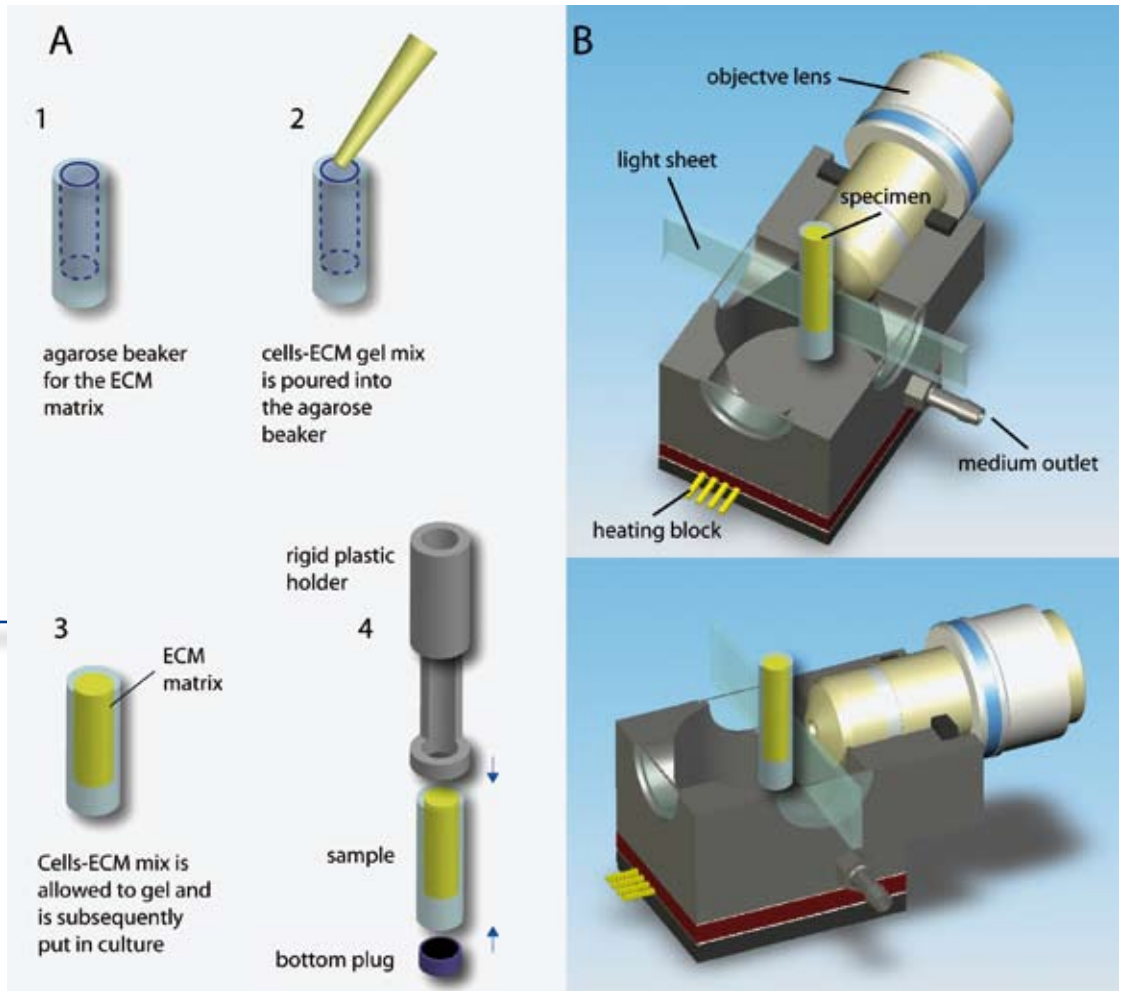

Fig. 3: Three-dimensional cell biology with light sheet-based fluorescence microscopy. A: Preparation of a stable, optically clear agarose beaker for three-dimensional cell cultures. 1. Liquid agarose is poured into a template and forms a small beaker. 2. A cell/ECM-gel mix is deposited into the beaker. 3. A plastic holder ensures stability for time-lapse studies. B: Autoclavable cell culture chamber for SPIM. An integrated heater maintains the temperature at 37 ± 0.1 °C. The objective lens is immersed into the medium.

ent (Dogterom & Yurke 1997). Moreover, research has also shown similar effects when comparing 2D *in vitro* and *in vivo* experiments. For instance, in the fission yeast Schizosaccharomyces pombe, microtubule bundles seem to bend rather than depolymerize spontaneously when they touch the yeast's cell membrane (a behavior that is quite in contrast to that observed with glass surfaces). Currently, we adopt our three-dimensional study to other dynamic cellular processes. We expect our methods and results to have a major impact on the understanding of the mechanical properties of tissue cells, an aspect that we will focus on next.

Three-dimensional Cell Cultures

An increasing amount of experimental data shows that growing cells within three-dimensional matrices reduces the gap between cell cultures and real tissues. In living tissues, cells interact through cell-cell and cell-ECM contacts (ECM: extracellular matrix). This signaling network extends in three dimensions and controls tissue specificity and homeostasis. Three-dimensional cell cultures mimic *in vitro* such physiological cell-cell and cell-ECM interactions. Therefore, they are a better model of real tissues when compared to conventional two-dimensional cultures.

Several studies show that the physiological relevance of cell-based assays is improved by employing three-dimensional cultures. A three-dimensional approach can increase the predictive power of *in vitro* drug and toxicity screenings, and contributes to the reduction of the number of test animals employed in both pharmaceutical industry and basic research.

Three-dimensional cultures are currently applied to a broad range of investigations in cell biology. These include tumor biology, cell migration, and epithelial morphogenesis.

Tumor biology. Mina Bissell pioneered the idea of culturing cells in three-dimensional basal membrane gel (Matrigel) in order to elucidate the steps leading to malignant transformation in breast cancer. Healthy and tumor cells are easily distinguished by employing a three-dimensional assay. In fact, healthy cells start organizing into mammary acini and to secrete milk in three-dimensional Matrigel, while cancerous cells grow to a disordered tumor-like mass. In contrast, two-dimensional cultures do not reveal any phenotypic difference between normal and neoplastic breast cells. By using three-dimensional assays, Bissel and collaborators showed that malignant breast cancer cells can be reverted to normally proliferating cells. This process is

started by inhibiting receptors involved in cell-matrix interaction, such as the β1 integrins or epithelial growth-factor receptors (Bissel et al. 2003).

By employing time-lapse imaging of three-dimensional cultures in collagen, Friedl and collaborators showed that invasive cancer cells easily change migration strategy. Metastatic cells can switch from mesenchymal (spindle-shaped cells) to amoeboid (spherical-shaped cells) motility. Such plasticity allows the cells to elude pharmacological treatment aimed to stop metastasis (Friedl & Wolf 2003).

The studies pioneered by Bissel and Friedl, and currently pursued by an increasing number of researchers worldwide, pave the road to novel cancer therapies targeting the cell's microenvironment rather the cell as an isolated entity.

Epithelial morphogenesis. The dichotomy between two- and three-dimensional cell culture systems is highlighted by the investigation of epithelial morphogenesis. Along with mammary cells, a very useful model system is represented by Madin-Darby Canine Kidney (MDCK) cells. MDCK cells cultured in three-dimensional collagen start an intrinsic differentiation program and form spherical monolayers with a hollow lumen (cysts), which resemble rudimentary epithelial suborgans (Fig. 4). Upon chemical stimulation (for example with hepatocyte growth factor), MDCK cysts undergo partial de-differentiation (epithelial-mesenchymal transition) developing branching tubules (a process called tubulogenesis). Cysts and tubules are fully polarized: they have an apical surface facing the cavity lumen and a basolateral surface contacting neighboring cells and the extracellular matrix. Interestingly, MDCK cells growing within the gel create their polarization cue autonomously, starting from a nearly isotropic situation. By contrast, in two-dimensional cultures it is the underlying substrate that provides an intrinsically ani-

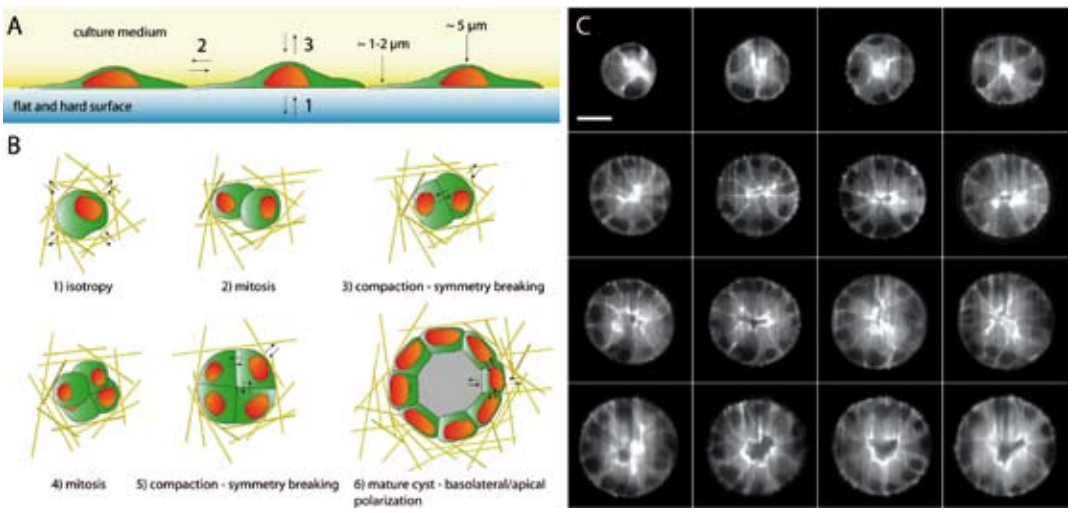

Fig. 4: Three-dimensional cell culture and MDCK cystogenesis.

A: Cell-cell and cell-environment interactions in 2D culture conditions. In the 2D experimental situation, cells are cultured as a monolayer on a hard and flat surface (e.g. glass slides, plastic Petri dishes). Cell-substrate interactions (1A-1). Cells receive a strong anisotropic mechanical cue from the underlying surface, and are stimulated to produce strong adhesions centres (e.g. the formation of focal adhesions and actin stress fibres is enhanced). Cell-cell interactions (1A-2). On monolayers, the cell-cell contact surface is thin and nearly two-dimensional. Cells stop growing when the monolayer reaches confluence (contact inhibition), but the insufficient lateral interactions do not allow the establishment of a defined lateral polarity. Cell-media interactions (1A-3). The cells in the monolayer receive nutrients, biochemical signals (e.g. from growth factors), and oxygen from the overlying culture media (1A-2). Cells also secrete biomolecules into the media. However, no mechanical stimulation is provided by the overlying liquid media.

B: Cell-cell and cell-environment interactions in three-dimensional cell culture. The cystogenesis process by Madin-Darby Canine Kidney epithelial cells (MDCK cells) in a three-dimensional hydrated collagen matrix is illustrated. Single MDCK cells are embedded in a soft gel. This environment, different from 2D culture surfaces, represents for the cell a mechanically and biochemically isotropic environment (C-1, the arrows represent mechano-chemical stimuli from the cell to the environment and from the environment to the cell). After mitosis (1C-2), the two daughter cells dramatically rearrange their architecture in order to create an extended cell-cell surface (compaction, 1C-3). Cell-cell surface creation is a symmetry-breaking event (1C-3, arrows) leading ultimately to full basolateral-apical polarization: an anisotropy axis directed from the plasma membrane in contact with the collagen matrix toward the cell-cell surface is created (1C-3). Cycles of mitosis and compaction are repeated, and cells aggregate to a cluster (1C-4, 1C-5). Subsequently, formation of a hollow lumen, by membrane separation and apoptosis create a third surface (the apical surface) for the cells. Such chain of cellular processes eventually leads to full cyst maturation (1C-6). A mature cyst is composed by a spherical monolayer of about fifty polarized cells surrounding a liquid-filled lumen. A cell in a cyst has a well defined basolateral-apical polarization: a basal surface in contact with the matrix, lateral contacts with the adjacent cells, and an apical surface facing the lumen (1C-6, arrows). Such a three-surfaces architecture creates a coherent information network (the "cell context") that ensures maintenance of cyst homeostasis.

C: Time-lapse SPIMaging of MDCK cystogenesis. These time series shows the development of a MDCK cyst (cystogenesis) observed with light-sheet fluorescence microscopy. MDCK cells were embedded in Matrigel-and cultured by employing the set-up illustrated in figure 4 (SPIM workstation for three-dimensional cell culture). Optimum culturing conditions were obtained by continuous perfusion of the culturing medium and by ensuring constant temperature and pH. Each frame represents the middle slice of a complete three-dimensional data set of a developing cyst. The cells were transfected with GFP-actin. The first frame shows a small 4-cells cyst. The cell divides and progressively the hollow internal lumen develops. The total acquisition time for this data set is 72 hours. The scale bar corresponds to 25 µm.

Fig. 5: Nervous system of a Medaka fish embryo. Maximum-intensity projections of two LSFM image stacks, showing a Medaka fish embryo with acetylated tubulin immunostaining in different orientations (relative angle 150°). The maximum-projection of each view is based on 2048 planes. The staining shows the embryo's entire nervous system. Detection via Carl Zeiss Plan-Neofluar 2.5x/0.075 lens. Scale bar 500 µm. Microscope development by Philipp J. Keller and Ernst H.K. Stelzer, sample preparation by Annette Schmidt and Lazaro Centanin (European Molecular Biology Laboratory), imaging by Philipp J. Keller.

sotropic cue for the establishment of the polarization axis. Moreover, MDCK monolayers grown on a flat substrate are only partially polarized since the nutrients have a limited access to the basal side (O'Brien et al. 2002).

Gene expression. Pioneering experiments performed by Bissell and collaborators over two decades ago showed for the first time that the ECM affected chromatin structure and thereby gene expression in mammary epithelial cell lines. Now, it is well acknowledged that cells cultured in three dimensions have a different gene expression compared to their two-dimensional counterparts. Melanoma cells cultured on flat substrates up- and down-regulate other genes if the same cells are cultured as three-dimensional spheroids. Interestingly, the genes that are up-regulated in the spheroids are also found to be up-regulated in tumor biopsies. Another example is provided by the GTPase protein Rac1. It was found that expression of Rac1 is fundamental for the establishment of epithelial polarity in cells that are cultured within three-dimensional collagen. However, Rac1 is not expressed in the same cells grown as monolayers on flat surfaces (O'Brien et al. 2001).

Developmental biology. Cell-cell and cell-environment interactions are essential for tissue morphogenesis in developing embryos. Time-lapse analysis of three-dimensional cell trajectories *in vivo* with confocal microscopy has provided new insights into such interactions. Large shear forces induced by blood flow are necessary for the correct heart development in zebrafish. *In vivo* studies on chick embryos revealed that the fate and the position of individual cells during somite boundary formation do not exclusively rely on gene expression patterns. Instead, multiple guidance cues are involved, among them mechanical forces within the developing tissue. Thus, previous models assuming strict molecular "pre-programming" have to be revised by taking into account bi-directional communication between cells and the surrounding microenvironment (Kulesa & Fraser 2002). The application of developmental biology concepts to cancer biology is providing new insights into the role of the microenvironment in cancer progression. Invasive human GFP-labeled melanoma cells were transplanted into the neural crest of an embryonic chick model and analyzed after several days of incubation. Instead of forming a tumor, melanoma cells responded to the embryonic microenvironment and reversed to a normal phenotype, as confirmed by the detection of melanocyte and neuronal markers not expressed at the time of transplantation (Kulesa et al. 2006).

The need for quantitative and physiologically relevant cellular systems is particularly perceived in the drug screening process. Currently, a drug candidate entering testing phase one will reach the bedside with a probability of 8 % only. A high failure rate and rising costs are serious challenges for pharmaceutical companies (USA-FDA 2004). Cell-based assays are assumed to improve the success rate at the early stages of the drug discovery process by providing a cell-specific response, which is missing in the target-oriented approach. Reproducing the phenotype of the target tissue in cultured cells is essential for obtaining reliable biomedical data. However, monolayer cell cultures lose their tissue-related functions rapidly, seriously impairing the predictive power of the assays. An example is provided by hepatocytes. If cultured as a monolayer, primary hepatocytes become undifferentiated after a few passages. Strikingly, the biosynthesis of drug-metabolizing enzymes, which is essential for toxicity assays in pharmaceutical research (toxic side-effects are one of the most common reasons for the failure of a drug candidate), is among the first functions to be lost (Gómez-Lechón et al.

1998). Studies have shown that re-establishing (at least partially) the original mechanical and chemical milieu preserves liver-specific functions for longer periods of time. This is achieved by embedding primary hepatic cells within three-dimensional matrices such as collagen and aggregating them to spheroids (Berthiaume et al. 1996).

Selected 3D model systems. A systematic collection of methods that helps scientists in the transition from monolayer cultures to three-dimensional systems is still lacking, despite detailed protocols start to be available. A closer collaboration between tissue engineers and cell biologists is required to fill this gap. Currently, several model systems are available.

Cellular spheroids. Cellular spheroids are simple three-dimensional systems, which take advantage of the natural tendency of many cell types to aggregate. Spheroids from a broad range of cell types are produced easily by the "hanging-drop technique". Spheroids can be obtained from single cultures or co-cultures (mono- or multicellular spheroids, respectively). The most obvious advantage of spheroids is that they do not require external scaffolds to aggregate. Cellular spheroids are the system of choice for therapeutically oriented biomedical studies.

Epithelial cell lines. Models of polarized epithelial tissues are obtained by growing nontransformed immortalized epithelial cell lines under three-dimensional conditions. Examples are the aforementioned MDCK cells and mammary cell lines (such as MCF-10A cells). Such cells grow as hollow spherical monolayers within ECM gels (Fig. 4B,C). The tissue counterparts of these suborgan structures are common to most of the glandular organs, such as breast, kidney, and salivary glands.

Organ explants. Organ explant slices can be cultured on semiporous membranes or embedded in three-dimensional collagen gel. Organotypic slice culture preserves the cytoarchitecture and the differentiation of the original tissue. Applications are in brain physiology, and in studies on the development of ureteric buds.

Living embryos. Embryos provide data on the behavior of cells in a truly physiological environment. Culturing drosophila, medaka, and zebrafish embryos *in vitro* allows some flexibility in the setting of environmental parameters. In contrast, mammalian embryos (e.g. mouse embryos) require controlled temperature and oxygenation to maintain their viability during an experiment. Different static culture systems suitable for time-lapse imaging of pre- and post-implantation embryos were developed (Jones et al. 2002).

Researchers working with three-dimensional cellular systems face several technical challenges. Large cellular aggregates require a careful control of the gas exchange as well as the diffusion of soluble nutrients and chemical agents. Biochemical analysis is complicated by the lower cell density and the additional steps required separating the cells from the matrix. Since most of the currently available ECM gels are extracted from animals or cultured cells, quality control is difficult. For example, the amount of undesired soluble components varies between batches. This reduces the reliability and reproducibility of the assays. Progress is achieved with fully synthetic fibrous biopolymer scaffolds. Gels resulting from molecular self-assembling of synthetic oligopeptides are now available for three-dimensional cell cultures (i.e. the commercially available Puramatrix). At pH and temperature conditions compatible with tissue culture, the oligopeptide building blocks form a well-defined scaffold made of nanometer-sized fibers. Nanometer-sized fibers and pores are essential to ensure a true three-dimensional environment for the cells. A further advantage is that such gels can be custom-tailored with specific amino-acidic sequences recognized by the cell's adhesion receptors. Progress in optical microscopy has to overcome the challenges preventing high-resolution live imaging of sensitive three-dimensional samples. A new SPIM-based workstation was specifically developed to investigate cell cultured in complex three-dimensional environments. Three-dimensional cell cultures can be observed for several days under tightly controlled pH and temperature conditions (Fig. 3). With this approach, three-dimensional fluorescence live imaging of MDCK cystogenesis was achieved (Fig. 4C).

Small Animal Model Systems

The ultimate goal of moving towards three-dimensional and close-to-life conditions is the study of living whole animals and organs. Apart from three-dimensional cell cultures, our current efforts are therefore focused on the three-dimensional investigation of embryo development. The study of the nervous system in Medaka fish embryos (Fig. 5) is an example of such an application. The embryo in figure 5 is seven days old and already approx. 3.5 mm long. The possibility to record multiple views of such large specimens with light sheet based fluorescence microscopy constitutes a simple way to address the issue of depth penetration in light microscopy. Although only two views of the same fish embryo are shown in figure 5, the acquisition of large and detailed multi-view data sets is straightforward, owing to the rotational degree of freedom in sample positioning and the long working distance lenses used in LSFM. Since single image stacks (i.e. single views) are typically recorded in under one minute in LSFM, a multi-view reconstruction of an entire embryo can be performed from the living specimen at a good temporal resolution (e.g. down to 5 minutes in an eight-view data set). Importantly,

the resulting good spatio-temporal resolution and manageable sample sizes clearly outperform the capabilities of confocal and multi-photon microscopies.

Outlook

The physiological relevance of three-dimensional cell cultures makes them a fundamental research tool in cell biology and will likely foster the further integration of genomics, proteomics and molecular cell biology data. This will result in improved models of tissues and organisms. Three-dimensional cell systems will allow more physiologically relevant screening assays for drug discovery and clinical research. Large-scale toxicity screenings like the recently started Registration, Evaluation and Authorization of Chemicals (REACH) Program of the European Union require the sacrifice of thousands of laboratory animals. Three-dimensional cell cultures could provide an alternative, which is attractive for both ethical and economical reasons.

Almost half a century ago, Karl Popper noted that the sciences, in particular the natural sciences, evolve by breaking a dogma and developing new ones. In the early 1900s, pioneers like Ross G. Harrison broke a central dogma of physiology by removing single cells from organisms and growing them in nutrient media. Such pioneering work separated cell biology from developmental biology and established the principle of cell culture, triggering a revolution that became mainstream and still helps us to address fundamental cellular phenomena. However, ongoing technical advances in tissue engineering and microscopy are now removing many obstacles in the growth and observation of cells in their natural tissue environment.

We believe that a more complete view becomes possible. Questions arising in biophysics, cell biology and developmental biology can be addressed with similar tools and with the same mind-set. Thus, seemingly different experiments become more relevant by relying on comparable compounds. Nevertheless, it is still a challenge to move into the third dimension in life sciences research. Although the scientific community is starting to realize the importance of introducing such approaches routinely, the main drive does not arise from basic research in cell biology but rather from the clinicians – those who would ultimately like to take advantage of the results of modern molecular biology.

Acknowledgements

The authors thank Klaus Greger for his many contributions to SPIM development. F.P. and E.H.K.S. acknowledge the Forschungsprogramm “Optische Technologien” der Landesstiftung Baden-Württemberg gGmbH for financial support. E.G.R. and E.H.K.S. acknowledge the support by the German BMBF. P.J.K. acknowledges the collaboration with Annie Rousselet.

References

[1] Stelzer E.H.K., Keller P.J., Innovation 7, 16–18 (2007).
[2] Stelzer E.H.K., Lindek S., Opt. Commun. 111, 536–547 (1994).
[3] Siedentopf H., Zsigmondy R., Ann. Phys. 10, 1 (1903).
[4] Huisken J., *et al.*, Science 305, 1007–1009 (2004).
[5] Greger K., *et al.* The Review of scientific instruments 78, 023705 (2007)
[6] Swoger J., *et al.*, Optics Express 15, 8029–8042 (2007)
[7] Verveer P.J., *et al.*, Nat Methods 4, 311–313 (2007).
[8] Engelbrecht C.J., Stelzer E.H.K., Opt. Lett. 31, 1477–1479 (2006)
[9] Bray D.: Cell Movements: From molecules to motility, Garland Publishing, 2001.
[10] Keller P.J., *et al.*, Curr. Op. Cell Biol. 18, 117–124 (2006).

The complete list of references is available within the online version.

Authors Biographies

Ernst H.K. Stelzer received his degrees in physics and has been a group leader at EMBL for almost twenty years. He started working on confocal fluorescence microscopy in 1983, developed the 4Pi microscope in the early 1990s and shortly afterwards introduced orthogonal and multi-lens detection schemes with theta microscopy. The latter work lead to the development of light sheet based fluorescence microscopy.

Philipp J. Keller is a second-year student in physics at EMBL and developed the next-generation light-sheet based microscope DSLM.

Francesco Pampaloni is a postdoctoral fellow at the EMBL and developed a 3D cell culturing workstation based on SPIM to investigate cell behavior regulation by mechanical forces.

Contact:

Dr F. Pampaloni
P.J. Keller
Dr M. Marcello
Dr E.G. Reynaud
A. Schmidt
Dr L. Centanin
Prof J. Wittbrodt
Dr E.H.K. Stelzer
European Molecular Biology Laboratory (EMBL)
Heidelberg (Germany)
Tel.: +49 6221 387 8354
stelzer@embl.de

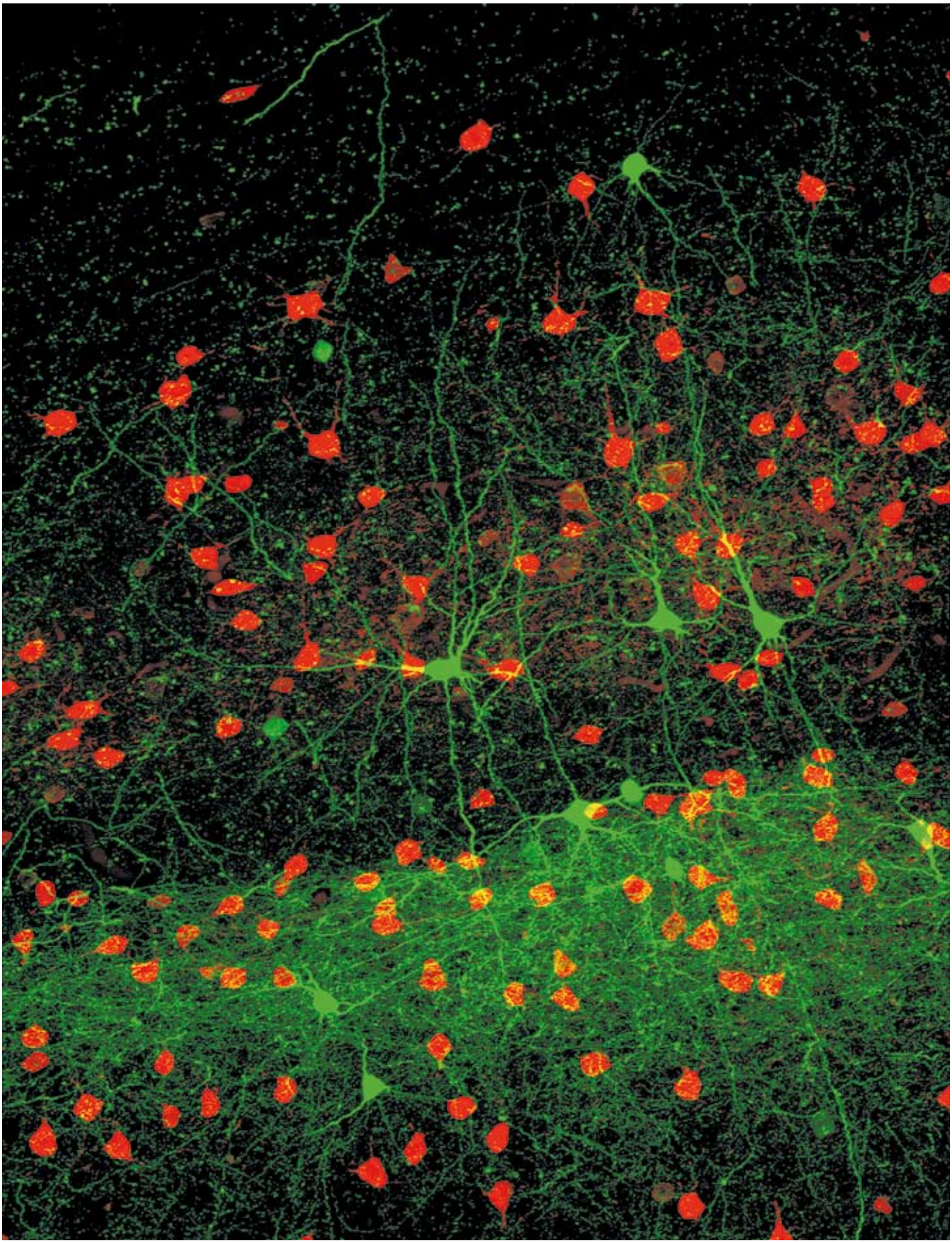

GFP expressing inhibitory interneurons (green) are located in the somatosensory cortex of a mouse brain. Parvalbumin is expressed by interneurons and surrounding neural cells, displayed in red (LSM 510)
Dr H. Hang, West Virginia University, Morgantown, USA

Visualizing Protein-protein Interactions

Correlation and Complementation

Microscopy utilizing fluorescence resonance energy transfer (FRET) with green fluorescent protein (GFP) derivatives has offered a first glimpse into the spatio-temporal aspects of biological activities. On the other hand, fluorescence cross-correlation spectroscopy (FCCS) has proven to be a promising technique for quantifying protein-protein interactions. Although FCCS does not produce direct images, it provides more quantitative information of the interactions since it is more sensitive than FRET. Also, bimolecular fluorescence complementation (BiFC) has been used to reliably analyze the occurrence and subcellular localization of protein-protein interactions in live cells. Although the irreversible binding of fluorescent protein fragments poses as a limitation of this technique, BiFC can provide high sensitivity, temporally-integrated information of protein-protein interactions.

生物機能の動的理解を目指して、さまざまな蛍光イメージング技術が注目されている。緑色蛍光タンパク質（GFP）の改変体を使った蛍光共鳴エネルギー移動（FRET）技術によって、生物機能の時空間制御が明らかにされつつある。一方、蛍光相互相関分光法（FCCS）は、測定点における生体分子間の相互作用に関する高感度かつ定量的な情報を与えてくれる。さらに、相補的蛍光生成（BiFC）を基にした技術は、生体分子相互作用を著しく高い感度で可視化することができ、その特性を利用すれば、相互作用の履歴を空間的にマップすることができる。

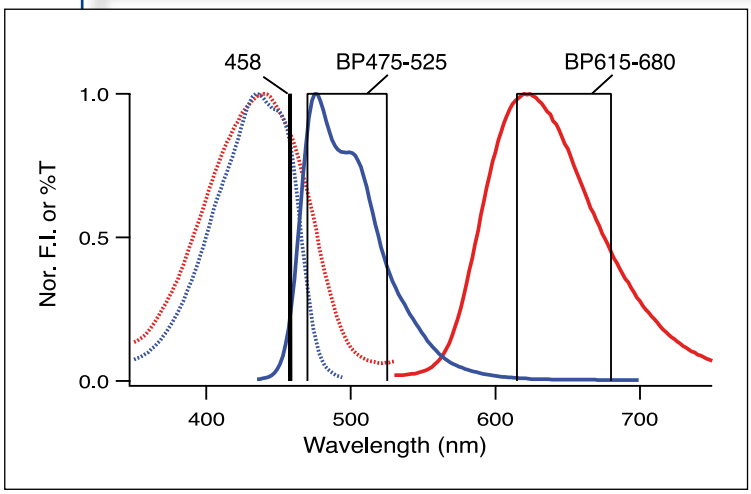

Fig. 1: Excitation (broken line) and emission (solid line) spectra of CFP (cyan) and mKeima (red). Nor. F. I.: normalized fluorescence intensity. The laser line (458 nm) and the transmittance spectra for the emission filters are indicated.

Keywords:

fluorescent protein / fluorescence resonance energy transfer / fluorescence cross-correlation spectroscopy / bimolecular fluorescence complementation / protein-protein interaction

In this review, the term 'fluorescent proteins' (FPs) is used to describe proteins that become spontaneously fluorescent via the autocatalytic synthesis of a chromophore [1]. With the emergence in the last decade of the spectral variants of *Aequorea* green fluorescent protein (GFP) along with GFP-like fluorescent proteins isolated from other animals, an increasing body of researchers have been earnestly anticipating the development of a tool for the direct visualization of biological functions [2]. Such a desire, increasingly realized by the marriage of FPs with fluorescence resonance energy transfer (FRET) [3], is further fueled by the need for more thorough post-genomic analyses of protein function. FRET imaging technologies using live samples permit analysis of the spatio-temporal patterns of many biological functions. Because live samples are highly dynamic, and because fluorescent signals are capable of reflecting current states, multiple time-lapse images are often collected to explore temporal regulation of biological functions. As the techniques that may complement FRET technique, here I will deal with fluorescence cross-correlation spectroscopy (FCCS) [4] and bimolecular fluorescence complementation (BiFC) [5]. I will also

explain the basic features of the chromophore and the β-barrel of FPs in order to clarify the underlying principles behind BiFC.

Dual-color Single-laser Fluorescence Cross-correlation Spectroscopy

Dual-color fluorescence cross-correlation spectroscopy (FCCS) is a promising technique which can quantify protein-protein interactions [4]. FCCS has several advantages over standard fluorescence correlation spectroscopy (FCS). Whereas FCS detects molecular concentration and mobility, FCCS enables the tracing of two spectrally distinguishable fluorophores, thereby extracting essential information about the kinetics of molecular interactions. In this technique, two different fluorescent labels are excited and detected simultaneously within a common measurement volume. In order to achieve simultaneous excitation, two lasers are aimed at the same confocal spot. Bringing two laser beams to a perfect and stable overlap, however, is often difficult. Although FCCS can be performed using a single laser line (SL-FCCS: single laser-line excitation FCCS) for single-photon excitation [6], complex mathematical computations are required to compensate for cross-excitation, cross-talk, and FRET when researchers use common fluorescent proteins which have broad excitation and emission spectra but modest Stokes shifts. One solution for efficient simultaneous excitation may come from two-photon excitation (TPE) microscopy [7], where two differently colored fluorescent proteins can be excited simultaneously by a single infra-red ultra-short pulse laser line due to the blue-shift effect. Although the TPE-SL-FCCS method has been shown to be successful [7], TPE requires expensive equipment and expertise of operation. Also, it is important to note that in TPE, the rate of bleaching per unit excitation increases supralinearly with pulse intensity [8]. This may add another decay component, thereby making analyses complex.

To generate a pair of fluorescent proteins having comparable excitation maxima but sufficiently different Stokes shifts, the development of fluorescent proteins that show large Stokes shifts was pursued. A recently developed far-red fluorescent protein, Keima, is endowed with a large Stokes shift [9]. It absorbs light maximally at 440 nm and emits maximally at 620 nm. Use of a monomeric version of Keima (mKeima) together with cyan fluorescent protein (CFP) allows for simple yet efficient FCCS using a single 458-nm argon laser line (Fig. 1). Due to the complete separation of the emissions of these proteins, this FCCS approach enables high sensitivity detection of the association of calmodulin (CaM) with CaM-dependent enzymes *in vitro* (Fig. 2A). Since the detection of molecular associations by FCCS is not usually affected by fusion design or the size of host proteins, this technique is applicable to high-throughput screening for interacting protein pairs. By contrast, FRET efficiency is highly sensitive to the way by which the two fluorescent proteins are fused to the host proteins; a substantial amount of work is required to obtain fusion constructs that give significant changes in FRET signal upon CaM/CaMKI association. However, reversible molecular interactions should be more difficult to detect in live cells than in *in vitro* experiments. Because cells contain endogenous unlabeled molecules that can interfere with the association between two distinct fluorescently labeled species, FCCS signals may be attenuated. The introduction of more labeled molecules into live cells may overcome this interference; unlike FRET, however, FCCS requires that the con-

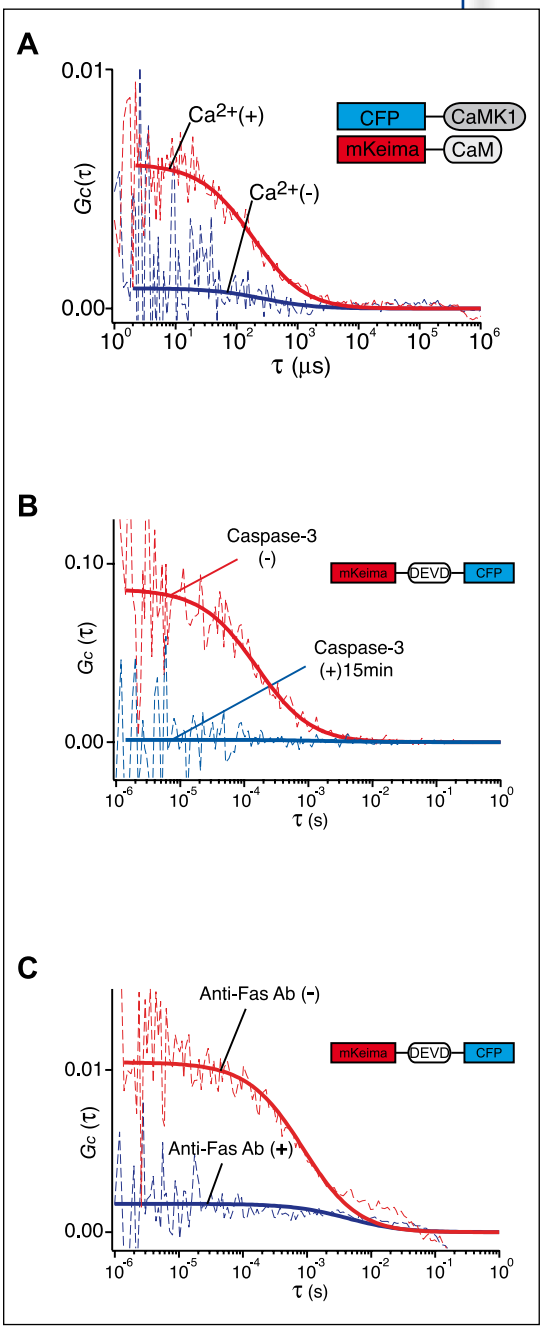

Fig. 2: Single laser wavelength (458 nm) excitation FCCS using mKeima and CFP. Gc(τ): the cross-correlation function. (A) Monitoring of the Ca^{2+}-dependent association between CaM and CaMKI. Cross-correlation curves were measured in the presence of 0.1 mM EGTA (blue, $Ca^{2+}(-)$) and then after the addition of 1 mM $CaCl_2$ (red, $Ca^{2+}(+)$). (B) *In vitro* cross-correlation analysis. Cross-correlation curves measured at 0 s (red) and 500 s (blue) after the addition of caspase-3. (C) Cross-correlation analysis in live HeLa cells. Cross-correlation curves measured from anti-Fas antibody-treated (blue) and non-treated (red) cells expressing the sensor protein.

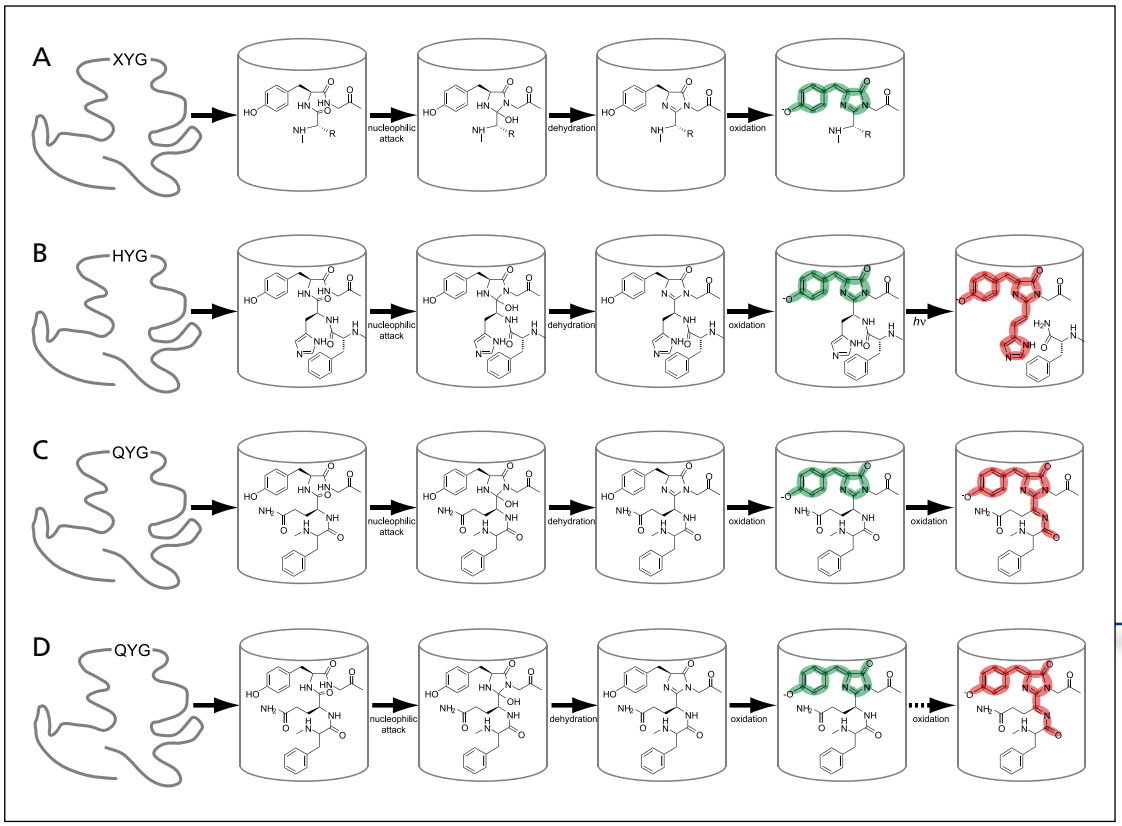

Fig. 3: Comparison of schemes for the formation and maturation of chromophores in FPs. The β-can structure represents the native conformation of the protein, while the denatured form is depicted as an irregular chain. π-conjugation for visible-light absorption is indicated in green or red. Neighboring amino acids (single-letter code) have been added. (A) Scheme for the formation of 4-(*p*-hydroxybenzylidene)-5-imidazolinone as the basic chromophore in green-emitting FPs, including the wild-type *Aequorea* GFP. (B) Scheme for the formation and photo-induced extension of the chromophore of Kaede or EosFP. (C, D) Scheme for the formation of 4-(*p*-hydroxybenzylidene)-5-imidazolinone and its autocatalytic modification in DsRed (C) and E5 (D).

centrations of labeled molecules be kept low to optimize fluctuating signals.

It should be noted that the interference problem does not affect the detection of proteolysis by FCCS because the cross-correlation signals from doubly labeled substrates are not affected by endogenous substrates. The carboxyl terminus of mKeima and the amino terminus of CFP were linked with a peptide containing the caspase-3 cleavage sequence DEVD. The recombinant protein (mKeima-DEVD-CFP) was examined in a chamber using an excitation wavelength of 458 nm. Significant cross-correlation was observed between the fluctuations in the two detection channels (Fig. 2B, caspase-3 (-)). Incubation of the same sample with activated recombinant caspase-3 (0.2 U/µl) at 25 °C for 7 minutes almost completely abolished the cross-correlation signal (Fig. 2B, caspase-3 (+)). Importantly, this proteolysis could also be examined easily in apoptotic cells. The same FCCS experiments were conducted with HeLa cells transfected with cDNA coding for mKeima-DEVD-CFP. The degree of cross-correlation was substantially different between anti-Fas antibody-treated and non-treated cells (Fig. 2C).

4-(*p*-Hydroxybenzylidene)-5-imidazolinone and green-to-red maturation

Most FPs share X-Tyr-Gly that serves as the chromophore-forming peptide. Known exceptions are the blue- and cyan-emitting variants of *Aequorea* GFP (BFP and CFP), which contain His and Trp instead of Tyr in the tripeptide, respectively. The wild-type *Aequorea* GFP contains the tripeptide Ser^{65}-Tyr^{66}-Gly^{67}. The process of chromophore formation is illustrated in figure 3A [1]. Concomitant or subsequent to the folding of the β-barrel an imidazolinone is formed by nucleophilic attack of the amide of Gly^{67} on the carbonyl of Ser^{65}, followed by dehydration. Molecular oxygen then dehydrogenates the α-β bond of Tyr^{66} to conjugate its aromatic group with the imidazolinone. The resulting chromophore is 4-(p-hydroxybenzylidene)-5-imidazolinone, which emits green fluorescence. Many other green-emitting FPs retain this chromophore throughout their lifetime.

Red-emitting FPs (RFPs) initially create the basic green-emitting chromophore, 4-(*p*-hydroxybenzylidene)-5-imidazolinone, but then an additional reaction occurs to expand the π-conjugated system.

Two coral fluorescent proteins, Kaede [10] and EosFP [11], contain the tripeptide His^{62}-Tyr^{63}-Gly^{64}, a green chromophore that is photoconverted to red (Fig. 3B). UV irradiation promotes an unconventional cleavage within the protein between the amide nitrogen and C_α at His^{62} via a formal β-elimination reaction. The subsequent formation of a double bond between His^{62}-C_α and -C_β extends the π-conjugation to the imidazole ring of His^{62}, creating a new red-emitting chromophore, 2-[(1E)-2-(5-imidazolyl)ethenyl]-4-(*p*-hydroxybenzylidene)-5-imidazolinone [12, 13].

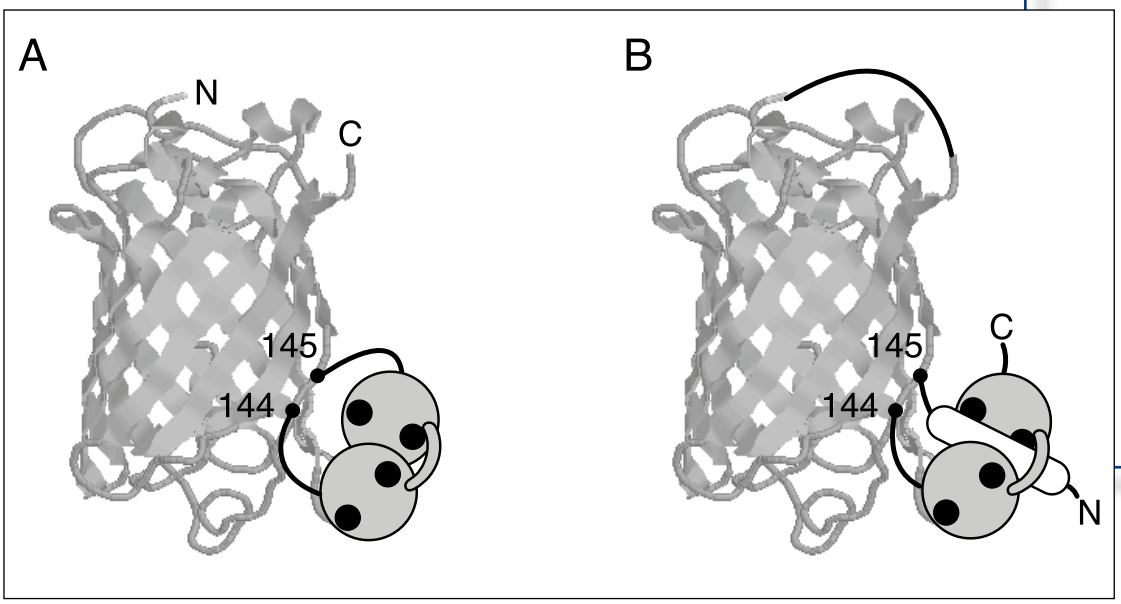

Fig. 4: Schematic drawings of two genetically encodable indicators for Ca^{2+}. (A) Camgaroo. (B) Pericam or GCaMP. Residues 144 and 145 localize in the region between a β-sheet and a surface-exposed loop region.

In common RFPs, additional oxidation occurs autocatalytically to modify 4-(*p*-hydroxybenzylidene)-5-imidazolinone. In certain precocious RFPs, such as DsRed, this oxidation is so efficient that the green intermediate exists only transiently (Fig. 3c) [14, 15]. Incomplete chromophore modification gives rise to residual green fluorescence, thus prohibiting the combined use of this molecule with green-emitting FPs in dual-color labeling experiments. Recently, a new generation of RFPs and engineered variants of DsRed featuring fast and complete green-to-red maturation have enabled researchers to overcome problems associated with slow and incomplete modification [16].

However, in some cases, a long-lived green state can be advantageous, especially for analysis of the duration of gene expression in cells. E5, a new mutant of DsRed, is particularly useful because it changes color from green to red according to a predictable time course (Fig. 3D) [17]. This feature allows for the ratiometric analysis of green to red emission as an estimate of the time elapsed after the initiation of reporter gene expression. Therefore, E5 functions as a 'fluorescent timer' that yields temporal and spatial information regarding protein translation and target promoter activity. For example, E5 was used to trace the expression of a homeobox gene, *Otx-2*, which is involved in the patterning of the anterior structures in *Xenopus laevis*. Green fluorescence indicated the onset of gene expression, whereas red fluorescence indicated that the expression was suppressed [17]. This approach of using E5 has also been employed to examine the functional segregation of secretory vesicles in neuroendocrine cells. By tagging atrial natriuretic factor (ANF) with E5, Duncan *et al.* analyzed the age-dependent distribution of large dense-core vesicles in bovine adrenal chromaffin cells [18]. They observed that newly assembled vesicles are immobile and docked at the plasma membrane shortly after biogenesis, whereas older vesicles are mobile and located at greater distances from the plasma membrane. Like DsRed, E5 forms an obligate tetramer. Although oligomerization does not prevent the use of E5 for reporting gene expression, it may preclude its use in certain fusion protein applications. A monomeric version of fluorescent timer proteins would be most suitable for analyzing age-dependent distribution of functional proteins.

β-Barrel Rearrangement

All FPs share a β-barrel structure. This elegantly woven three-dimensional setup is indispensable for chromophore formation. At first glance, its function may seem to be easily compromised with the introduction of rearrangements. Nevertheless, in 1999, researchers performed substantial operations on the β-barrel of *Aequorea* GFP variants. Baird *et al.*

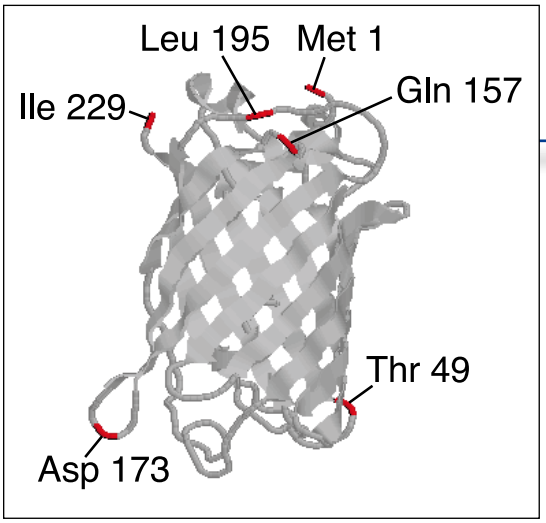

Fig. 5: Three-dimensional structure of *Aequorea* GFP with Met1, Thr49, Gln157, Asp173, Leu195, and Ile229 indicated. These residues are all positioned in surface-exposed loop regions. Thr49, Gln157, Asp173, Leu195, and Ile229 become new amino termini of circularly permuted GFPs, in which the natural amino and carboxyl termini are connected via the pentapeptide linker, GGSGG.

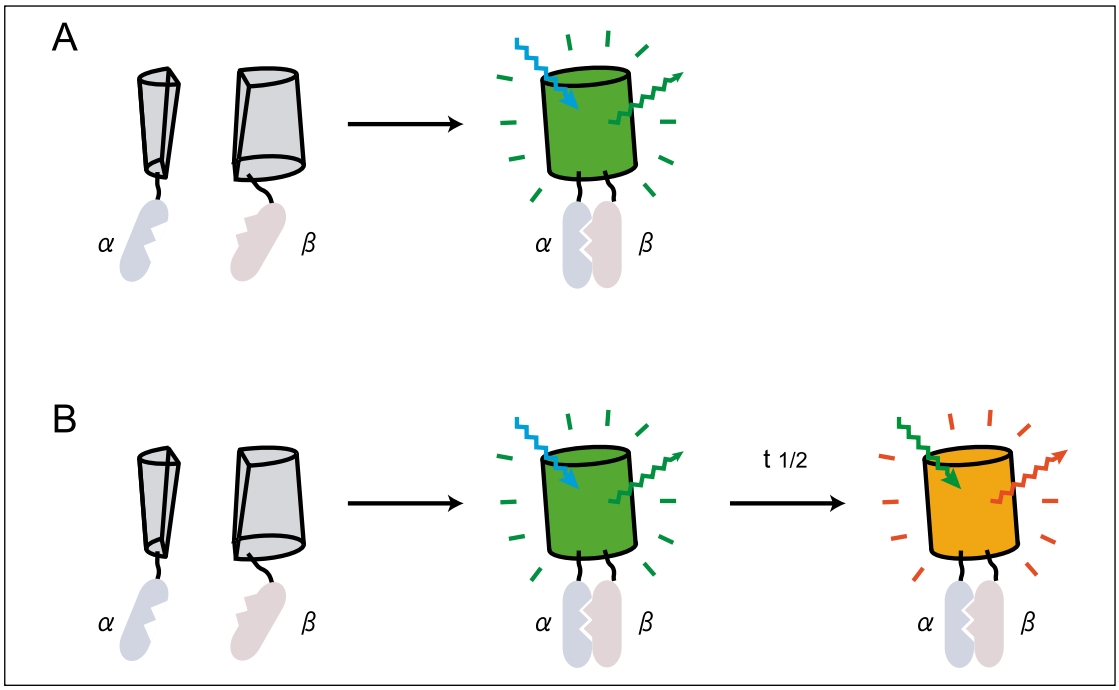

Fig. 6: Principle of bimolecular fluorescence complementation assay. (A) This assay is based on the formation of a fluorescent complex (β -barrel) by fragments of an FP brought together by the association of two interacting partners (α and β) fused to the fragments. (B) A schematic of the BiFC technique setup combined with a fluorescent timer protein.

identified specific positions that can tolerate the insertion of additional protein sequences [19]. Furthermore, the authors succeeded in producing circular permutations at these positions. These rearranged proteins, whose amino and carboxyl portions were interchanged and rejoined with short spacers, proved to be fluorescent.

Interestingly, the position extensively used for insertion and circular permutation by the authors was Tyr145, a residue located in the peripheral region of a β-sheet [19]. Therefore, a chimeric FP containing a conformationally sensitive receptor could potentially modulate the fluorescence of *Aequorea* GFP variants in response to ligand binding. This principle was demonstrated by the insertion of CaM at Tyr145 of EYFP [19]. The fluorescence of this protein was enhanced upon Ca^{2+} binding (Fig. 4A). This EYFP-CaM, named "camgaroo," functions as a genetically encoded Ca^{2+} indicator with an apparent K_d for Ca^{2+} of 7 µM and a Hill coefficient of 1.6. Since *Aequorea* GFP variants circularly permuted around Tyr145 are sensitive to conformational changes, they have also been used as sensors for detecting interactions between two protein domains. A circularly permuted YFP was fused to CaM and its target peptide, M13. Chimeric proteins "pericam"[20] and "GCaMP" [21] are fluorescent and their spectral properties change reversibly as a function of Ca^{2+} concentration. As the mechanism for this spectral shift, it is proposed that the interaction between CaM and M13 alters the microenvironment surrounding the chromophore (Fig. 4B).

The development of fluorescent circularly permuted *Aequorea* GFP variants could be facilitated by inverting sequences at a site within a surface-exposed loop region of the β-barrel. The resulting intact β-sheet structures should be insensitive to conformational changes. In our laboratory, circular permutations were performed on Venus (the bright version of YFP) with a pentapeptide linker, GGSGG, to connect natural amino and carboxyl termini [22]. New termini were introduced into surface-exposed loop regions of the β-barrel. The resulting proteins, cp49Venus, cp157Venus, cp173Venus, cp195Venus, and cp229Venus, were given new N termini at Thr49, Gln157, Asp173, Leu195, and Ile229, respectively (Fig. 5). When expressed in bacteria and mammalian cultured cells, they matured efficiently and showed similar resistance to acidification to their parent protein. These cpVenus proteins produced significant variations in the relative spatial orientation of the yellow chromophore within the Venus-containing protein complex, since Met1, Thr49, Gln157, Asp173, Leu195, and Ile229 reside at different sites on the β-barrel.

Cameleons are genetically encoded fluorescent indicators for Ca^{2+} based on *Aequorea* GFP variants and CaM [23]. They are chimeric proteins consisting of a short-wavelength variant of GFP, CaM, a glycylglycine linker, the CaM-binding peptide of myosin light-chain kinase (M13), and a long-wavelength variant of GFP. Ca^{2+} binding to CaM triggers an intramolecular interaction between CaM and M13, which changes the chimeric protein from an extended to a more compact conformation, thereby increasing FRET efficiency. Yellow cameleons (YCs) have cyan and yellow fluorescent proteins (CFP and Venus) as FRET donor and acceptor, respectively. In order to achieve a large Ca^{2+}-dependent change in the relative orientation and distance between the two fluorophores, cp49Venus, cp157Venus, cp173Venus, cp195Venus, and cp229Venus were tested on YCs. Cp173Venus incorporated in YC absorbs a greater amount of excited energy from CFP in its Ca^{2+}-saturated form, thereby increasing the Ca^{2+}-dependent change in the ratio of Venus/CFP by nearly 600 % [22].

Bimolecular Fluorescence Complementation (BiFC)

Distinct proteins containing the amino- and carboxyl-terminal halves of an FP do not spontaneously assemble into a functional FP if co-transfected into cells. The bimolecular fluorescence complementation (BiFC) assay is based on the reconstitution of an FP from two non-fluorescent fragments [5]. If these two fragments are brought into close proximity by a physical interaction between proteins fused to each fragment (Fig. 6A), the β-barrel structure will be reconstituted, and fluorescence will be produced. *Aequorea* GFP variants are usually separated between positions 154 and 155 or between positions 172 and 173, since these positions are located in loop regions Kerppola and colleagues initially used EYFP residues 1 – 154 (YN) and residues 155 – 238 (YC) as the two fragments for studying BiFC [24]. By generating fusion proteins to the basic leucine zipper (bZIP), and members of Rel transcription factor families to YN and YC, they identified intracellular locations where the association of these proteins occurs. By employing different *Aequorea* GFP variants, such as GFP, CFP, and BFP, Hu and Kerppola further extended this technique to multi-color BiFC, which permits direct visualization of multiple protein interactions within the same cell and allows for the comparison of complex formation efficiencies with different interacting partners [25]. The color range available for BiFC has been extended to red with the development of an improved monomeric red fluorescent protein (mRFP1-Q66T) that is amenable to fragmentation [26]. Furthermore, the efficiency of BiFC has been greatly improved [27] by using newly-identified FP fragments derived from Venus [28] and Cerulean [29], which are *Aequorea* GFP variants that show fast maturation.

The association of FP fragments in BiFC has been thought to be irreversible, although a unique BiFC system with reversibility has been reported [30]. A potential drawback of this irreversible assay is that the interaction of the fused proteins may also be irreversible. This could interfere with the cellular physiological state of the system and impede the investigation of dynamic protein interactions. However, the major drawback of the technique also confers a major advantage; irreversible binding makes BiFC a highly sensitive assay. It may allow for the visualization of transient or low affinity interactions, such as those between enzymes and substrates. The power of this sensitivity may also be harnessed to obtain integrated fluorescence signals for protein-protein interactions that occur prior to imaging. This feature may be particularly useful for studying biological events transpiring in deep regions such as tissue in the brain. If a monomeric version of fluorescent timer proteins can be compatible with fragmentation and reconstitution, BiFC using the protein will permit studies that aim to examine the temporal aspect of protein-protein interactions [31] (Fig. 6B).

Acknowledgements

I thank Drs. Hideaki Mizuno, Satoshi Karasawa, and Takako Kogure for preparation of figures, and Dr. David Mou for critically reading the manuscript.

Literature:

[1] Tsien, R. Y. Annu. Rev. Biochem. 67, 509–544 (1998).
[2] Miyawaki, A. Neuron 48, 189–199 (2005).
[3] Miyawaki, A. Dev. Cell 4, 295-305 (2003).
[4] Kim, S. A., and Schwille, P. Curr. Opin. Neurobiol. 13, 583–590 (2003).
[5] Kerppola, T. K. Nat. Rev. Mol. Cell Biol. 7, 449–456 (2006).
[6] Hwang, L. C., and Wohland, T. J. Chem. Phys. 122, 114708 (1–11) (2005).
[7] Heinze, K. G., et al., P. Proc. Natl. Acad. Sci. USA 97, 10377–10382 (2000).
[8] Patterson, G. H., and Piston, D. W. Biophys. J. 78, 2159–2162 (2000).
[9] Kogure, T. *et al.*, Nat. Biotechnol. 24, 577–581 (2006).
[10] Ando, R., *et al.*, A. Proc. Natl. Acad. Sci. USA 99, 12651–12656 (2002).

Author Biography

Atsushi Miyawaki received his M.D. in medicine at Keio University School of Medicine in 1987 and his Ph.D. in signal transduction at Osaka University School of Medicine in 1991 (Dr. Katsuhiko Mikoshiba). He served as a researcher and then an assistant professor in the Institute of Medical Science, the University of Tokyo from 1991 to 1998. His main research was focused on calcium signaling. He also joined Department of Pharmacology (Dr. Roger Y. Tsien), the University of California, San Diego as an HFSP long-term fellowship and a research pharmacologist from 1995 to 1998, to work on technological innovations in fluorescence imaging. In 1999, after returning to Japan, he set out a laboratory, Laboratory for Cell Function Dynamics at Brain Science Institute (BSI) of RIKEN. From 2004 he has been directing Advanced Technology Development Group of BSI.

Contact:

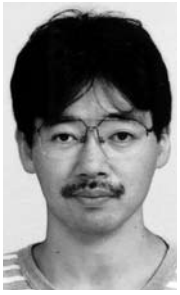

Atsushi Miyawaki, MD, PhD
Group Director
Advanced Technology
Development Group
Laboratory Head
Cell Function Dynamics, Brain
Science Institute, Riken, Japan
Tel.: +81 484 675917
matsushi@brain.riken.jp
http://cfds.brain.riken.jp/mta.html

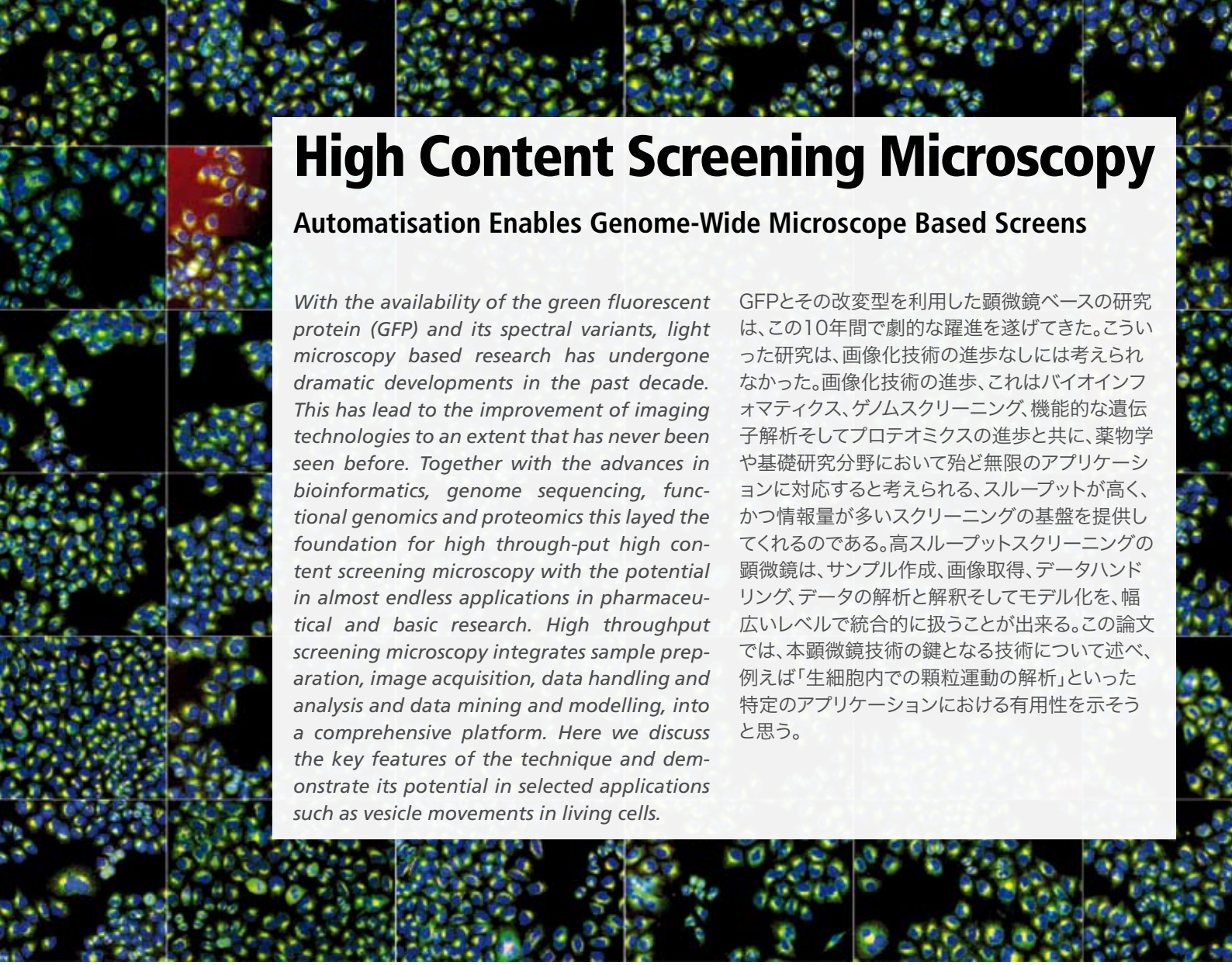

High Content Screening Microscopy

Automatisation Enables Genome-Wide Microscope Based Screens

With the availability of the green fluorescent protein (GFP) and its spectral variants, light microscopy based research has undergone dramatic developments in the past decade. This has lead to the improvement of imaging technologies to an extent that has never been seen before. Together with the advances in bioinformatics, genome sequencing, functional genomics and proteomics this layed the foundation for high through-put high content screening microscopy with the potential in almost endless applications in pharmaceutical and basic research. High throughput screening microscopy integrates sample preparation, image acquisition, data handling and analysis and data mining and modelling, into a comprehensive platform. Here we discuss the key features of the technique and demonstrate its potential in selected applications such as vesicle movements in living cells.

GFPとその改変型を利用した顕微鏡ベースの研究は、この10年間で劇的な躍進を遂げてきた。こういった研究は、画像化技術の進歩なしには考えられなかった。画像化技術の進歩、これはバイオインフォマティクス、ゲノムスクリーニング、機能的な遺伝子解析そしてプロテオミクスの進歩と共に、薬物学や基礎研究分野において殆ど無限のアプリケーションに対応すると考えられる、スループットが高く、かつ情報量が多いスクリーニングの基盤を提供してくれるのである。高スループットスクリーニングの顕微鏡は、サンプル作成、画像取得、データハンドリング、データの解析と解釈そしてモデル化を、幅広いレベルで統合的に扱うことが出来る。この論文では、本顕微鏡技術の鍵となる技術について述べ、例えば「生細胞内での顆粒運動の解析」といった特定のアプリケーションにおける有用性を示そうと思う。

Keywords:

fluorescence microscopy, genome-wide screening, green fluorescent proteins, automatisation, image analysis

Introduction

In the past decade, light microscopy technology has undergone dramatic developments. With the availability of the green fluorescent protein (GFP) and its spectral variants, fluorescent labeling of virtually every protein encoded by the genome of a species under view is in principle possible [1]. This has stimulated systematic approaches that aim e.g. at the determination of the localization and dynamics of the proteins of an entire proteome (see review by [2]). An almost endless number of GFP-based reporter systems that read out biochemical reactions such as protein-protein interactions or post-translational modifications in living cells have been designed [1]. In parallel to these improvements in the fluorescent labeling of molecules in living specimens, advanced light microscopy methods such as fluorescence recovery after photobleaching (FRAP), fluorescence resonance energy transfer (FRET) or fluorescence correlation spectroscopy (FCS) have been further developed and can now be much easier and more efficiently performed than ever before [3]. These methodological advances in light microscopy have also been fertilized by the continuous developments and improvements of commercially available or custom built imaging equipment, including for example confocal laser scanning microscopy, total internal reflection fluorescence (TIRF) microscopy or fluorescence lifetime imaging (FLIM). New developments such as the single plane illumination microscopy (SPIM), photoactivated localization microscopy (PALM) or high-resolution microscopy such as STED offer now completely new light microscopy applications. Not least the continuous increase in performance of computer technology, that is essential for the control of imaging hardware, data storage and image analysis software packages, contributed significantly to the developments in light microscopy technology.

Coincidently with these improvements in light microscopy, genome sequencing, functional genomics, proteomics and bioinformatics techniques have equally fast developed in the past decade and generated a wealth of information and reagents. With these means at hand, the remaining challenge is now to integrate all this genomic and proteomic information into a physiological context of

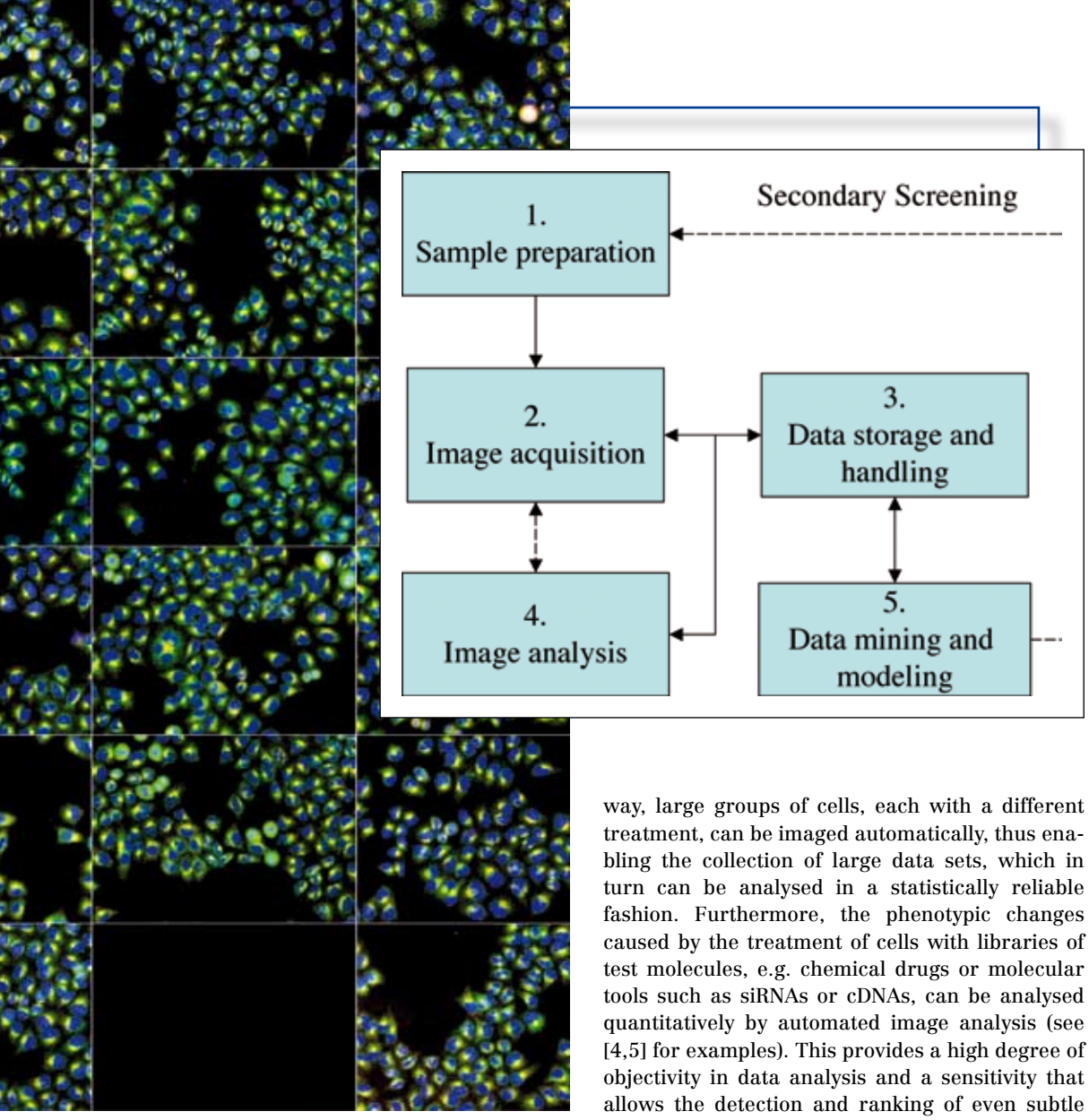

Fig. 1: The key steps in high-content screening microscopy. A high-content screening microscopy experiment comprises at least five different steps: (1) Sample preparation, (2) image acquisition, (3) data storage and handling, (4) image analysis and (5) data mining and modelling. Automated sample preparation in 96 or 384 well plates includes cell transfections, drug delivery, fixation and staining of the sample. These steps are typically conducted by liquid handling robotics. Several automated widefield and confocal microscopes linked to appropriate data storage and handling systems are commercially available for image acquisition (Table 1). Image processing is central for each high-content screening microscopy approach and needs to be adapted for each new assay that is developed. Therefore, it is currently a bottleneck of the technology. The huge amount of data generated in a screening project requires the linking of sample preparation, image acquisition and results from image analysis as well as quality control analysis in a project database. In this way, the project's results can also conveniently be combined with bioinformatic analyses and data models can be generated. These models will identify candidate reagents or genes that may be subjected to more detailed and more complex secondary screening experiments. In such secondary experiments image analysis could be performed online during image acquisition with the aim to identify objects of interest in the sample that thereafter may be subjected to time consuming high resolution 3D imaging.

living cells or model systems with the aim to develop new strategies for diagnostics and cures for serious human diseases such as cancer or viral infections. In order to achieve this goal, quantitative and large scale analyses in living cells or organisms is required. One such method is fluorescence microscopy, which has only recently been demonstrated that it could be used to complement genomic and proteomics approaches in physiologically relevant systems (see e.g. [4,5, 10]).

High Content Screening Microscopy

Applying fluorescence microscopy at large scale needs a considerable degree of automation of all the steps involved in an experiment. These are sample preparation, image acquisition, image analysis, data storage and handling as well as data mining and modelling (Fig. 1). Such automated fluorescence microscopy enables unsupervised data collection with high information content on the temporal and spatial distributions and states of fluorescent markers (see review by [6]). In this way, large groups of cells, each with a different treatment, can be imaged automatically, thus enabling the collection of large data sets, which in turn can be analysed in a statistically reliable fashion. Furthermore, the phenotypic changes caused by the treatment of cells with libraries of test molecules, e.g. chemical drugs or molecular tools such as siRNAs or cDNAs, can be analysed quantitatively by automated image analysis (see [4,5] for examples). This provides a high degree of objectivity in data analysis and a sensitivity that allows the detection and ranking of even subtle phenotypes, which could easily be missed by manual data evaluation. Several automated fluorescence light microscopy systems and image analysis software packages for large-scale screening and high information content microscopy analyses are available commercially or as open source and are listed in Table 1 and Table 2, respectively. In addition to these dedicated high throughput microscope systems, many current confocal and widefield systems, are equipped with hardware and software that allow, systematic scanning of samples and thus even multi-position time-lapse microscopy in living cells. Although complete automatisation may not be possible with such systems, as essential components such as automated focus identification are lacking, they are very instrumental in acquiring systematic image data at a low throughput.

Assay Development and Sample Preparation

One of the key steps in high content screening microscopy is the development of an appropriate microscopy read out (assay) that reports quantita-

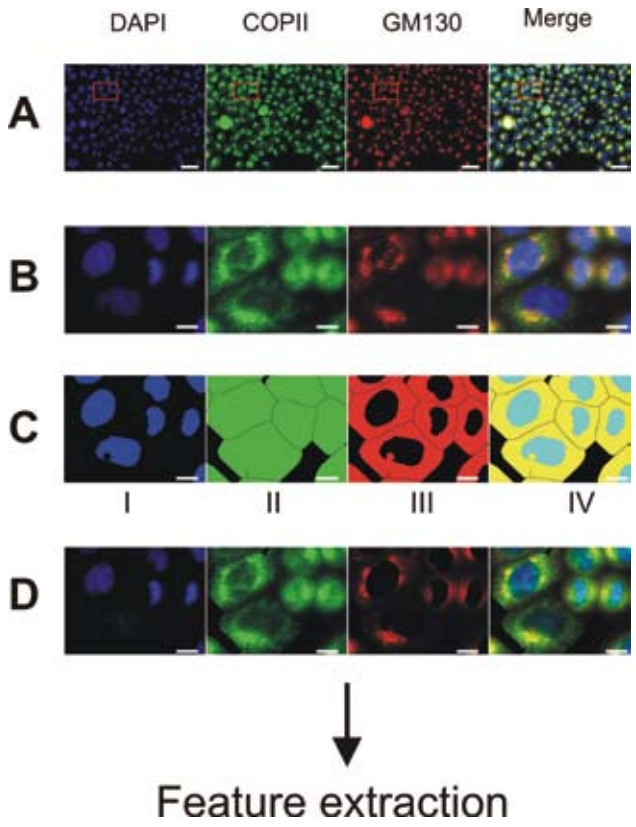

Fig. 2: Example for quantitative image analysis in high content screening microscopy.
HeLa cells were reverse transfected in LabTek tissue culture dishes (see Fig. 4) for 48h and subsequently fixed and stained for cell nuclei (using DAPI, blue), the vesicular coat complex COPII (Alexa 488, green) and the Golgi complex marker GM130 (Cy3, red). Subsequently samples were imaged with a Zeiss Cellobserver HS. The objective used was an LD-Plan Neofluar 40x/0.6 Korr. Ph2. Autofocussing was done on the DAPI channel with a software-based approach implemented in the Axiovison software. The existing offset between the focal planes of the nucleus and the other compartments was determined manually on several cells before the imaging session was started. The mean of these offset values was taken as the offset between the focal plane for the DAPI staining and the other cell compartments. Exposure times were 20 ms for the DAPI channel, 200 ms for the ALEXA488 and 800 ms for Cy3channel. The complete LabTek could be imaged within less than two hours.
To image all the cells in each of the 384 spots (diameter of 400 µm, see Fig. 4) of the LabTek dish, four partially overlapping images were taken and stitched together afterwards. In (A), the four stitched images are shown. Scale Bars=50 µm. In (B), magnifications of the areas highlighted by the red box in (A) are shown. Scale Bars= 10 µm. (C) Image analysis: To automatically identify the cell locations and their boundaries, images are first low pass filtered and then cell nuclei are identified in the DAPI channel using single threshold techniques (I). After subsequent image processing steps including dilation and a watershed algorithm, the cell boundaries are determined (II) leading to the generation of four different digital masks (cell nuclei (I), the entire cell including nuclei (II), cytoplasm (III) and nuclei and cytoplasm (IV)). Multiplication of these digital masks with the images shown in (B) returns images with signals of the regions of interest in individual cells only (shown in D). From these images and for each of the channels a number of object features (e.g. intensity, contrast, shape, etc.) are finally extracted. In this way, a multidimensional feature "space" can be defined and quantitatively determined for each object in the image and for each spot on the LabTek dish, which is then used to discriminate between different morphological phenotypes obtained (see [4,8]).

tively on the feature of interest, e.g. cell growth, protein secretion, speed of cell division or organelle movement, and can be completely automated for large scale analyses. Such assays are mostly based on well-established experimental set-ups that have already been used and tested in small-scale experiments. Nevertheless, they have to be adapted and tested for high throughput image acquisition and automated image data analysis, which may cause increased experimental errors compared to small scale, well-controlled manual experiments. Examples for two assays are shown in figure 2 and figure 3. While automated image acquisition protocols for different assays may often be very similar and solutions developed for one assay may be easily adapted to another one, image analysis of the data mostly requires considerable changes to existing solutions and very often completely new developments.

Sample preparation for imaging at high throughput requires a very high degree of reproducibility as data from different samples need to be compared quantitatively. Therefore, automated methods for cell transfections, drug delivery and, if required, cell fixation and fluorescent staining are typically carried out on liquid handling robots that can deal with the throughput required (see e.g. [5]). For this purpose cells are cultivated in multi-well tissue culture dishes with a glass bottom, which is compatible with high-resolution light microscopy which require objectives with short working distances and need immersion media for imaging. A very effective method for high throughput cell transfection with plasmid DNAs or siRNAs is reverse transfection of cells in LabTek tissue culture dishes (see [7] and Fig. 4). In this method, the reagents to be transfected are spotted onto the bottom of a LabTek tissue culture dish (step II in Fig. 4) onto which subsequently cells are seeded (step III in Fig. 4) and thus transfected at each place of a spot with the respective reagent. This miniaturization of the tissue culture format facilitates high throughput imaging considerably, one reason being that the demands for automatic focus identification are less time-consuming than in multi-well plates. Also, treatment of cells with drugs or staining of fixed cells (step IV in Fig.4) is much easier and does not require the use of expensive liquid handling robots (see [7] for further discussions).

Image Acquisition

Several microscope systems that are commercially available and are able to acquire images fully automatically exist (see Tab. 1). A key feature of these systems is the automated identification of the focal plane. In the case of confocal microscopes, identification of the optimum focal plane, which for example contains the maximum number

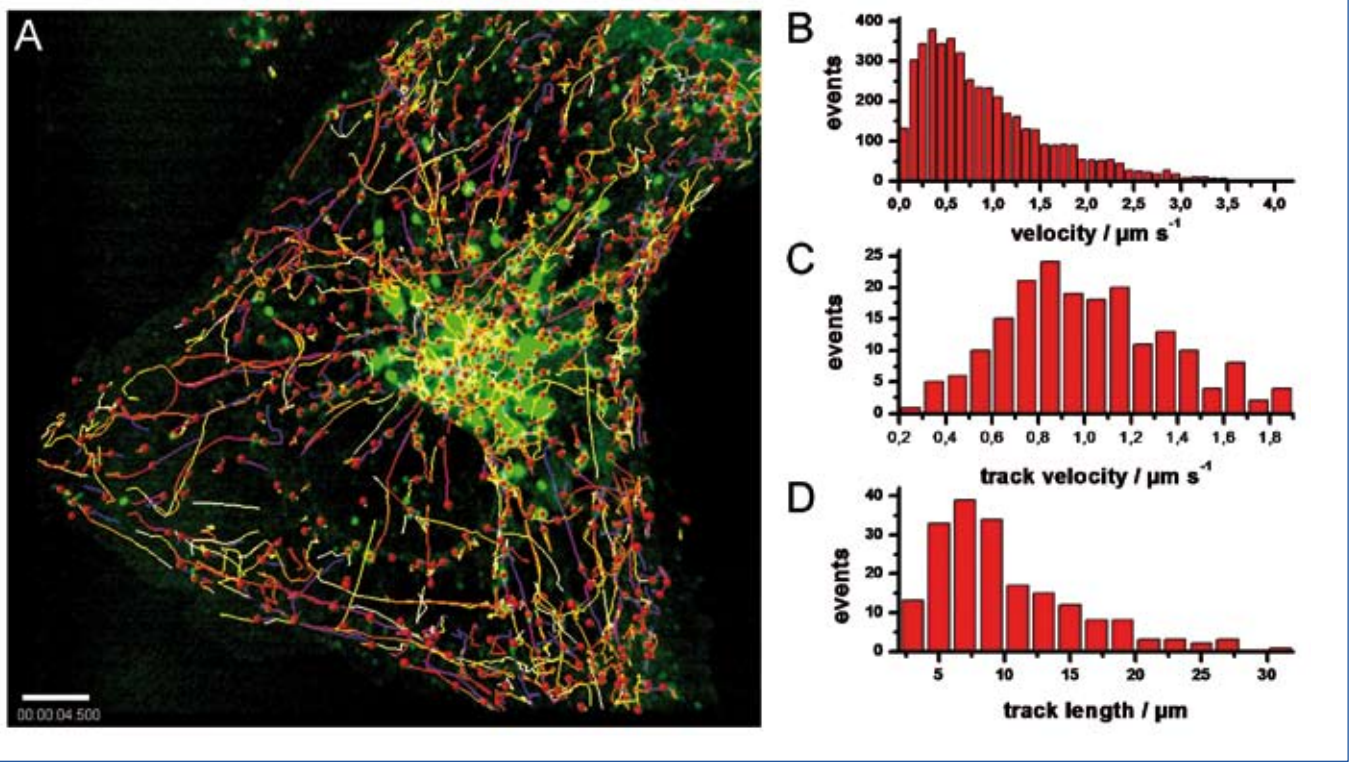

of objects of interest, is equally important. Examples of fixed cells stained with fluorescent antibodies and imaged automatically are shown in figure 2. In this example, cells have been counterstained with the DNA stain DAPI (Fig. 2A), which thus highlights cell nuclei. As this DAPI signal is usually very bright and shows very little cell to cell variations, it is often used to determine the plane of focus at each position and to identify the cell nucleus by simple image segmentation procedures (see legend to Fig. 2). A fixed offset from the cell-nuclei- determined focal plane is then used for the acquisition of the images for different cellular structures such as vesicular membranes or the Golgi complex, which reside predominantly in image planes different from the cell nucleus (Fig. 2). Depending on the number of different stainings in such samples, image acquisition may take up to 2h and even longer for the imaging of an entire 384 well plate. Automated image acquisition of living samples at high throughput has also been demonstrated recently [4]. An example of life cell imaging and automated quantification of organelle movement in single cells is shown in figure 3. As living cells suffer from repeated illumination that is required for automated focus identification, it is advisable to identify the focal plane of the specimens only once at the beginning of an imaging session and then repeat this procedure only if focus drift occurs in the sys-

Table 1: Examples of commercial high-throughput screening microscope systems

Name of instrument	Manufacturer
Live cell imaging possible	
IN Cell Analyzer 3000*	GE Healthcare, www.gehealthcare.com
Pathway HT*	BD Biosciences, www.bdbiosciences.com
Scan^R§	Olympus, www.microscopy.olympus.eu/microscopes/Life_Science_Microscopes_scan_R.htm
KineticScan§	Cellomics, www.cellomics.com
Opera*	Evotec Technologies, www.evotec-technologies.com
Cell Observer§	Carl Zeiss, www.zeiss.com
Live cell imaging not possible	
ArrayScan§	Cellomics, www.cellomics.com
Discovery§	Molecular Devices, www.moleculardevices.com
cellWoRx§	Applied Precision, www.api.com
Acumen Explorer	TTP LabTech, www.ttplabtech.com
iCyte	CompuCyte, www.compucyte.com
NDP	Hamamatsu, http://jp.hamamatsu.com/products/life-science/pd267/nzoomb/index_en.html
Cell Lab IC 100§	Beckman Coulter, www.beckmancoulter.com

*: Confocal microscopy
§: Widefield microscopy

Fig. 3: Example for automatic tracking and quantification of vesicle movement in living cells
HeLa cells expressing YFP-tagged vesicular stomatitis virus glycoprotein that moves from the endoplasmic reticulum to the plasma membrane in a temperature sensitive manner were imaged (see [10] for details). Images were acquired on a PerkinElmer Ultraview RS spinning disk confocal microscope with a PLAN-Apochromat 63x/1.4 NA oil immersion objective lens (Carl Zeiss) at time intervals of 300 ms between single images.
A, Overview of the tracks obtained by automatic tracking of 100 time-points using Imaris 5.7.2 (Bitplane) software package. Only spots above 0.65 µm in diameter were tracked by the autoregressive tracking module (parameters used were: maximum distance of 2 µm/frame and maximum gap of 1 time point). Only tracks longer than 10 time points and more than 0.4 µm of total displacement were chosen for display and quantification. Scalebar=10 µm.
B, Histogram of the velocities of all tracks at every time point derived from the time-lapse sequence described in (A).
C, Histogram of the average track velocities derived from the time-lapse sequence described in (A).
D, Histogram of the track length derived from the time-lapse sequence described in (A).
This figure is accompanied by Movies 1 and 2.

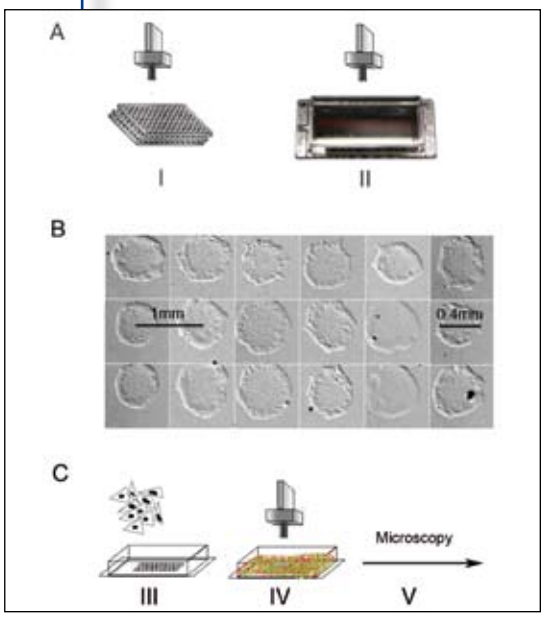

Fig. 4: Reverse transfection in LabTek culture dishes. Reverse transfection is a recent method to introduce material into tissue culture cells as it is required in high content screening microscopy experiments (see [7] for a comprehensive description). (A) In a first step all reagents required for transfection of cells (transfection reagent, gelatine, fibronectin and the material to be transfected) are mixed in 384 well plates. Thereafter, the reagents are spotted onto the bottom of glass bottom LabTek culture dishes using a commercially available DNA spotter. (B) Examples of images of the dried spots acquired with a Scan'R screening microscope equipped with a 10X objective. In our laboratory the spots have a size of 1mm and the inter spot distance is 400µm. (C) After the spotted samples have dried for a few days, cells can be plated onto them to become transfected only at the place of the spots. This generates 384 cell colonies with different transfections. Thereafter, samples are either directly subjected to microscopy or, if cells need to be fixed and stained, they will be prepared with standard laboratory equipment before they are placed onto a screening microscope.

tem. Some of the imaging systems listed in Table 1 use a combination of hardware and software auto focus identification. In these cases, the hardware auto focus procedure identifies the bottom of the cell support (e.g. glass bottom of a LabTek tissue culture dish) and subsequently moves a pre-defined offset into the sample to image the structures of interest. Focus optimization may then be achieved by acquiring a few images in different z-planes and then analyzing them with software auto focus procedures online. In this way, the total sample illumination time is significantly reduced and helps survival of the specimens during the time-lapse screening procedure.

Data Handling and Image Analysis

The amount of data acquired in high content screening microscopy projects very quickly reaches the several tens of terabyte range. This is the case in particular when time-lapse data or image stacks over the entire depth of the sample are acquired. Depending on the subsequent way images are to be analysed, image compression may help to save storage space. Because of this huge amount of image data to be analysed, any speed optimization of the image analysis routines used are an advantage. The use of multiprocessor computer systems for analysis may also help to overcome the problem.

Of particular importance in high content screening microscopy is the development of image analysis algorithms that return quantitative data in a reliable manner. Very often, fluorescence intensities are compared as readout of the assay. In these cases, image analysis is straightforward, and commercially available solutions as they are delivered together with the imaging systems (see Table 1) or as stand alone image analysis software (see Table 2) can be used for analysis. However, many interesting questions that aim to exploit the unique strength of the microscopy-based screening rely on the description of complex cellular patterns that will change under different treatments of cells. One strategy to address this problem is exemplified in figure 2 (see also [4,8]). In this approach, images are first processed and background corrected and objects automatically recognized. Thereafter, several user defined object features are calculated for each object and used to discriminate different morphological phenotypes from each other. Images showing particular morphological phenotypes may be pre-defined by the user to determine the phenotype specific values of the associated features and their cell-to-cell variations. With such "training information" the pre-defined morphological phenotypes, as they occur in the images of the actual screening experiment, can be discriminated with high precision ([4, 8]). A drawback of this approach is that phenotypes that have not been trained may be associated with the closest pre-defined phenotype and are thus not properly classified. A further important limitation of this else very powerful analysis approach is that it is sensitive to variations of the imaging conditions during the screening. Such variations can be introduced by intensity fluctua-

Table 2: Examples of image analysis packages suitable for the development of high throughput image data analyses

Name of software package	Manufacturer	More information at:
Cellenger	Definiens	http://www.definiens.com/
Axiovision	Carl Zeiss	http://www.zeiss.com/micro
MetaMorph	Molecular Devices	http://www.moleculardevices.com/
Scan'R	Olympus SIS	http://www.olympus-sis.com/
Acapella	Evotec Technologies	www.evotec-technologies.com
Imaris	Bitplane	www.bitplane.com
Cell Profiler	Open source	http://www.cellprofiler.org/
BioConductor	Open source	http://www.bioconductor.org/
Image J	Open source	http://rsb.info.nih.gov/ij/

tions of the excitation light source in fluorescence microscopy or changes in the optical or detector system during the course of the screening project.

Data Mining and Modeling

The huge amount of data generated by a high content screening project including information about reagents and sample preparation, raw image data and results of the image analyses requires an integration of all these parameters into a database that can be easily queried. Such databases, if accessible via WEB browsers, are also an important tool to make the data and results generated accessible to the community. Databases are also compatible with the bioinformatics information available on the reagents used in the screening experiments or the genes associated. This allows combining the results of the screening project with pre-existing data.

Conclusions and Outlook

High-content screening microscopy is an emerging technology that has numerous applications in basic research and drug development. Quantitative fluorescence microscopy-based multi-parameter analyses at high throughput will provide the opportunity to conduct analyses at the systems-level in order to understand how biological entities are formed and function. Although high-content screening microscopy has all these promises, it still poses serious challenges for the future. Considerable hardware and image analysis software developments are needed before work with living cells will become a routine high-throughput technology at the time resolution required. Also, exploitation of powerful fluorescence microscopy techniques such as fluorescence resonance energy transfer (FRET), fluorescence correlation spectroscopy (FCS) or fluorescence recovery after photobleaching (FRAP) (see [9] for review) in high-throughput still needs to be developed.

Acknowledgements

We thank Brigitte Joggerst and Dr. Jeremy Simpson for providing the samples used to generate the data shown in figures 2 and 3. We thank Dr Vito Smolej and Dr Markus Neumann from Carl Zeiss Imaging Solutions GmbH for their support of generating data and results shown in figure 2. The authors would like to acknowledge funding by the German Federal Ministry of Education and Research (BMBF) in the framework of the National Genome Research Network (NGFN) (NGFN-2 SMP-RNAi, FKZ01GR0403 and NGFN-2 SMP-Cell FKZ01GR0423, NGFN-1 FKZ01GR0101, FKZ01KW0013.). Further support by the Landesstiftung Baden Wuerttemberg in the research programme "RNS/RNAi" is acknowledged. We also apologize to our colleagues for the numerous work in the literature that we could not cite in this article due to space limitations.

References

[1] Giepmans BN, et al., Science 312, 217–224 (2006).
[2] Simpson J., et al., Genome Biol. 8, 211 (2007).
[3] Presley J. Biochim Biophys Acta, 10, 259–272 (2005).
[4] Neumann B. et al., Nat Methods 3, 385–390 (2006).
[5] Pelkmans L et al., Nature 436,78–86 (2005).
[6] Pepperkok R. and Ellenberg J., Nat Rev Mol Cell Biol. 7, 690–696 (2006).
[7] Erfle H. et al., Nat Protoc. 2, 392–399 (2007).
[8] Conrad C. et al., Genome Res. 14, 1130–1136 (2004).
[9] Bastiaens P.I. and Pepperkok R., Trends Biochem Sci. 25, 631–637 (2000).
[10] Starkuviene V. et al., Genome Res. 14, 2004 1948–1956 (2004).

Author Biography

Rainer Pepperkok studied physics at the University of Heidelberg from 1982 to 1988. He finished his PhD studies in 1992 in cell biology at the University of Kaiserslautern, Germany. For his postdoctoral work, he joined the group Prof. Dr. T Kreis at University of Geneva, Switzerland. He was lab head at the Imperial Cancer Research Fund, London, UK, between 1996 and 1998. He has been team leader of the advanced Light Microscopy Facility (ALMF) at EMBL Heidelberg, Germany, since 1998.

Contact:


Dr Yury Belyaev


Dr Stefan Terjung


Dr Arne Seitz


Dr Rainer Pepperkok

Dr Arne Seitz
Dr Stefan Terjung
Dr Yury Belyaev
PD D Rainer Pepperkok
Teamleader Advanced
Light Microscopy Facility
Cell Biology Cell Biophysics Unit
Heidelberg
Tel.: + 49 6221 387 0
pepperko@embl.de
www-db.embl.de/jss/EmblGroupsHD/g_50.html and
http://www.embl.de/almf/

Zoom-in Beyond Light Microscopy

A New Approach for Biological Structure Research – Correlative Light and Electron Microscopy on one and the Same Sample

The structure researchers dream to fly through several orders of magnitudes in scale on the identical pre-selected sample area has become realistic with the establishment of a new freeze-substitution protocol after high pressure freezing. Samples prepared in such a way allow in a multimodal approach to choose between LM (FLM, CLSM) and EM (SEM, FIB/SEM, TEM) imaging modes for structural studies of complex tissue and cell structures. One and the same structure can now be investigated at mm to nm range in 2D and 3D.

生物の構造を研究する人たちは、高圧凍結法後に生み出された新しいサンプル作成法によって得られるようになった観察領域を、様々な観察倍率で自由に飛び回る（観察する）事を夢見ることが出来るだろう。この方法で作成したサンプルは、複雑な組織や細胞構造のイメージングに用いられる「光学顕微鏡やレーザ顕微鏡」と、「*SEM*、*FIB/SEM*、*TEM*などの電子顕微鏡」でのスケールの間隙を、様々な観察倍率で行える。同一の構造観察が、今や*mm*から*nm*レベルで*2*次元*3*次元イメージング、解析が可能となったのである。

Keywords:

correlative microscopy, 3D microscopy, high pressure freezing, freeze substitution, block-face, FIB/SEM

Introduction

Qualitative evaluation of the cellular complexity and structural integrity of tissue samples, e.g. skin biopsies, had been used by scientists for decades to gain insight into structure and function of complex organs. The well-accepted correlation between the tissue structure and its function conveys fundamental knowledge for the development of experimental models for the study of normal and – in the framework of experimental scenarios – specifically altered or treated tissue. The implementation of physiologically relevant models has made it possible to study the intrinsic cell regulation pathways. Furthermore, it has provided compelling evidence for the role of e.g. certain skin compartments in directing cellular function in dysfunction.

In order to translate the findings from basic cellular research into a holistic understanding of the tissue, all biopsy-based system investigations need the absolute preservation of the 3D-organisation and the multi-cellular complexity of the tissue.

The reason why the 3D tissue comes more and more into the focus of systems-biology is that there is a big difference between a flat layer of cells and a complex, three-dimensional tissue. But until recently, many scientists have glossed over this fact.

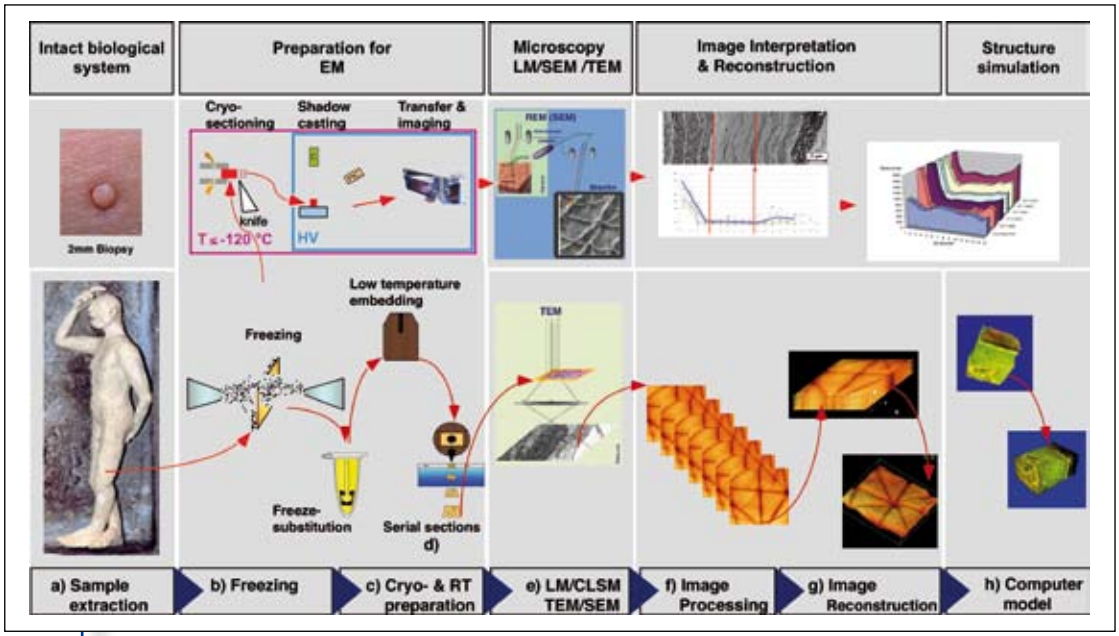

Fig. 1: Flow process chart and scheme of the "information-transfer-chain" for microscopic investigation of tissue biopsies: a) A life-like and environmental sampling of biomaterial e.g. microbiopsies b) Freezing this material in milliseconds, thus trapping dynamic cellular processes and functional hydrated states; in the case of complex material this is only possible by high pressure freezing c) Preservation of the native molecular arrangement of biomaterial by cryo-preparation and cryo-transfer techniques d) Serial sectioning of freeze-substituted and low temperature embedded material e) Direct or tomographic imaging in the light or electron microscope at high resolution f) Section alignment and structure rendering for digital processing g) 3D-reconstruction and h) 3D-model analysis, interpretation and simulation

In addition the recent elucidation of the complete genomes of several organisms, including that of humans, has increased our awareness that most interactions in cells and tissues take place not simply on the level of single macromolecules, but within the framework of extended higher order structures. Additional to this high structural complexity, there is a complex feedback context of organelles and cells, e.g. the differentiated layered cell groups assembling the epidermis in human skin, which functions in a highly coordinated manner. How essential this context information is, becomes even clearer, if we investigate the highly efficient skin barrier itself. This most efficient barrier structure in nature is formed after the cells went through apoptosis. Its formation is completely controlled by self-assembly – i.e. all the essential molecules have been delivered at the life-death transition zone. In this article, we give a brief overview how such complex structures can be studied by taking advantage of applying state-of-the-art correlative light and electron microscopy approaches (1).

A Dream…

The structure researcher's dream – in order to study a complex morphological context in its native functional state – is an imaging tool, which allows *in vivo* continuous zooming-in from a millimetre (mm) scale down to a few nanometres (nm) at different tissue levels. Due to the physical limitation of the excitation wavelength, such a device will never exist, because it would have to cover wavelengths from hundreds of nanometres (photons, ultrasound) to sub-nanometer (electrons). Thus, the structure-researcher faces a methodological problem, if he wants to study a tissue like skin on a large resolution and information level scale.

This problem has been partially solved by establishing preparation techniques, which allow investigating the same tissue biopsy with different imaging techniques and hence circumvent the physical limitation by using a multimodal imaging strategy on optimally preserved tissue samples (2). Although cryo-immobilisation by high pressure freezing provides the best structural preservation (3,4), it is used routinely only for electron microscopic (EM) investigations, while, unfortunately, for light microscopy (LM) chemical fixation protocols or simplified cryo-fixation protocols (e.g. Fig. 2a+b) have been established. These chemically invasive fixation protocols have the drawback of introducing unpredictable fixation artefacts (3,5,6). Therefore, comparative histological (i.e. LM) and ultrastructural (i.e. EM) results are usually obtained from different samples that have not been prepared identically and never by examining exactly the same features. To overcome these handicaps, we have modified the well-established freeze-substitution technique (FS), allowing the investigation of resin-embedded cryo-immobilised tissue by confocal laser scanning microscopy (CLSM) prior to EM examination (2). Thus, selected cells can be depicted throughout the whole tissue block by CLSM (2, Fig. 3 & 5) and subsequently, they can be selectively prepared by targeted sectioning for follow-up investigation of the identical structure by TEM.

Here we would like to show that, with this approach, the dream of a structural analyst to zoom through several orders of magnitude in scale on one an the same sample area becomes partially true. And we would also like to describe what kind of knowledge and coherent context information

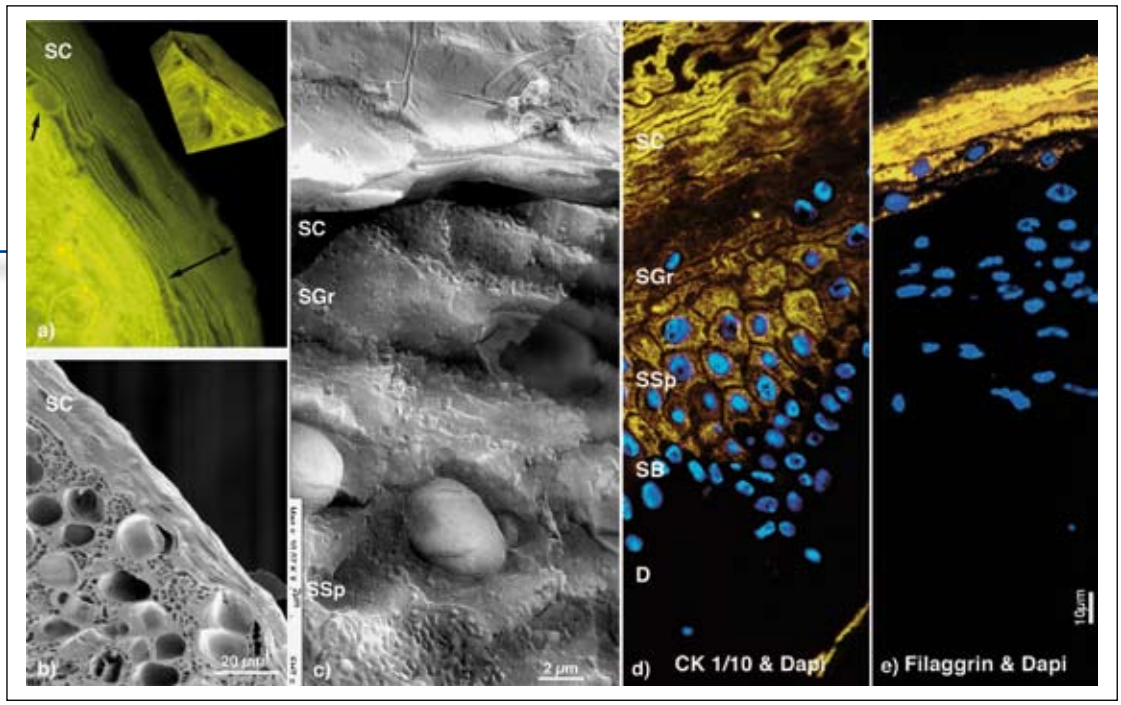

Fig. 2: Structure preservation and information depth of human skin biopsies viewed fully hydrated with cryo-SEM or after freeze substitution after immunocytochemical staining with LM.
a+b) liquid nitrogen frozen biopsy cross-section imaged a) with a CLSM after nile red staining or b) with a cryo-scanning electron microscope (cryo-SEM) c-e) high pressure frozen human skin biopsies imaged c) with a cryo-SEM at about -120 °C or d-e) with a LM after freeze substitution, thin sectioning, labelling against different antigens (cytokeratin 1/10, Filaggrin) and DNA (Dapi) . Due to the better time resolution, better epitope preservation and better structure preservation of biopolymers by high pressure freezing, images with a very high information density and with a higher precision in localization of epitopes (stratum corneum (SC), stratum granulosum (SGr), stratum spinosum (SSp) can be generated

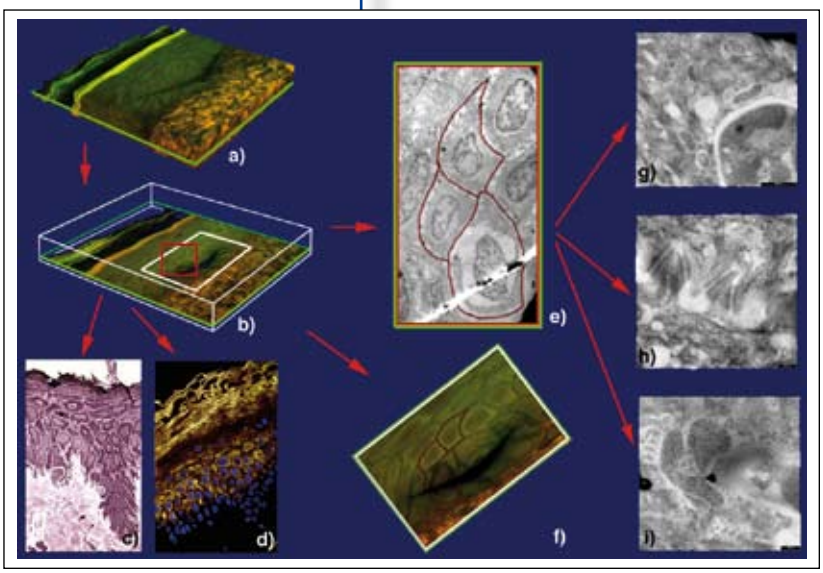

Fig. 3: Scheme of the imaging strategy in the case of high pressure frozen, freeze substituted and embedded skin biopsies: one sample for multimodal imaging . After embedding and preparation of a plain block-face through the skin sample in the polymer matrix, the specimen can first be examined by CLSM in 3D (a, b+f) prior to further preparation steps. Selected sections of defined planes from the embedded biopsy can be depicted and either stained for histological or immuno cylological investigations (c+d) or areas of interest (a+b green layerlines) can be depicted and prepared for TEM examination (e-i). Such samples are optimal for histological investigations (Fig. 3 c+d), for investigating complex 3D-tissue structures by confocal light microscopy (Fig. 3 a, b+e) as well as for describing ultrastructure and constituents of the identical cells by electron microscopy (Fig. 3 f-i).

such a multimodal imaging approach offers to a research community, e.g. dermatology. Due to the complexity of the different imaging and preparation techniques we only show the major route and refer to literature for more details.

General Preparation Strategy: An "Information-Transfer Chain"

The challenge we have to face is that we deal with a biological, dynamic and hydrated specimen, which needs constant environmental conditions to avoid changes of the morphological context during manipulation, preparation and imaging (5, 6). Therefore, the gap between basic histology and high-resolution electron microscopy, which is the method of choice to analyse and understand the nano-organization of life-like biological material in context (7), can only be closed by a dedicated and careful preparation. Our goal is to use the information obtained by EM analysis for the investigation and description of the biological nano-molecular organisation on the basis of intact cells and tissues at a defined differentiation state, and still explore these structures in their natural context.

This can only be reached by cryo-immobilisation and cryo-processing techniques that vitrify the cellular water (3,5,7), simultaneously rapidly arresting all physiological processes and preventing artefact-induced changes during specimen processing. Routing techniques to put this goal into practice are given in figure 1, which briefly shows the "information-transfer chain" for investigation of e.g. human skin biopsies: a) Life-like and environmental sampling of biomaterial, e.g. microbiopsies. b) Freezing this material in milliseconds, thus trapping dynamic cellular processes and functional hydrated states; in the case of complex material, this is only possible by high pressure freezing. c) Preserving the native molecular arrangement of biomaterial by cryo-preparation and cryo-transfer techniques. d) Serial sectioning of freeze-substituted and low temperature embedded material. e) Direct or tomographic imaging in the light or electron microscope at high resolution. f) Section alignment and structure rendering for digital processing. g) 3D-reconstruction and h) 3D-model analysis, interpretation and simulation. For more details on critical steps in the "information-transfer chain" see figure 1.

Structure Preservation and Information

Figure 2 shows the gain in structural context after high pressure freezing (HPF) of human skin biopsies (Fig. 2c,d,e) compared to standard rapid freezing techniques being routinely used for LM such as plunge freezing in liquid nitrogen (Fig. 2 a+b) or freezing on solid carbon dioxide. Figure 2b shows a liquid nitrogen frozen biopsy cross-section imaged using a cryo-scanning electron microscope (cryo-SEM) after the water had been removed by freeze-drying. Holes are revealed in the tissue where water had segregated from the biological tissue in order to form ice crystals during the freezing process (8). These holes are surrounded by compressed biological matrix and therefore resemble an artificial organisation of the biological tissue with huge delocalisation of bio-molecules. Due to the "grace of the low resolution power", even in confocal light microscopy (CLSM) images one is not directly aware of the structural changes induced by freezing, except if one considers that this skin cryo-section was stained with a lipophilic stain (nile red – Fig. 2a). Nile red should only stain lipid containing areas between the Corneocytes (50-100 nm) in the Stratum Corneum (SC) as shown in detail in figure 4, but it should not be spread in the intercellular space nor in the cytoplasm in viable cell layers of the epidermis as extensively as shown in figure 2a. Nevertheless, it allows a wonderful description of the Corneocyte stacking in the SC.

Due to the better time resolution, better epitope preservation and better structure preservation of biopolymers by high pressure cryo-fixation (4,9), images with a very high information density can be generated with a more precise localisation and identification of specific molecules by immunocytochemical labelling inside an intact nano-morphology for light microscopic (Fig. 2d+e) as well as for electron microscopy investigations (see Fig. 2c; 3 and 4). Figure 2c shows a high pressure frozen and freeze fractured skin biopsy and therefore reveals the compactness and the complexity of the outermost layers of human epidermis in its frozen hydrated native state. Note that there are neither holes nor areas without fine structural details – thus it reflects the native nano-bio-organisation of the tissue at the time-point of tissue extraction and immobilisation. This cellular complexity can

only be further investigated either with the help of high resolution SEM imaging by morphological identification of macromolecular complexes, or by freeze-substitution and identification of single antigens with the help of antibodies. The second approach may also be taken after the tissue has first been investigated in a cryo-SEM or immediately after high pressure freezing as described in more detail in Figure 3 and in Biel et al. (2,10).

One Biopsy for Multimodal Imaging – the Principle

A detailed structural investigation of skin biopsies requires the coupling of optimal structural preparation of arrested frozen samples with preserved detailed information, gained by high pressure freezing, with image collection at both, the light and electron microscopic level. In order to overcome the handicap of comparing data derived from differently prepared samples as well as to introduce the superior structural preservation of HPF into LM investigations, we have developed a new freeze-substitution protocol (2) suitable for LM and EM investigations (Fig. 3).

The well-established freeze-substitution technique (FS) was modified, to allow the investigation of resin-embedded cryo-immobilised tissue by LM or CLSM prior to EM examination. This is facilitated by the addition of specific fluorescent dyes during the first freeze-substitution exchange step. Selective binding properties of various dyes to different cellular structures allow a direct histological description of the tissue at the light microscope level (for more detail see 3) or preserve intrinsic fluorochromes, e.g. GFP. After embedding and preparation of a plain block-face through the skin sample in the polymer matrix, the specimen can first be examined by CLSM (Fig. 3 a, b + f) or sections may be taken (Fig. 3 c+d) for histological or immunological investigations. For areas of interest, the depth in the resin block is determined with the help of the CLSM (Fig. 3 a+b, green layerlines) followed by removal of the tissue lying above with an ultramicrotome. Now, the tissue can be cut into a series of ultrathin sections and examined by TEM for determination of the sub-cellular and nano-structural organisation in 2D (Fig. 3 e, g-i) and/or 3D. Samples prepared like this turned out to be optimal for histological investigations (Fig. 3 c+d), as well as for the investigation of complex 3D-tissue structures by CLSM (Fig. 3 a, b+e), and for a description of the ultrastructure and the constituents of the identical cells with electron microscopy (Fig. 3 f-i).

This approach allows cells throughout the whole tissue block to be depicted by CLSM (white and red box in Fig. 3 b) and subsequently to be selectively prepared by targeted sectioning for follow-up investigation of the identical structure by TEM (Fig. 3 e+f).

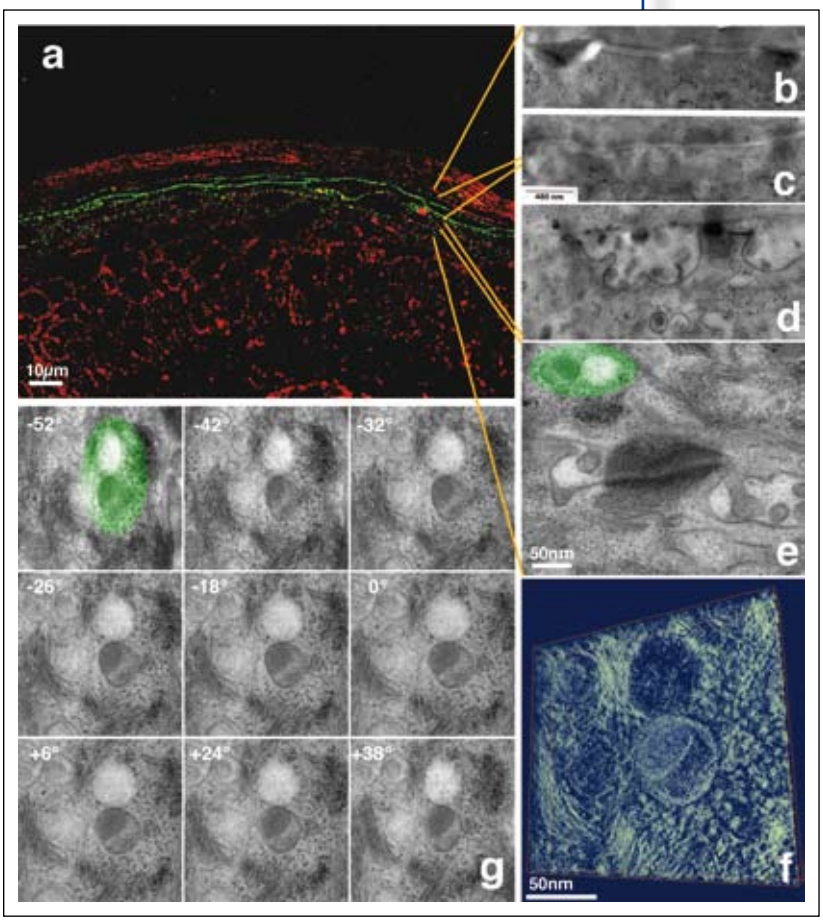

Fig. 4: Lipid layers in human skin imaged after high pressure freezing and freeze substitution a) Antibodies were used against a Ceramide (red) and its glucosylated precursor (green) on semi-thin sections (200 nm) to show that the various lipid species can be specifically localised after cryo-preparation. The antibodies were detected with a fluorescence-labelled secondary antibody and visualised with the help of a CLSM. In order to study the organisation of the lipids at the molecular level, sections were taken for electron microscopy (b-e). b) shows an area from the SC with desmosomes and lamellar lipids in the intercellular space, c+d) an area of the last layer of the SGL with vesicular structures in the intercellular space. e) shows an area in the SGL. A lipid vesicle is highlighted in green, corresponding to one dotted green vesicle as revealed in a). The same vesicle was tilted in the TEM from -60° to +60° and some images from the TEM tomogram are shown in the gallery g). Under different tilting angles it becomes obvious that the vesicles contain several (here three) entities of lipid stacks arranged within an organelle membrane. A reconstruction of the lamellar body is shown in f).

Finally, this approach also solves the problem of finding an area of interest for EM investigation within a complex tissue context known as the "searching for a needle in a haystack" problem. The major advantage of such an approach is that the cellular complexity stored in a single section becomes manageable by transferring this kind of morphological information into digital information packages, so called "data sections" at different resolution levels. This may be one way to overcome the "complexity dilemma" in structure research for life science.

Lipid Structure – Often Ignored in Biology, Perfectly Resolved by HPF

Major components for the permeability properties of the skin barrier are lipids arranged between the cornified corneocytes in the stratum corneum (SC) (11, 12). The extensive diversity of these lipids is rarely appreciated in ultrastructural investigations due to the lack of lipid arrangement preservation by the various preparation techniques used. This is drastically improved by the use of high pressure freezing (13) combined with freeze-substitution (4). Preservation of the lipid within its natural context is only one part of the story, since the spacing of lipid lamellae is in the range of 3-5 nm it becomes essential to view these lamellae exactly edge on in TEM (electron beam parallel to

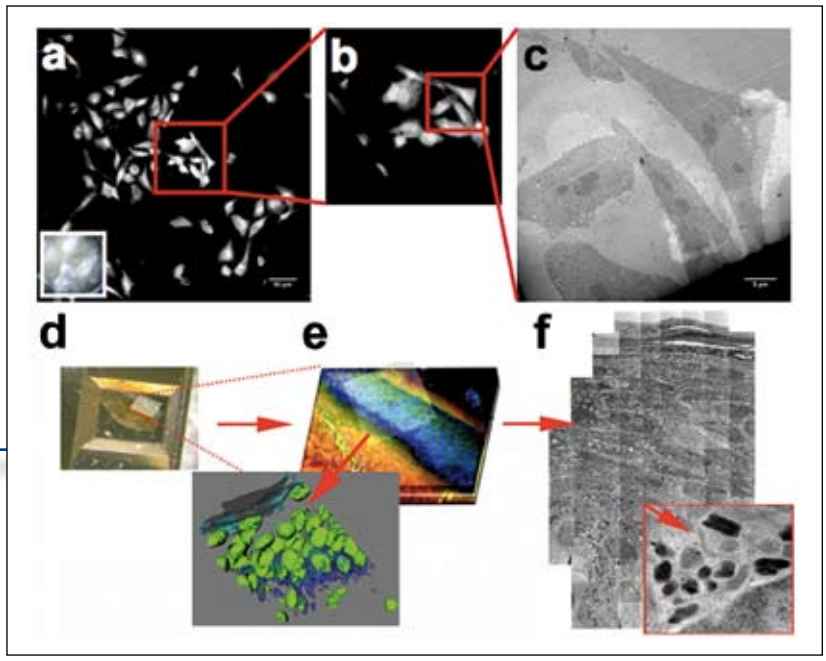

Fig. 5: Block-face embedded material: some possible application and imaging modes a-c) monolayer cultured cells prepared after specific treatment of cells for CLSM and TEM investigations – the aim is to pre-select areas of interest for further TEM and TEM tomography investigations. d-f) embedded tissue (skin) investigated by CLSM and corresponding 3D model followed by large scale imaging at higher resolution with TEM for stereological investigation of sub-cellular pigment distribution in human skin.

lipid sheet) in order to reveal significant contrast of the layered structure. This can only be reached with modern electron microscopy techniques such as TEM tomography (Fig. 4) – (1).

In figure 4a, antibodies were used against a Ceramide (red) and its glucosylated precursor (green) (9) on semi-thin (200 nm) sections of a high pressure frozen and freeze-substituted human skin sample to show that the various lipid species can be specifically localised after cryo-preparation. The antibodies were detected with a fluorescence-labelled secondary antibody and visualised with the help of a CLSM. The CLSM was equipped with a spectrometer for a better separation of the signal revealing the single entities of lipid vesicles as dotted green structures in the stratum granulosum (SGr) at its best resolution power. Electron microscopy is essential to further study the organisation of such lipid vesicles, also called lamellar bodies (14) or other lipid arrangements (Fig. 4b-f). E.g. imaging the intercellular space in the transition zone between the SGr to the SC allows visualising the extrusion of lamellar lipids (Fig. 4c+d) into the intercellular space as well as the rearrangement of lipids in this space (Fig. 4c+b). To reveal the molecular arrangement of the lipids in one of the dotted green vesicles as revealed in figure 4a, it is essential to tilt the ultrathin section (100 nm) in the TEM and view the preserved and embedded structure under various tilting angles (Fig. 4e). In doing this, it becomes obvious that the vesicles contain several (here three) entities of lipid stacks arranged within an organelle membrane. By continuously tilting the specimen in 1 degree steps with the help of modern TEM specimen stages, it is possible to acquire a tomographic tilt series, which allows to reconstruct the 3D objects in the 100 nm ultrathin section with the help of 3D visualisation software. Such a reconstruction of the lamellar bodies in figure 4e is shown in figure 4f. It highlights the three different "lamellar bodies" surrounded by one organelle lipid bi-layer which is embedded in a dense cytoplasm matrix enriched with filaments, ribosomes and multivesicular bodies.

Figure 3 and 4 clearly show the benefit of a better structure preservation and a multimodal imaging strategy helping to address questions of skin tissue organisation at the macromolecular level towards a better understanding of the nano-organisation of biological matter.

Learning from Multimodal Imaging Approaches

Modern preparation and imaging techniques allow to close the bridge from *in vivo* to the nanomorphology of biological tissue as microstructure has been demonstrated e.g. for the skin barrier structure (1). On one side, this allows to fulfill the dream of having a zoom-in imaging-tool throughout the different resolution levels for investigation of biological samples. On the other side, this helps to reduce workload in processing statistically relevant amounts of samples to compensate for the biologically intrinsic variations. Starting from *in vivo* by pre-selecting areas of interest with a multiphoton laser scanning microscope (MPLSM) the structures are recorded prior to taking a biopsy for further investigations at higher resolution (1). With the help of CLSM investigations of samples prepared as described above it is possible to visualise a broad range of characteristic structures within the selected biopsy at optimal structure preservation. 3D information from MPLSM and CLSM can then be used for the reconstruction of continuous structures within single cells as well as for the visualisation of the whole tissue sample (3D histology) and can be brought into register with histological and immunological images from a single selected section of the embedded material. Alternatively, after CLSM examination, (S)TEM of targeted ultra-thin sections can be used to find answers to ultrastructural questions on structures pre-selected by 3D light microscopy. Thus, a clear-cut TEM description of these structures eliminates the risk of (over-) interpreting light microscopic staining patterns by precisely defining the stained structures, e.g. membranes. Zooming from the sample overview into ultrastructural details within a multimodal dataset is a prerequisite for a holistic structural analysis. This allows to close the gap between histology and ultramorphology in 2D and even in 3D for the first time. Identifying macromolecular arrangements in their histological context and precisely describing exactly the same structures at high resolution becomes possible. This is the only way to cope with biological structural variance. With TEM tomography becoming a routine technique, 3D analysis of biological details can be pushed from LM level to a level allowing the nano-bio-morphology (e.g. Fig. 3 lamellar lipids in vesicles) to be described in 3D.

If the hydration state of a tissue is of interest, alternatively, processing the sample in its frozen-hydrated state is the method of choice (8), allowing to study e.g. effect of hydration or dynamic events (schematically described in Fig. 1, upper row).

Future Learning from Skin Research for Structural Biology

As discussed above, the aim of merging information at different information levels is to get a holistic model and hence a better understanding of the biological system under investigation.

By combining new dedicated preparation and imaging techniques in more than a correlative and coordinated way, one can not only produce synergies on the experimental side but also improve the view and hence the imagination and models of a structure under investigation (1). The basis is a common, very high structure preservation quality close to the native structure, so that data from different imaging approaches can be directly compared and merged. This leads to far more than comparing data from the same structure and deducing common features – it is the "sine qua non" for a multimodal integrative structure modelling as well as a virtual modelling strategy for computer models based on real structural data.

Real correlative zoom-in structures may be generated from cell monolayer culture (Fig. 5 a-c) by reallocating single cells of interest in a cell population and reinvestigating the region of interest (selected event or localised changes) at higher magnification by TEM. Or in tissue samples (Fig. 5 d-f), allowing the 3D histology to be studied by CLSM of e.g. the melanosome pigment distribution (Fig. 5 e – blue structures) and its corresponding ultra-structural background by TEM at higher resolution, i.e.resolving the individual melanosomes (Fig. 5 f – dens particle) for further stereological evaluations.

Further 3D investigations at higher resolution are available either by serial sectioning and 3D reconstruction of the structure of interest by TEM (Fig. 6 a) or by SEM (15). A complete new approach has become available by the establishment of FIB/SEM 3-D imaging, first established for material science, and since recently, also available for life-science application by collecting consecutive 20 nm section planes from an embedded tissue sample (Fig. 6 b).

Whether serial mechanical sectioning or ion beam sectioning will be the method of choice for 3D structure investigations on the cellular and tissue level needs to be investigated and carefully evaluated in the near future. One big additional benefit of FIB/SEM is that, even though it is also an invasive method, FIB/SEM allows to stop the process and pin point extract an ultra-thin TEM lamella for further investigation at higher magnification in a (S)TEM. Combined with CLSM 3D imaging, this would allow to shortcut the time of searching an area of interest for high resolution structure investigation once more.

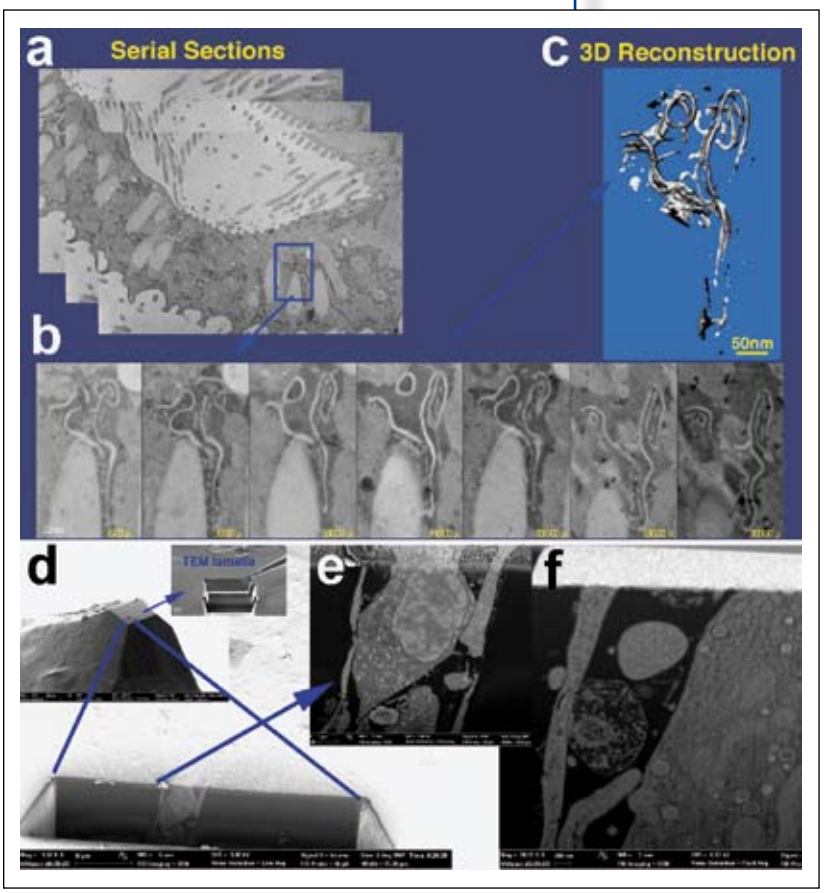

Fig. 6: Block-face embedded material: some possible application and further imaging modes
a-c) Serial sections of embedded Paramecia for TEM investigations – an image stack of a selected area can be reconstructed to a 3D model of a structural feature. d-f) embedded tissue (pancreas) investigated in a FIB/SEM by ion beam milling of an area of interest followed by serial sectioning of the tissue by ion beam sectioning.

The advantage (Fig. 7) of investigating samples which, after high pressure freezing, have been embedded in resin for structure research, can be summarised in brief as follows:

- Only one biopsy (sample) is needed to cover a large order of magnitudes in scale (mm to nm), reducing cell and animal experiments and biopsy material required for the investigation.
- Life-like "embedded" structural information – data blocks – become long time storable.
- Investigation and reinvestigation of embedded samples at any scale becomes time independent, hence re-investigation is possible at any time after gaining new insights and new information.
- Biological variance can be overcome by investigating one and the same sample at different scales.
- 2D and 3D stereological investigations are possible at different scale levels (zoom-in studies).
- At low resolution: *in vivo* light microscopy investigations prior to freezing can be correlated with histological and immunological structure data on one an the same area.
- At medium resolution: 3D histological evaluation by CLSM can be extended by 3D SEM block-face ultra-structural investigations (serial sectioning or ion milling) or serial sectioning for TEM.
- At high resolution: 3D FIB/SEM data can be selectively refined by FIB-lamella (S)TEM investigations.

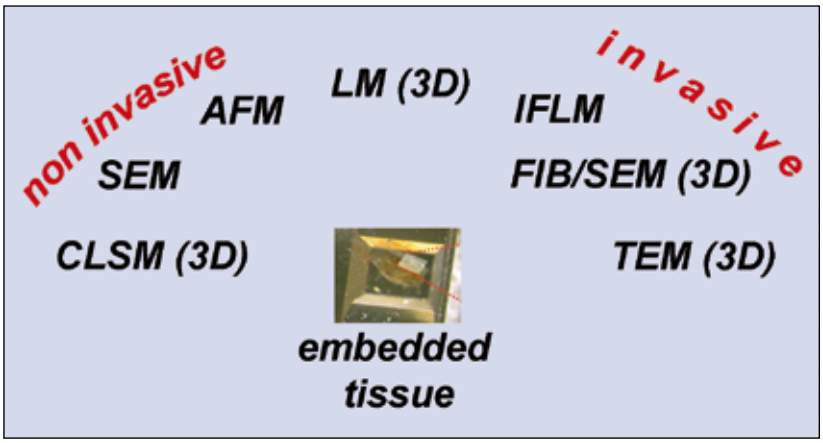

Fig. 7: Multimodal imaging potential on one and the same optimally preserved and stained biological samples embedded in resin
Left: non invasive imaging is possible by CLSM, SEM and AFM (16) on the resin blockface; right: for 3D reconstruction the embedded sample has to be mechanically sectioned or removed layer by layer (invasive treatment)

These are all prerequisites for describing functional or dynamic interactions of different cells or cellular components acting as parts of a trans-cellular information network reflecting proliferation, differentiation, apoptosis and special synthesis on different resolution levels.

By preserving the life-like material until imaging, it becomes possible to use the low-resolution map and continuous zooming-in to the details of interest at macromolecular and molecular level, therefore enabling us to study functional units, molecular networks and to still keep the "overview" in mind.

Author Biography

Roger Wepf is Director of the Electron Microscopy Centre ETH Zurich (EMEZ) since May 2006. Born in Strassbourg (F), he received his PhD in cell biology in 1992 at the ETH. After a postdoctoral fellowship, he joined the physical instrumentation program at EMBL in Heidelberg in the group of Max Haider, developing cryo-technology for corrected LVSEM and EM applications. In 1996 he was appointed junior group leader in the cell biology program at EMBL. Before he moved to the ETH, he was nine years with Beiersdorf AG, as head of the analytical microscopy department, in the research division in Hamburg. Working mainly on human skin morphomics and nano-analytic technology research in-vivo and ex-vivo at the level of light to electron microscopy, spectroscopy and SPM with a focus on developing cryo-technology for microscopy. His major research at ETH Zurich is now focused in the field of correlative microscopy, automatic sample preparation and imaging techniques for particle imaging technology.

Acknowledgements:

We thank S. Biel, K. Dunckelmann, T. Richter, S. Wessel, J. Vietzke for support and excellent work on the skin barrier structure. Special thanks go to U. Hintze, Beiersdorf AG for his enthusiastic support over several years and to L. Diener for sample preparation as well as, and to E. Müller, EMEZ, for corrections of the manuscript.

Literature:

1) Wepf, R., et al., In: „Bioengineeering of the Skin 2nd Ed: Skin Imaging and Analysis ", Informa Healthcare, New York, Oxon 2007
2) Biel, S.S., et al., J. Microsc. 212: 91-99, 2003.
3) Echlin, P. In: Low-Temperature Microscopy and Analysis, Plenum Press, New York 1992.
4) Pfeiffer, S., et al., J. Invest. Dermatol. 114: 1031-1038, 2000.
5) Hohenberg, H., et al., J. Micros. 183: 133-139, 1996.
6) Droste, MS., et al., J Biomed Opt. 10 (6):064017-10, 2005
7) McIntosh, JR., et al., J Cell Biol., Vol. 153(6), F25-32 (2001).
8) Richter, T., et al.; J. Microsc.; Vol 225, Issue 2, 201-20, 2007
9) Vielhaber, G., et al., J. Invest. Dermatol. 117: 1126-1136, 2001
10) Biel, S.S., et al., Imaging & Microscopy 7: 26-29, 2005.
11) Hohenberg, H., et al., J. Microsc. 175: 34-43, 1994
12) Wertz, P.W., Acta Derm. Venereol. Suppl. (Stockh.) 208: 7-11, 2000
13) Vietzke, J., Lipids 36 (3): 299-304, 2001
14) Norlen, L., et al., J Invest. Dermatol. 120:555-560, 2003
15) Landmann, L., J. Invest. Dermatol. 87: 202-209, 1986
16) Denk, W., et al., PLoS Biol. 2(11):e329. Epub 2004
17) Efimov, AE., et al. J Microsc. 226 (Pt3): 207-17 2007

Contact:

Prof Heinrich Hohenberg
Heinrich-Pette-Institute
for experimental Vilology
and Immunology,
University of Hamburg, Germany

Dr Andreas Schertel
Carl Zeiss NTS GmbH
Oberkochen, Germany

Dr Miriam S. Droste
Dr Roger Wepf
Head Electron Microscopy
ETH Zurich (EMEZ),
Switzerland
Tel.: +41 44 633 4558
Fax: +41 44 633 1336
roger.wepf@emez.ethz.ch
www.emez.ethz.ch
www.cimst.ethz.ch

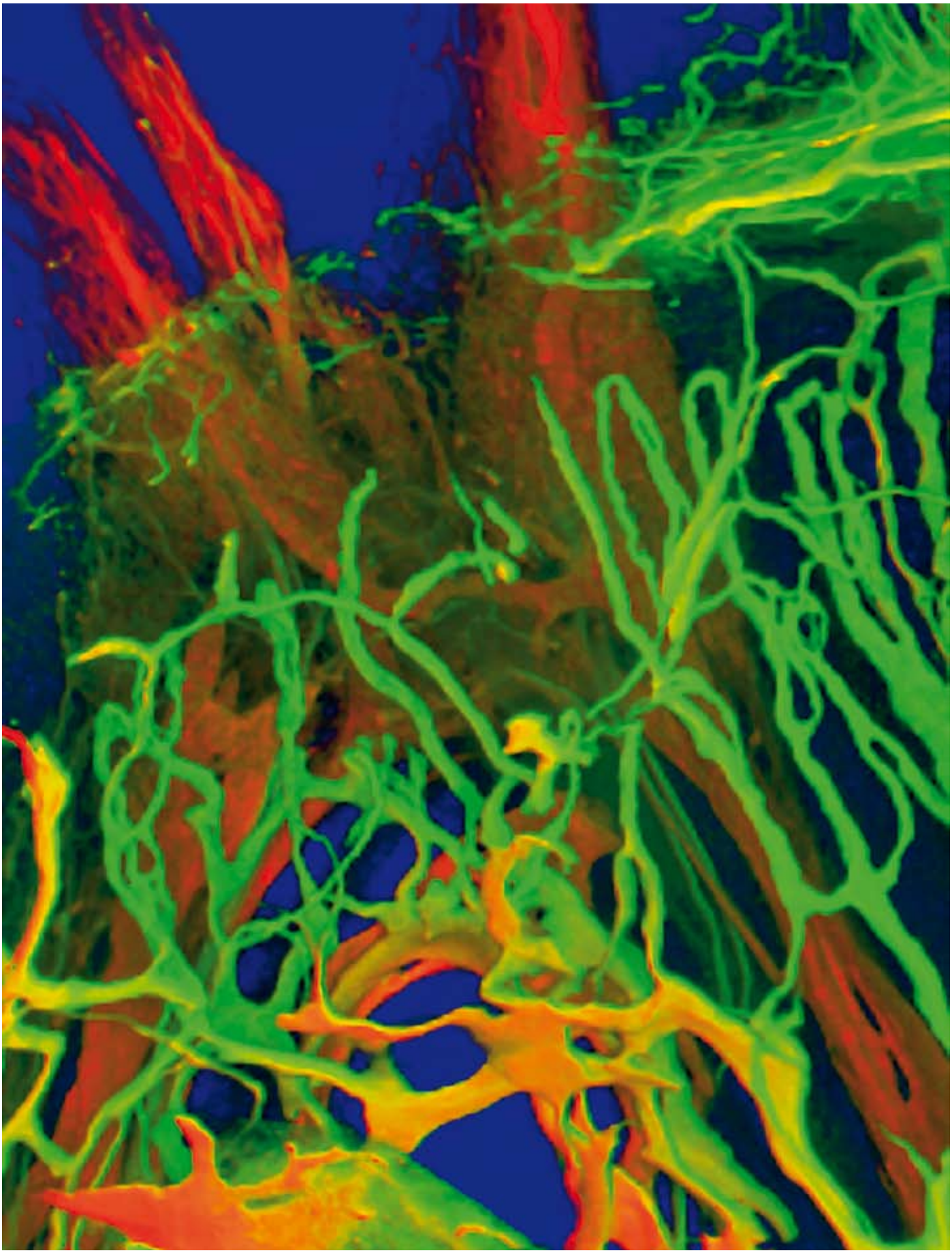

Section through jaw and tooth of an adult mouse stained with FITC / TRITC gelatine, showing a part of a 3D reconstruction; colours indicate the depth of each structure (LSM 510)
Dr Hashimoto and Dr Kusakabe, Jikei University, Tokyo, Japan

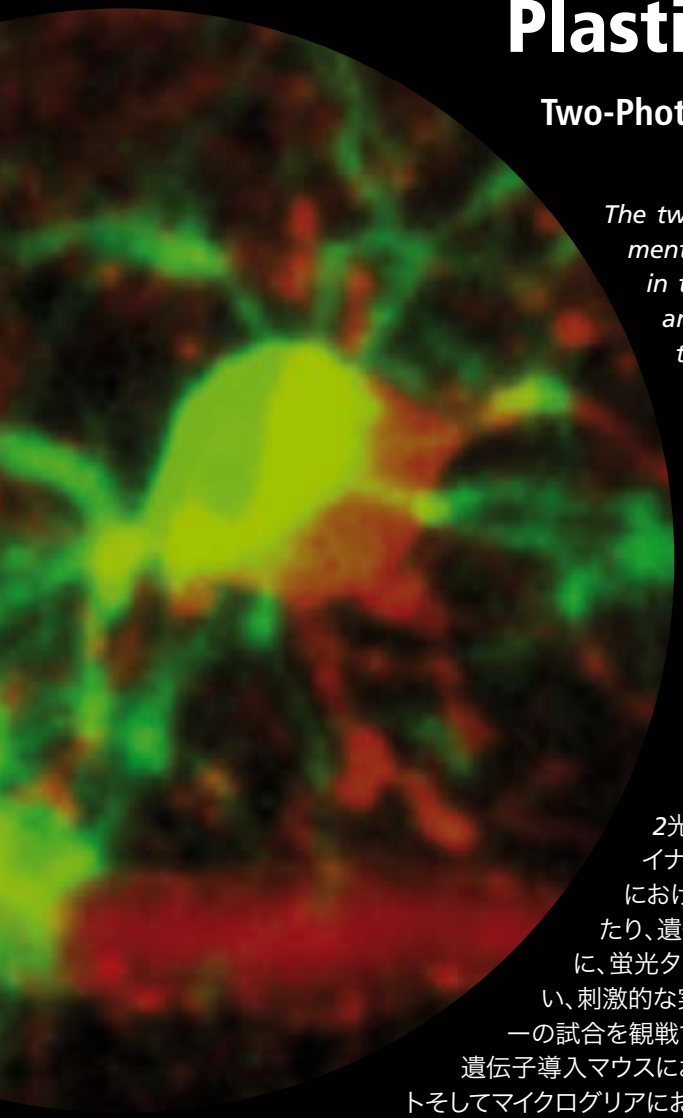

Plastic Structures in the Brain

Two-Photon Imaging Uncovers Dynamic Cell-cell Interactions

The two-photon laser scanning microscope represents a fascinating instrument which allows the direct observation of dynamic cell-cell interactions in the nervous system of living animals. However, its powerful appearance at the neuroscience stage was and still is dependent on the simultaneously occurring development of novel fluorescent dyes which either selectively label defined structures in the brain or which are genetically encoded and can be used in transgenesis. In particular, the numerous mouse lines with cell-type specific expression of fluorescent proteins (FP) offer a wide range of novel exciting in vivo experiments in which the experimentator is a direct observer like a football supporter following, the game of his team in the stadium. In transgenic mice well characterised regulatory DNA elements control the expression of FPs in neurons, astrocytes, oligodendrocytes and microglia. In the following, I will provide an overview of the most prominent plastic changes observed in the nervous system during development, in the adulthood and during neurodegeneration.

2光子レーザ走査顕微鏡は、生きた動物の神経系における細胞間相互作用のダイナミクスを直接観察するシステムとして魅力的である。一方で、神経科学分野における頼もしい状況は、かつて、そして今でも、脳の特定構造を選択的に標識したり、遺伝的にコードして発現させて用いられる新規の蛍光標識に依存している。特に、蛍光タンパクを細胞の種類特異的に発現させた多くのマウス類は、*vivo*での幅広い、刺激的な実験系を提供している　–研究者はまるでスタジアムでの地元チームのサッカーの試合を観戦するサポータの様な感じで直接的に観察できるのである。
遺伝子導入マウスにおいては、充分に制御された*DNA*が神経細胞、星状細胞、オリゴデンドロサイトそしてマイクログリアにおける蛍光タンパクの発現をコントロールしている。以下の本文では、発生過程、成育期、そして神経退化過程における神経構造の、特徴的な可塑性について述べてみたい。

Keywords:

cell-cell interaction, nervous system development, synaptic/axonal plasticity, two-photon laser scanning microscopy

Remodelling of Brain Structures is a Common Process in the Nervous System

Synapses, these tiny structures connecting nerve cells, are the major sites of brain communication pathways. Understanding the regulation of synaptogenesis, i.e. the formation of synapses and also their elimination, is regarded as prerequisites to understand brain function. Already quite early it was recognised that synapses undergo a high turnover in the growing nervous system. Initially, a substantial surplus of synapses is formed with subsequent use-dependent elimination. While classical techniques (such as electron microscopy and immunohistochemistry) can only describe changes in synapse density and structure, the felicitous combination of molecular biology and life imaging as it comes with *in vivo* two-photon laser-scanning microscopy (2P-LSM) and transgenic mice expressing fluorescent proteins in a cell-type specific manner generated a wealth of novel information on dynamic processes occurring in the developing, adolescent and adult brain (Grutzendler and Gan, 2006; Helmchen and Denk, 2005; Nimmerjahn et al., 2004; Nolte et al., 2001; Feng et al., 2000). In parallel to the generation of transgenic mice with fluorescently labelled cells, also viruses have been constructed that allow the labelling of neural structures also in species which are less accessible to germ line manipulation, such as higher rodents or even non-human primates.

Thanks to these technological improvements, we are now in a position to study brain dynamics in diverse nervous systems as found in the fly, worm, fish, mouse, rat and monkey.

Dynamics of Axons and Spines are Heterogeneous in Various Regions of the Brain

The most common experimental model to study brain dynamics *in vivo* are transgenic Thy1-GFP or Thy1-YFP mice in which the expression of green or yellow fluorescent proteins (FPs) is regulated by the Thy1 mini-gene (Feng et al., 2000) (Fig. 1). The reporter protein expression is found almost exclusively in neuronal cell populations only, particularly, in projection neurons such as cortical pyramidal neurons, cerebellar Purkinje cells, retinal ganglion cells or spinal motoneurons. But granular neurons of hippocampus and cerebellum are also found to be fluorescently labelled. Interestingly, individual transgenic founder lines are heterogeneous in respect to the pattern of FP expression. In some lines, only few cells are labelled, while others show an almost ubiquitous expression in almost all cells of a distinct neuron population. Although this appears disadvantageous at the first glance, during the last years it turned out, that this provides a major virtue. In animals with sparse labelling, the observation of distinct structures (axons or spines) is much easier, and the identification of single spines or axons is facilitated during subsequent imaging sessions over months.

The neuronal connectivity, i. e. the formation of synapses by axonal terminals and postsynaptic specialisations of the innervated neuron, determines brain function.

Synapses are not only formed during development, their structural changes are also thought to underlie learning and memory. However, until very recently little was known about synaptic reorganisation *in vivo*. To address this question, Wenbiao Gan and his colleagues observed the spines of layer 5 pyramidal cells in the visual cortex of Thy1-EYFP mice for several months using transcranial 2P-LSM (Grutzendler et al., 2002) (Fig 2). They found that in young mice, i.e. within the critical period of visual cortex development, the vast majority of spines (about 75 %) appeared stable during the observation period of a few weeks, while simultaneously numerous small filopodial extensions were detected that transiently emanated from the dendritic shafts and which were retracted within less than an hour. Interestingly, similar filopodia could not be detected in adult mice. Although it was hard to detect the formation of new spines, elimination of spines was seen more often. In adult mice, however, almost all spines (more than 95 %) remained stable over the complete life of the animal. The mean half-life of these spines was found to be 13 months.

Similar experiments have been performed by the group of Karel Svoboda in the mouse barrel cortex combining 2P-imaging with subsequent electron microscopic processing of the imaged brain region (Trachtenberg et al., 2002) (Fig. 2). The generation of bona fide synapses were found after transient extension of filopodia. In the barrel

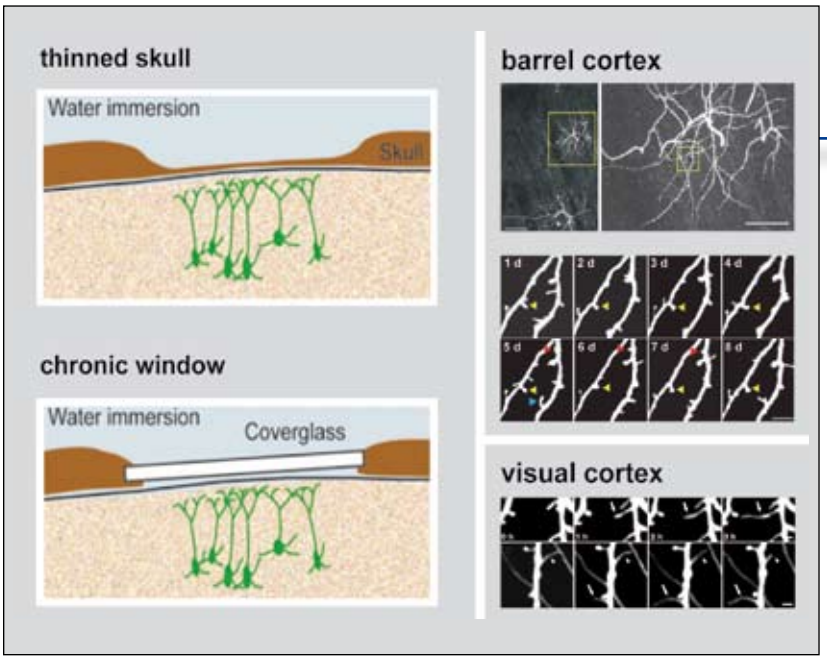

Fig. 1: *In vivo* two-photon laser scanning microscopy (2P-LSM) of the mouse cortex.
Two different variants of brain access to image neural plasticity. Through the thinned skull (20 to 40 µm) prelabelled neural structures such as green fluorescent protein-expressing neurons of transgenic Thy1-GFP mice can be readily observed without induction of injuries to the cortical neuropile. In the chronic window approach, a small hole of a few mm in diameter is inserted into the skull. Dyes or viruses can be applied locally for staining purposes. Subsequently, a glass coverslip covers the craniotomy to reduce pulsation of the exposed brain and to allow repetitive imaging.
The latter approach has been used to perform chronic time-lapse imaging in the barrel cortex. The high-resolution images display transient, semi-stable and stable spines of layer 5-pyramidal neurons as indicated by blue, red and yellow arrowheads. Scale bars 100, 50 and 5 µm.
The thinned skull preparation has preferentially been used to image neurons in the visual cortex. The two panels display dynamic filopodial extensions (arrows) and retractions (arrowheads) imaged in two different 1-month-old mice at 1-h-intervals. Scale bar 1 µm.
Modified from (Helmchen and Denk, 2005;Trachtenberg et al., 2002;Grutzendler et al., 2002).

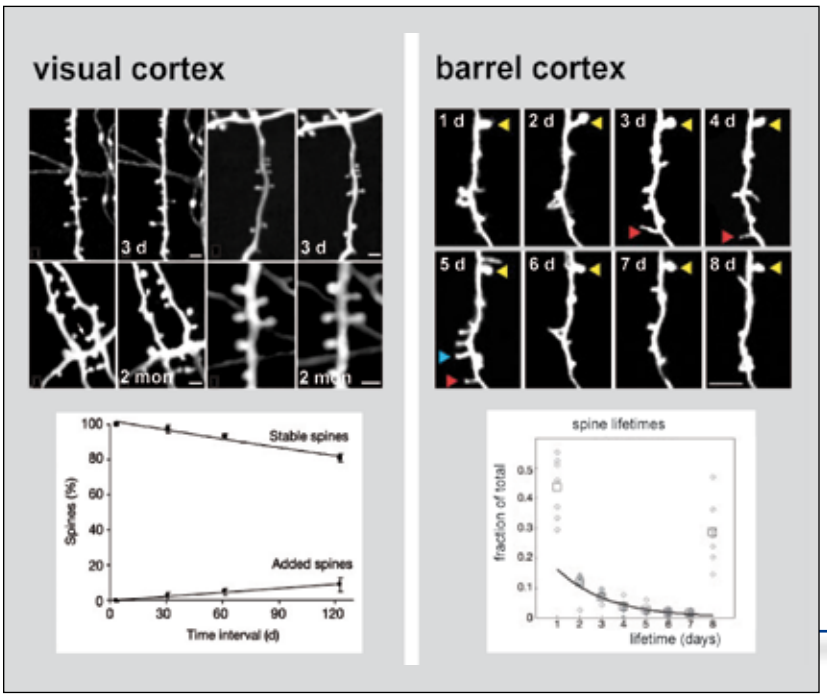

Fig. 2: Long-term imaging of cortical spines *in vivo*.
In the visual cortex of adult mice, dendritic spines demonstrate long-term stability. The individual images represent four different sites which have been recorded with time intervals of three days or two months, respectively. More than 90 % of spines remain stable over a time period of three months.
In contrast, spines of the the barrel cortex seem to be more plastic. Spines appear and disappear with broadly distributed lifetimes. Transient and semi-stable spines make up about 40 %, while only 60 % of spines are stable for more than a week.
Modified from (Grutzendler et al., 2002;Trachtenberg et al., 2002).

cortex, however, the spine turnover, and hence spine plasticity, seemed to be more pronounced than in the visual cortex. Spine lifetimes varied significantly, ranging from days to months. But only 50% of spines persisted for more than a month, a rather small percentage when compared to the 95% of stable spines in the visual cortex.

To further reveal regional heterogeneity of spine plasticity in the brain cortex, a comparative analysis has been performed for the visual, auditory and somatosensoric cortices in juvenile 4-week-old mice (Majewska et al., 2006). And, indeed, significant differences in the basal rate of spine motility in the same type of pyramidal cells of layer 5 were uncovered. As reported previously, neurons of the visual cortex revealed the lowest rate of spine turnover. In young adult mice of 2 to 3 months, the synapses, both terminals and spines, appeared rather stable, with more than 80% persisting over a 3-week-period in all sensory regions. Remarkably, axon terminals were more stable than postsynaptic, dendritic spines.

These data together clearly demonstrate that the largest proportion of synapses formed during development can persist for the whole life of an animal. It is tempting to speculate that these synapses contribute to stable, long-term memory. However, there was also a significant percentage of synapses with fast use-dependent turnover, which might represent adaptive remodelling of neural circuits. Therefore, it is very likely that processes underlying learning and memory predominantly occur through changes in the strength and efficacy of existing synapses, but structural plasticity, i.e. remodeling of connectivity, with loss and gain of synapses contributes also to brain function.

Experimental Modulation of Synaptic Plasticity

To shed some light on distinct mechanisms which might regulate either changes of synaptic efficacy or the turnover of synapses, experimental manipulation of sensory inputs has to be performed in combination with *in vivo* 2P-LSM. For that purpose, Majewska et al. (2006) studied whether the differences observed between the motility of dendritic spines in different cortical areas would depend either on the nature of the sensory, innervating input or on local cues intrinsic to the cortical area itself. They performed surgeries on neonatal mice which routed the retinal input to the auditory thalamus instead of the lateral geniculate nucleus. As a consequence, the auditory cortex instead of the visual cortex received visual information. Since subsequent 2P-imaging in grown-up mice did not show any differences in dendritic spine motility of neurons in the auditory cortex when compared to untreated mice, these data clearly hint towards an intrinsic regulation of structural plasticity rates in cortical regions.

Interestingly, the loss of synapses seems to be an important property of brain development and maturation indicating the establishment of stable neuronal circuits (Zuo et al., 2005; Holtmaat et al., 2006).

In the somatosensory, barrel cortex it was observed that long-term sensory deprivation through whisker trimming prevented a net spine loss (Zuo et al., 2005) (Fig. 3). Although a preferential decrease in the rate of ongoing spine elimination rather than a generation of new spine formation was predominant in young mice, synaptogenesis still persisted in adulthood. Spine elimination could again be accelerated by restoring sensory experience after adolescent deprivation.

Therefore, it is conceivable that adaptive modulation of brain circuits occurs via selective generation and loss of persistent spines upon novel sensory experience. To test this hypothesis, Holtmaat et al. (2006) repeatedly imaged dendritic spines for one month after trimming alternate whiskers, a paradigm that induces adaptive functional changes in neocortical circuits. A checkerboard-type of whisker trimming led to a reorientation of axon terminals in neighboring barrels with subsequent stabilization of new spines and desta-

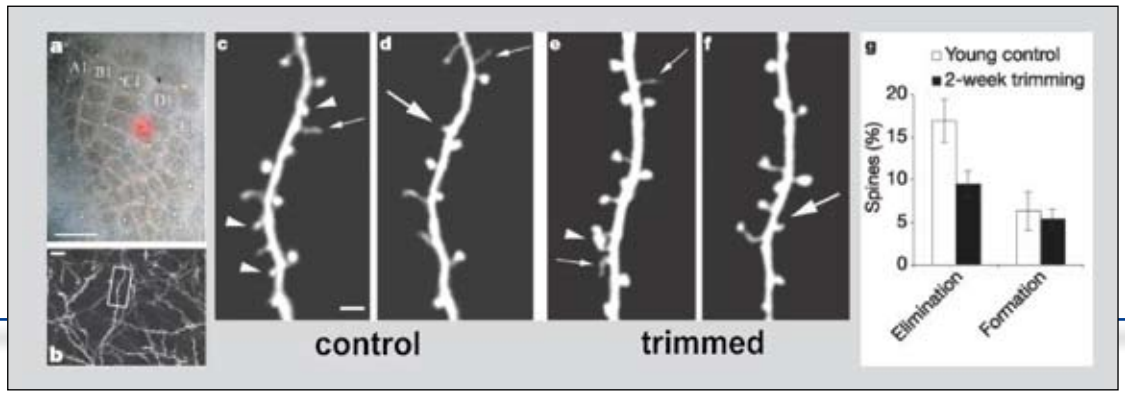

Fig. 3: Whisker trimming reduces the use-dependent spine elimination in the barrel cortex of young mice.
Retrograde DiI labelling visualizes the distinct perceptive fields of individual whiskers (a) and indicates the barrel fields in which plastic spine changes of layer 5 neurons were observed for two weeks (b, low maginification). Repeated imaging at high-magnification reveals plastic changes, primarily spine elimination (arrowheads), but also new spine formation (large arrows) and filopodium turnover (small arrows) in control (c, d) and whisker-trimmed (e, f) mice. Spine elimination but not formation is significantly reduced after whisker trimming (g). Scale bars 500, 10 and 2 µm. Modified from (Zuo et al., 2005).

bilization of previously persistent spines. New stable synapses were preferentially formed on a selective subclass of layer 5 neurons with complex apical tufts rather than simple tufts.

From these studies it can be concluded that throughout almost the whole life-span, experience, i.e. activation of neuronal network activities, regulates synapse remodelling and turnover, but particular critical phases exist during adolescence.

Also Axons Display Plasticity

So far, numerous studies demonstrated a clear heterogeneity of spine development, its turnover and synapse remodelling in a region-, age- and experience-dependent manner. But even axons, their branches and boutons, are highly plastic, in rodents as well as in primates (De Paola et al., 2006; Stettler et al., 2006).

In layer 1 of the mouse barrel cortex, axons originating from the thalamus and layers 2/3/5 or layer 6 pyramidal cells can be identified based on their distinct morphologies (Fig. 4). Similar to the stability of synapses, branching patterns and sizes were preferentially found to be stable over months, but cell type-specific rearrangements could also be observed. Thalamocortical afferents could elongate and retract branches of more than 100 µm in a few days. The majority of their boutons, however, seemed to persist throughout life. In contrast, terminaux boutons of layer 6 axons were highly plastic. Only 40 % of them persisted for more than a month. The other intracortical axon boutons showed intermediate levels of plasticity. Retrospective electron microscopy revealed that the new boutons formed synapses.

Similar results were found in the visual cortex of adult Macaque monkeys in which axons were fluorescently labeled by adeno-associated viruses (Stettler et al., 2006). The large-scale branching patterns were stable, but subsets of small branches associated with terminaux boutons and en passant boutons appeared and disappeared every week, further strengthening the view of input cortices as dynamic structures in which a small, but significant number of local circuits are permanently rebuilt.

Dynamic Shape Changes are Key Features of all Glial Cell Types

Plastic interactions of astroglial processes with active synapses

The most recent view of a functional synapse has integrated the neighboring compartment, i.e. the astroglial processes (Halassa et al., 2007). Within this tripartite structure, the enwrapping glial ensheathment regulate synaptic transmission by transmitter uptake and by direct transmitter release. But, in addition, the astroglial processes are highly motile as well as it could be shown in acutely isolated slices prepared from the brainstem of transgenic TgN(GFAP-EGFP) mice (Hirrlinger et al., 2004) (Fig. 5). At synaptic regions, astroglial process endings displayed two defined modes of spontaneous motility: (i) gliding of thin lamellipodia-like membrane protrusions along neuronal surfaces and (ii) transient extensions of filopodia-

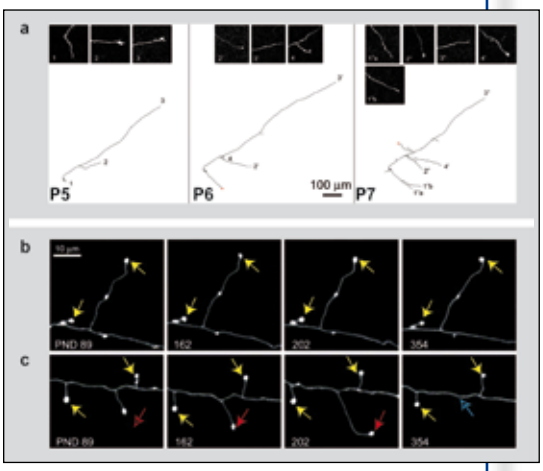

Fig. 4: Plasticity and stability of thalamocortical axons in the mouse cortex.
During the first postnatal week, substantial axon growth with formation of collaterals occurs within layer 1 of the mouse cortex (a). In contrast, imaging of thalamocortical axons in adult mice reveals a long-term stability from the 3rd to 12th month of age (b). Only a few of the axon branches are either retracted or show further outgrowth (c). Modified from (De Paola et al., 2006).

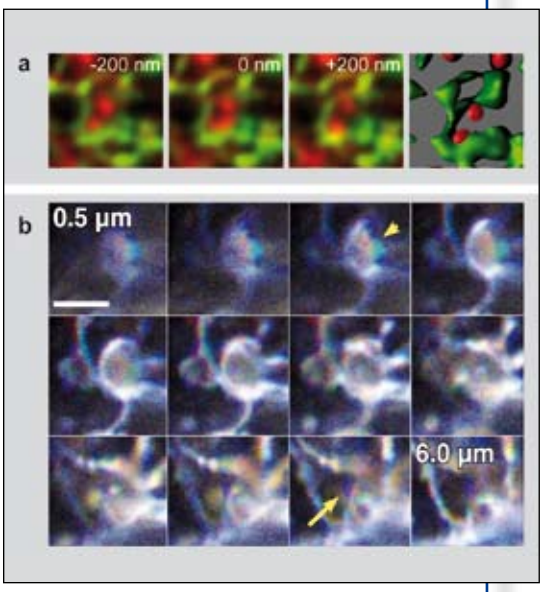

Fig. 5: Astroglial processes are highly dynamic at synapses.
Single optical sections of an acutely isolated and FM1-43 stained brainstem slice show active synaptic terminals (red) and their close interactions with astroglial processes (green)(a). The right image represents a 3D reconstruction of a stack of 2P-LSM images. Astroglial processes appeared very motile as assessed by overlaying a set of three consecutive stacks (12 optical planes separated by 0.5 µm), recorded at 30 s intervals and coloured in red, green and blue. Stationary structures appear in white while motile structures show up in distinct colours (additive in the RGB colour space with blue revealing process extension and red retraction, respectively (b)). Scale bars 1 (a) and 2 (b) µm.
Modified from (Hirrlinger et al., 2004).

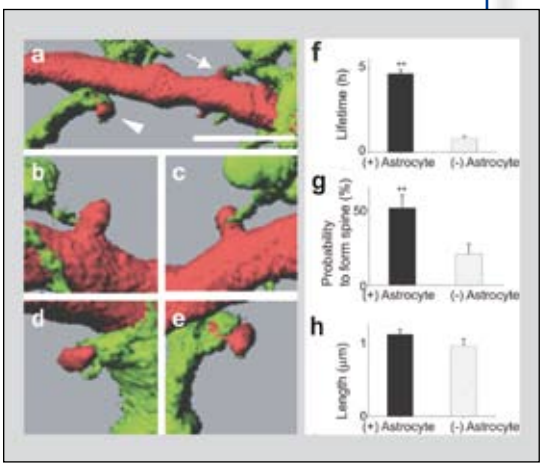

Fig. 6: Contacts with astrocytes stabilize neuronal spines.
3D-modelling of two-photon image stacks reveal that the contact sites are either large enough to encircle the neck of dendritic protrusions (arrowhead in a, magnified views in d, e) or are confined to a small area (arrow in a, enlarged in b, c). 2P-LSM stacks were recorded from organotypic slice cultures of early postnatal mouse hippocampi. Astrocytes were GFP-labelled by viral infection, neurones by electroporation with rhodamine-dextran, respectively. The contact of astroglial processes increases the lifetime of spines (f) and the probability of their formation (g). Spine length, however, is not modulated by astroglial interactions (h). Scale bar 5 µm.
Modified from (Nishida and Okabe, 2007).

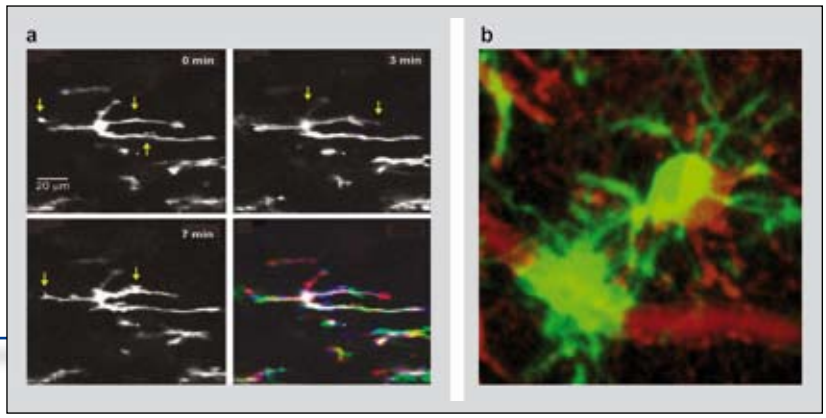

Fig. 7: Microglial processes are very motile, continuously surveying the CNS parenchyma and reacting upon acute injuries. Time-lapse recording of microglia in the spinal cord of genetically modified mice in which EGFP is expressed from the CX3CR1 locus (a). Microglial processes are longitudinally orientated along axonal fiber tracts. Some small membrane protrusions (arrows) emanate from the major processes within minutes, whereas others are retracted simultaneously. These terminal processes constantly survey their cellular neighbourhood. The lower right image is an overlay of the three grey images colour coded in red, green and blue. The static portion of the cell therefore appears in white and the moving processes in different colours. Laser-evoked micro-lesions of cortical capillaries induce immediate attraction of microglial processes which shield the injured site from the neighboring tissue (b). Modified from (Giaume et al., 2007;Nimmerjahn et al., 2005).

like processes into the neuronal environment. Similar data could also be observed in organotypic slice cultures of the hippocampus (Benediktsson et al., 2005; Nishida and Okabe, 2007). Shigeo Okabe and his coworker could further identify ephrin-A3 and EphA4 as an important mechanism of synaptic neuron-glia interaction (Nishida and Okabe, 2007). They showed that thin neuronal filopodia were stabilized by astroglial processes leading subsequently to thick, mushroom-like spines receiving synaptic input (Fig. 6). These studies highlight the active role of astrocytes in synaptic remodelling, modulation of synaptic transmission and hence, tuning of neuronal circuits.

Unfortunately, astroglial processes and, in particular, their fine membrane protrusions are significantly thinner (20 to 50 µm) than the spatial resolution of 2P-microscopy (300 µm). Therefore, astroglial process imaging has so far been restricted to brain slices obtained from neonatal mice in which the processes are less densely compacted as in the adult. So we are still awaiting observations from living mice.

Oligodendroglial Motility as a Mechanism to Achieve Proper Spacing of Myelin Units Along Axons

Although transgenic mice with expression of fluorescent proteins in oligodendrocytes, the myelinating glial cells of the central nervous system exist (Fuss et al., 2000; Belachew et al., 2001; Hirrlinger et al., 2005), they have not yet been used to study and visualize the dynamics of processes along neuronal fiber tracts. Myelinating oligodendrocytes arise from migratory and proliferative oligodendrocyte progenitor cells (OPCs). Complete myelination requires that oligodendrocytes are uniformly distributed and form numerous, periodically spaced membrane sheaths along the entire length of target axons. The mechanisms how oligodendrocyte assemble along axons and initiate the spiralling of myelin sheaths are not yet known.

Exciting observation of oligodendroglia during these initial phases of myelinogenesis were made in the transgenic zebrafish (Kirby et al., 2006).

At the onset of myelination oligodendroglial progenitor cells continuously extended and retracted numerous filopodiuma-like processes, as similarly seen in astrocytes. During this phase, they migrated toward the axons forming a linear array with defined separating distances. Dynamic contacts with neighboring progenitors seemed to define the intercell distance at the axon. Therefore, the process motility before axon wrapping might serve as a surveillance mechanism facilitating uniform spacing of oligodendrocytes and complete myelination.

Motile Microglial Processes Survey their Microenvironment and Respond to Acute Brain Injuries

Microglial cells represent the immune system of the mammalian brain and are therefore critically involved in various injuries and diseases.

Until very recently, microglial cells have been regarded as rather quiescent cells during normal brain function. By taking advantage of a genetically modified mouse line in which the fractalkine receptor CX3CR1 was replaced by the green fluorescent protein EGFP (Jung et al., 2000), and applying *in vivo* 2P-imaging to the neocortex, an unprecedented degree of process motility was observed in microglia (Nimmerjahn et al., 2005; Davalos et al., 2005). Although microglial cells were assumed to be at their so-called resting state, they continually surveyed their cortical microenvironment. Permanently, thin processes and membrane protrusions were extended and retracted almost randomly (Fig. 7). Microglial processes, however, were perfectly suited to react also directionally. Small, highly localized disruptions of the blood-brain barrier provoked immediate and focal attraction of microglial processes. Injury-sensing cells changed their behavior from a patrolling state to a protective phase by shielding the injured site (Fig. 7). The bifunctional molecule ATP, acting as an energy metabolite as well as a transmitter, could be shown to mimic the rapid chemotactic response upon injury (Davalos et al., 2005; Haynes et al., 2006). The regulation of microglial branch dynamics by extracellular ATP was further confirmed in mice lacking the metabotropic purinoreceptor P2Y12 (Haynes et al., 2006). Within the nervous system, this receptor is selectively expressed on microglial processes only. In P2Y12 knockout mice not only the ATP-dependent attraction of microglial processes is blocked, but the attraction of processes towards small necrotic lesions is also impaired.

Structural Adaptations in the Chronically Diseased Brain

The brain of patients suffering from Alzheimer's disease (AD) is characterized by proteinaceous ex-

tra- and intracellular deposits termed amyloid plaques and neurofibrillary tangles, respectively. Interestingly, the formation of amyloid plaques can be followed in a transgenic mouse model of AD by *in vivo* 2P-LSM using the fluorescent compounds thioflavin S and T as well as their derivatives (Bacskai et al., 2003). When thioflavin staining of the cortical neuropile is applied in mice with viral or transgenic FP expression the interaction of plaques with various cellular compartments can readily be studied, even during the complete progression of the disease (Tsai et al., 2004; Spires et al., 2005). Substantial spine loss and shaft atrophy of dendrites were often observed in the vicinity of fibrillar amyloid deposits (Fig. 8). In addition, adjacent axons developed large varicosities, irregular bendings, and abrupt branch ending as a consequence of neurite breakage. Therefore, AD plaques can cause wide-spread and permanent disruption of neuronal connections. Interestingly, also some process sprouting could be detected. Careful investigation of human post mortem brain revealed similar changes, demonstrating the validity of data obtained in the mouse model (Grutzendler et al., 2007). Prevention and early clearance of amyloid plaques have to be the prime target for any therapeutic approach targeting AD.

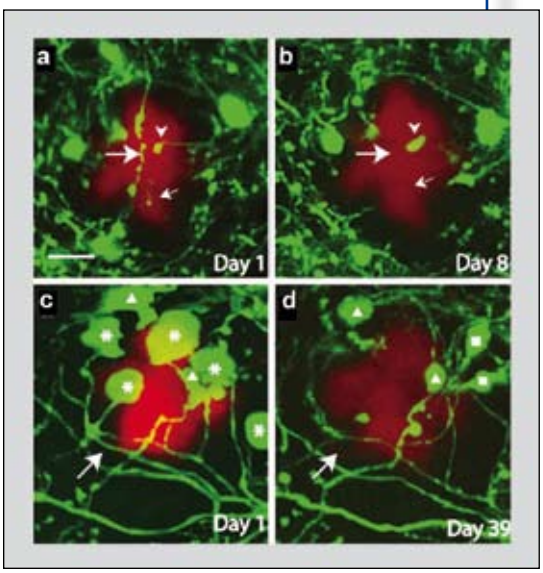

Fig. 8: Disintegration of neurites in the vicinity of amyloid plaques imaged by *in vivo* 2P-LSM. Two neuronal processes (arrows) adjacent to a plaque of Aβ deposits disappeared within the observation period of a week. A third process (arrowhead) retracted and left a retraction bulb behind (c). Axonal varicosities show substantial, but variable changes at amyloid plaques. While some disappear (asterisks), others are newly formed (square) or remain stable (triangle). The arrow indicates a disappearing axonal branch. Scale bar 10 µm. Modified from (Tsai et al., 2004)

Outlook

The last decade has witnessed a substantial increase in our knowledge of plastic changes in the healthy and diseased brain. A prerequisite for the success of numerous studies was the combination of transgenic mice with FP expression and *in vivo* 2P-LSM. So far, most studies used only a single or sometimes two different fluorescent dyes. Future studies will take advantage of novel neurogenetic strategies allowing the visualization and distinction of complete neural networks. In addition, genetically encoded biosensors will help to study signalling pathways, and light-modifiable proteins will allow the manipulation of neural cell properties directly by the investigator.

Author Biography

PD Dr. Frank Kirchhoff studied biochemistry at the University of Hannover (1981-1986). In 1990, he obtained his PhD degree in neurobiology at the University of Heidelberg (Dr. rer.nat.). After postdoctoral periods at the University of Heidelberg (1990-1994) and the Max Delbrück Center of Molecular Medicine in Berlin (1995-1999), he became head of the research group Glial Physiology and Imaging in the Department of Neurogenetics at the Max Planck Institute of Experimental Medicine, Göttingen. Since 1998, he is also lecturer of biochemistry (venia legendi) of the Free University of Berlin (Faculty of Biology, Chemistry and Pharmacy). His research interests are (1) molecular and cellular mechanisms of neuron-glia interactions in the CNS, (2) development of transgenic mouse models to visualize neuronal and glial properties, (3) development of transgenic mouse models to modulate glia function and (4) imaging techniques to study neuronal and glial network activities *in situ* and *in vivo*.

Acknowledgements

Research work of the author is supported by grants provided by the Deutsche Forschungsgemeinschaft and the Max Planck Gesellschaft.

References

[1] Bacskai B.J. et al., Proc Natl Acad Sci U S A 100, 12462–12467 (2003).
[2] Belachew S., et al., Dev Neurosci 23, 287-298 (2001).
[3] Benediktsson A.M., et al., J Neurosci Methods 141, 41–53 (2005).
[4] Davalos D., et al., Nat Neurosci 8, 752–758 (2005).
[5] De Paola, V., et al., J Neurosci 49, 861–875 (2006).
[6] Feng G., et al., J Neurosci 28, 41–51 (2000).
[7] Fuss B., et al., Dev Biol 218, 259–274 (2000).
[8] Giaume C., et al., Cell Death Differ 14, 1324–1335 (2007).
[9] Grutzendler J. and Gan W.B. NeuroRx 3, 489–496 (2006).
[10] Grutzendler J., et al., Ann N Y Acad Sci 1097, 30–39 (2007).

The complete list of references is available within the online version.

Contact:

PD Dr Frank Kirchhoff
Glial Physiology and Imaging
Dept. of Neurogenetics
Max Planck Institute of
Experimental Medicine
Göttingen, Germany
Tel.: +49 551 3899 770
Fax: +49 551 3899 758
kirchhoff@em.mpg.de
www.em.mpg.de

Imaging Mitochondrial Physiology

Application of Fluorescence Imaging to Study Mitochondria

Live cell imaging has opened up a wealth of knowledge of cell physiology. In this essay, we show how the approach lends itself to the study of mitochondrial function. Mitochondria play a pivotal role in cell life and death. Understanding the integration of mitochondrial physiology into cell signalling pathways is therefore central to much of cell physiology, and by implication, to much of medicine. The list of diseases for which mitochondrial dysfunction is implicated as a pathogenic mechanism continues to grow. It is therefore essential to understand the impact of mitochondrial function on cell physiology and the impact of pathophysiological contexts on mitochondria if we are to make progress in understanding the processes that define these diseases.

生きた状態の細胞や組織を顕微鏡下で捉える、いわゆるライブセルイメージングは、細胞生理学の価値を切り開いて来た。ここでは、どの様なアプローチがミトコンドリアの機能解析に有効なのか？について述べてみたい。
ミトコンドリアは細胞の生と死に関して中核的な役割を担っている。細胞内情報伝達系に関わるミトコンドリアの役割を理解することは、故に細胞生理学の核心的な理解につながり、それは薬の開発にもつながると期待される。
ミトコンドリアの機能不全が病態メカニズムとして関わっている「病気」は増え続けている。
故に様々な「病気」を定義する過程を進んで理解しようとするならば、細胞生理学におけるミトコンドリア機能の影響力を理解すること、そしてミトコンドリアが関与している病態生理学の実情を理解することが非常に重要となる。

Fluorescence imaging has had a spectacular impact on our understanding of physiology, from details of molecular mechanisms and cell signalling pathways to the complexities of intercellular communication. The technical demands of microscopy and imaging have fostered a reductionist approach, driving the development of instrumentation with ever higher spatial and/or temporal resolution to explore function in cells, parts of cells or proteins. It seems that there is now a growth towards a more integrative approach, seeking to explore signalling pathways within tissues to explore ways in which signalling pathways identified at the cellular or subcellular level contribute to the complexities of organ system function.

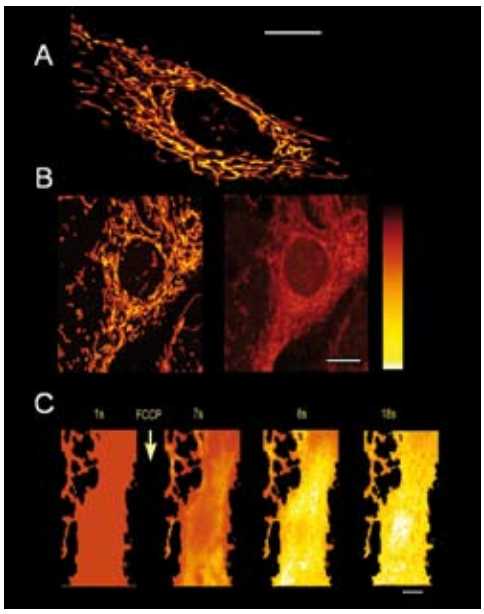

Fig. 1: Mitochondrial membrane potential (Δψm) measured with TMRM. A. An astrocyte loaded with TMRM (25 nM) at equilibrium illustrates accumulation of the dye into mitochondria. B. Collapse of Δψm using the ionophore FCCP (tight) promotes redistribution of the dye. C. Using the 'dequench' protocol, mitochondrial depolarisation and loss of dye from the mitochondria increases the fluorescence signal in the cytosol. In these images, extracted from a sequence, the images have been divided by the first image to show relative changes in signal.

Keywords:

mitochondria, intracellular calcium, FLIM, gluathione, NADH, mitochondrial potential

In approaches that were initially driven by the application of indicators of intracellular calcium concentration, we now have a huge armamentarium of physiological fluorescent indicators at our disposal that allow measurements of cytosolic calcium concentration, calcium concentration in specific compartments – in ER or mitochondria – intracellular magnesium, zinc, pH, membrane potential, secretion, redox state, free radical generation… and so the list goes on. Great advances have come from the ability to use probes with different spectral properties – arising from the availability of probes with excitation and emission spectra that range throughout the spectrum and in the exquisite optics of modern microscopes that allow simultaneous or near simultaneous excitation or emission of multiple wavelengths. Such advances are key to understanding the relationships between different aspects of signalling, allowing measurements of multiple variables at the same time and so the relationships between them.

Introducing Mitochondria

Our interests focus on understanding cellular metabolism, its interaction with other aspects of cell physiology and the role of disordered metabolism in pathological systems. Figure 2 shows a cartoon to illustrate the major mechanisms involved in driving mitochondrial oxidative phosphorylation. Mitochondrial function is central to so many aspects of cell physiology that it follows inevitably that mitochondrial dysfunction will lead to disease. Irreversible damage to mitochondria is key in defining the point of no return in ischaemic injury in heart, brain, kidney and no doubt other less studied tissues. More subtle aspects of mitochondrial injury are associated with diabetes, with many of the neurodegenerative diseases (including Parkinson's, Huntington's, Alzheimer's Diseases and motoneuron disease) and genetic mitochondrial dysfunction underlies the family of diseases encompassed by the mitochondrial encephalomyopathies. How then is it possible to investigate mitochondrial function in order to gain a better understanding of the mechanisms that underlie these horrible diseases? For a recent review see Duchen, 2004.

The great power of imaging (compared to traditional biochemical approaches) comes into its own where we want to compare mitochondrial and cell physiology in a heterogeneous cell preparation or an intact tissue or where the yield of cells available from a small structure does not allow standard biochemistry. Then we can identify the cells under the microscope and explore their physiology directly or compare the physiology of different cell types side by side.

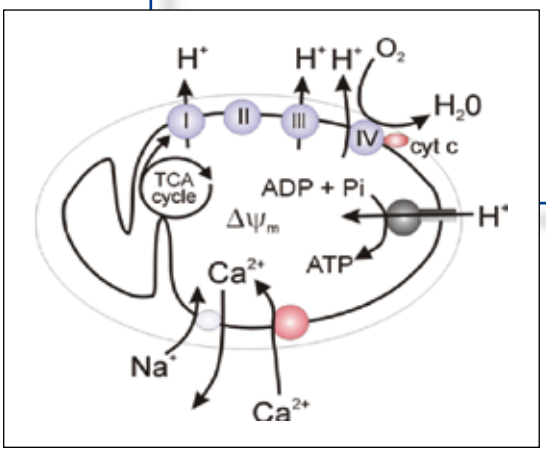

Fig. 2: Substrates enter the tricarboxylic acid (TCA; Krebs') cycle where NAD+ is reduced to NADH and FAD^{2+} to $FADH_2$. These are oxidised at the respiratory chain, which carries electrons to molecular oxygen. In the process, protons are translocated across the membrane, generating an electrochemical gradient expressed as a potential difference across the inner membrane ($\Delta\psi_m$), estimated at about 150 mV negative to the cytosol. The potential provides the energy to drive ATP synthesis, protein import and calcium accumulation.

Measuring Mitochondrial Membrane Potential

Fluorescence imaging provides a number of approaches to illuminate aspects of mitochondrial function. Perhaps the most widely employed measure of mitochondrial physiology is the measurement of mitochondrial membrane potential ($\Delta\psi m$). These measurements rely on dyes such as tetramethyl rhodamine methyl ester (TMRM) or rhodamine 123, lipophilic cations that partition between cellular compartments according to differences in potential. Mitochondrial potential dictates the rate of ATP generation, calcium accumulation and protein import. At very low (nM) concentrations, the dyes partition into mitochondria (Fig. 1A) so that fluorescence intensity is a simple function of dye concentration which is in turn a simple (logarithmic or Nernstian) function of potential. Under such conditions, it is possible to allow the dye to equilibrate and then make direct comparisons of potential between cell populations simply by measuring the intensity of signal from the mitochondria. Good examples of such applications include exploring the potential in cells from a mutant animal versus control, in cells treated with some agent versus control, changes in potential with time during the progression of apoptosis or measurements of potential in a cell transfected with a protein perhaps lying adjacent to a non-transfected cell where the impact of the protein expression on mitochondrial function is compared directly. It is important to stress that if high resolution imaging is used, the mean signal from mitochondria can be measured, with the background signal from the cytosol thresholded out. The measured signal is independent of mitochondrial mass or density – it is a function solely of the dye concentration within individual mitochondria and so will be brighter or darker according to potential, no matter how dense the mitochondrial network might be. The main limitation is in calibration – measurements can be quantitative and

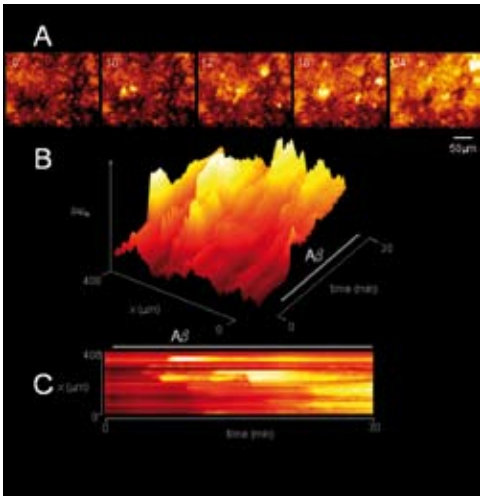

Fig. 3: Mitochondrial potential undergoes fluctuations in astrocytes following exposure to the amyloid β peptide (Aβ1-24) associated with Alzheimer's Disease. This is a mitochondrial response to fluctuations in intracellular calcium and oxidative stress following activation of the NADPH oxidase by Aβ. A shows images extracted from a time series (see animation of this series on line). B shows a representation of the changes in space and time, plotting the intensity profile along a line across the image. A surface view of the pot is shown as C. Each flash of signal represents transient mitochondrial depolarisation in a cell – the images were acquired at x20 magnification using a cooled CCD camera and include many cells (see Abramov et al., 2003, 2004).

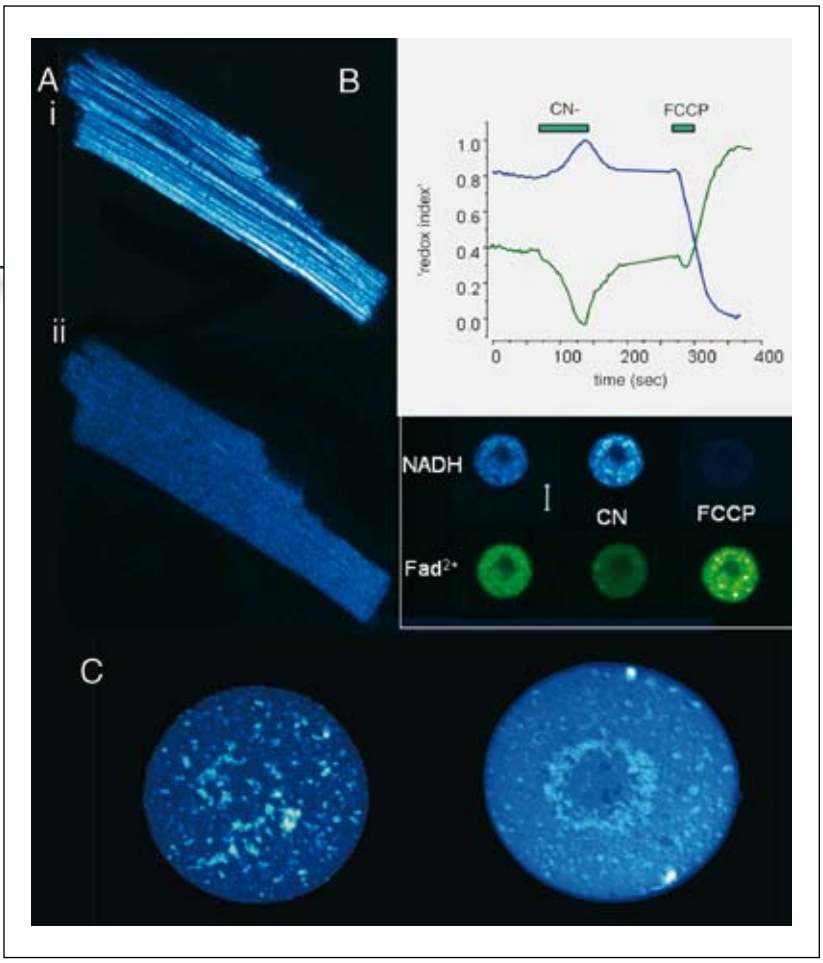

Fig. 4: NADH is imaged in cells. A an isolated ventricular cardiomyocyte shows NADH fluorescence from densely packed mitochondria which run parallel to the long axis of the cell. The mitochondrial signal vanishes after the cells are exposed to FCCP, which stimulates respiration and so oxidation of NADH. B. Mitochondrial NADH and flavoprotein signals are manipulated using CN to inhibit respiration and promote maximal reduction, and FCCP to promote maximal oxidation. Sample images (from an adipocyte) taken from a time series are shown below the plot of intensity with time in which the signals have been normalised to the maximally reduced ('1') and maximally oxidised ('0') levels. This cell shows a relatively reduced resting 'redox index'. C. In mouse oocytes, pyruvate (left) promotes oxidation of cytosolic NADH and reduction of the mitochondrial pool (the mitochondria are brighter against a darker background). Lactate promotes a strong cytosolic NADH signal (shown on the right) determined by LDH activity (Dumollard et al., 2007). Fig. 4a: the cell is about 100 microns in length. Fig. 4c: the cell is about 100 microns in diameter.

proper statistical comparisons made, but true estimation of potential is generally not practical or reliable.

In response to dynamic changes in potential during cell signalling, it is possible to follow the redistribution of the dye as mitochondrial potential is lost, but quantification is complex and requires identification of mitochondrial and cytosolic signals (Fig 1B). Instead, we often use an approach in which higher concentrations of dye are used. The concentration of dye within the mitochondria may reach a concentration at which the dye undergoes a phenomenon of autoquenching through the interaction of dye molecules or the formation of non-fluorescent multimers. Mitochondrial depolarisation then causes the redistribution of dye to the cytosol where the quench is relieved, causing a dramatic increase in fluorescence. This is often referred to as a 'de-quench' protocol and it is a useful way of amplifying changes in potential (Figs. 1C and 3). While this approach may be less rigorously satisfying than the former, but it has merit, in that it does not require high resolution imaging. We can image a field of cells at low power and follow changes in signal with time in response to a treatment. An increase in signal then gives an unambiguous measure of mitochondrial depolarisation without having to resolve individual mitochondrial structures (Fig. 3). This is not the place for a detailed treatment of the use of these dyes or comparisons between dyes and for this I refer those interested to Duchen et al., 2003.

Measuring (mitochondrial) Redox State

Measurements of mitochondrial redox state provide an invaluable further insight into mitochondrial metabolism. The mainstay of classical bioenergetics is the oxygen electrode. However, we are often faced with situations where the cell number is too small or cell populations are heterogeneous – say cells have been transfected with a protein and we have a mixture of transfected and non-transfected cells side by side on a cover slip. Mitochondrial respiratory rate is reflected in the redox balance of mitochondrial pools of NADH and $FADH_2$. These can be measured because in each case, only one member of the redox pair is fluorescent and so the fluorescence is related to the balance of $NADH/NAD^+$ (NADH is the fluorescent partner) or $FAD^{2+}/FADH_2$ (FAD^{2+} is fluorescent). While these are complex functions of the rate of oxidation by the respiratory chain and substrate supply, a decrease in $\Delta\psi_m$ associated with increased reduction of the pool must indicate an impaired respiratory chain, while if NADH is more oxidised it is likely that potential is reduced due to an increased ion flux across the membrane – a 'leak' or increased ATPase activity – which drives an increase in respiratory rate. On this note I must also make the point that a decrease in potential is not inevitably 'a bad thing' – it may simply point to higher ATP turnover.

NADH fluorescence is excited in cells or tissues using a UV light source with optimal excitation at 350 nm or with multiphoton imaging with excitation around 720 nm (Huang et al., 2002 – see Figs. 4 and 7). Emission is in the blue, with a peak at about 550 nm (Chance and Baltscheffsky, 1958). The fluorescence of FAD^{2+} is shifted by about 100 nm – we use the 458 line of an argon laser- and emission peaks at ~550 nm. Much of the basis for these measurements was established in the 1950's from the work of Britton Chance. With a Zeiss 510 LSM, 'multitracking' allows us to switch back and forth between these measurements so that the two signals are measured effectively simultaneously (Fig. 4B). It seems crucial to us to understand that the basal signal is meaningless without reference to landmarks that effectively define the dynamic range of the signal. We routinely use CN- to inhibit respiration and to push the redox system to its maximally reduced state after which the CN- is washed out to be replaced by an uncoupler, such as FCCP, which drives respiration to its maximal capacity and so promotes complete oxidation of the redox pairs (Fig. 4A, B). The position of the basal signal relative to these extremes then gives us a measure of resting redox state in the cell.

In most cell types, NADH is predominantly mitochondrial, and the majority of UV excited blue autofluorescence is derived from mitochondrial NADH. In the mammalian egg, which has an extraordinary metabolism, much of the NADH signal is cytosolic (Dumollard et al., 2006). This is defined by LDH activity. Figure 4C illustrates the way that the balance can be driven by either lactate (which promotes cytosolic NADH generation) or by pyruvate, which promotes oxidation of the cytosolic pool while it is taken up into mitochondria and promotes reduction of the mitochondrial pool. This approach has allowed a dissection of metabolic pathways in the egg to illuminate the metabolism of a cell type where the small numbers of cells available make routine biochemistry very hard or impossible.

We are still limited in interpretation of autofluorescence signals as it remains a complex task to tease out contributions to the signal from cytosolic versus mitochondrial components, while NADPH also has such a similar spectrum that it is not practically separable. One possible approach that might help separate these signals is fluorescence lifetime imaging, or FLIM. The collection of photons following excitation of fluorescence from a pulsed light source allows the tracking of the times of arrival of photons following the pulse. These are built into a time distribution to measure the decay rate constants of the excited signal (Fig. 5). Free NADH in solution has a mean lifetime of around 400 psec, while enzyme bound NADH has a mean lifetime of around 2 nsec. In cells it is possible to resolve lifetime distributions of NADH autofluorescence signals as (at least) bi-exponential fits with time constants representing these two forms and giving remarkably similar values (Fig. 5). The measurements remain time consuming, but as the technology develops, perhaps this approach will allow further exploration of the factors that determine the balance of free and bound NADH pools.

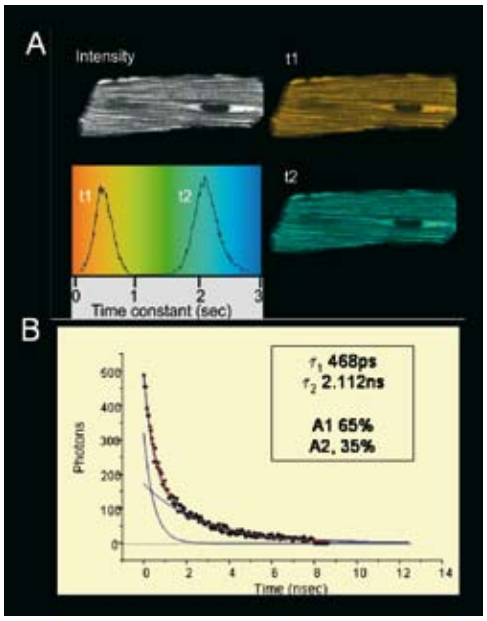

Fig. 5: Lifetime imaging differentiates pools of bound and free NADH. Lifetime images of NADH in an isolated ventricular cardiomyocytes were acquired using a Zeiss NLO system, Coherent chameleon laser (at 720 nm), collecting fluorescence between 435-485 nm using a Becker and Hickl TSCPC system. The lifetime signal was well fit by the sum of two exponentials (shown for a single pixel in B). As the cell is packed with mitochondria, the bulk of signal is mitochondrial and the distribution lifetimes reflects mitochondrial NADH. 65 % of the signal arose from the short lifetime form (free NADH). The images show the intensity distribution, the distribution of lifetimes at tau 1 and tau 2 and the distribution histograms for signals at tau 1 and tau 2.

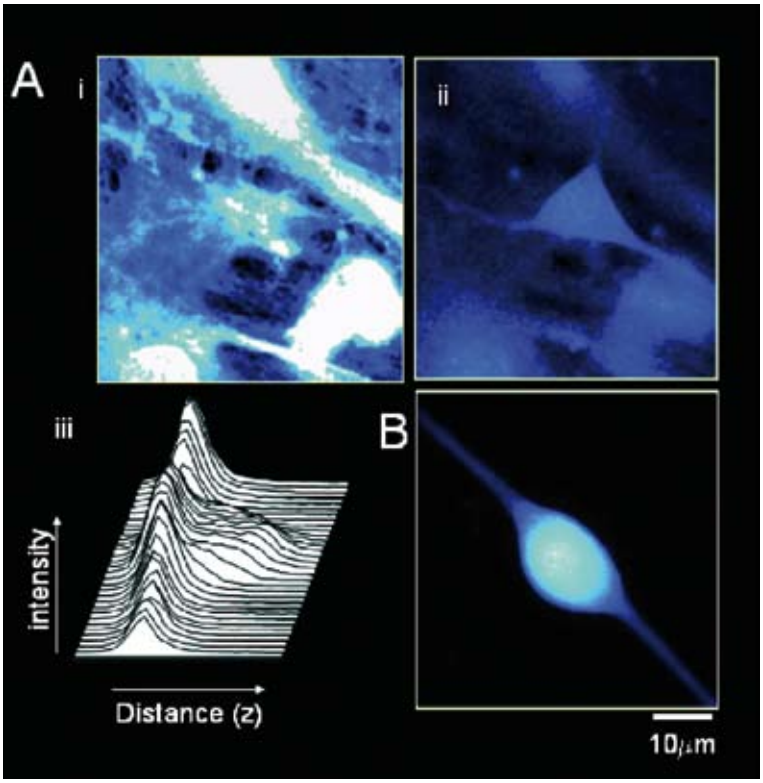

Fig. 6: Measurements of glutathione using monochlorobimane (MCB). A. images from a Z-stack from a preparation of hippocampal neurons and astrocytes in co-culture. The Z-stack passes first through the astrocytes (i) in which the signal is close to saturation. At higher focal planes, the neurons become visible (ii) and show a much lower signal confirming that astrocytes have a much greater GSH content than neurons. The intensity in Z is plotted through the stack in iii. Thus, measurements can be made in different cell types growing side by side in the same culture. The image in B is a projection of a z-stack showing MCB fluorescence in a neuron in culture.

Glutathione and Oxidative Stress

Mitochondrial dysfunction is inextricably linked with changes in cellular redox state and possibly with oxidative stress. Damage to the respiratory chain can increase electron leak from the respiratory chain generating superoxide anion, while oxidative stress due to generation of oxygen free radical species may deplete cellular antioxidant defences including glutathione. Glutathione depletion in turn alters the redox balance of the cell and causes mitochondrial dysfunction in neurons (Vesce et al., 2005) and can cause cell death. A number of probes are used to follow the generation of oxygen radical species, including hydroethidine and carboxyfluorescein and the mitochondrially targeted hydroethidine derivative, mitoSOX. All are non-fluorescent derivatives of a parent fluorescent dye (ethidium, fluorescein) and are oxidised to the fluorescent product by free radical species. A number of probes based on fluorescent proteins are now available whose fluorescence changes according to a change in redox state, but none of these is in widespread use and their relative merits remain to be established.

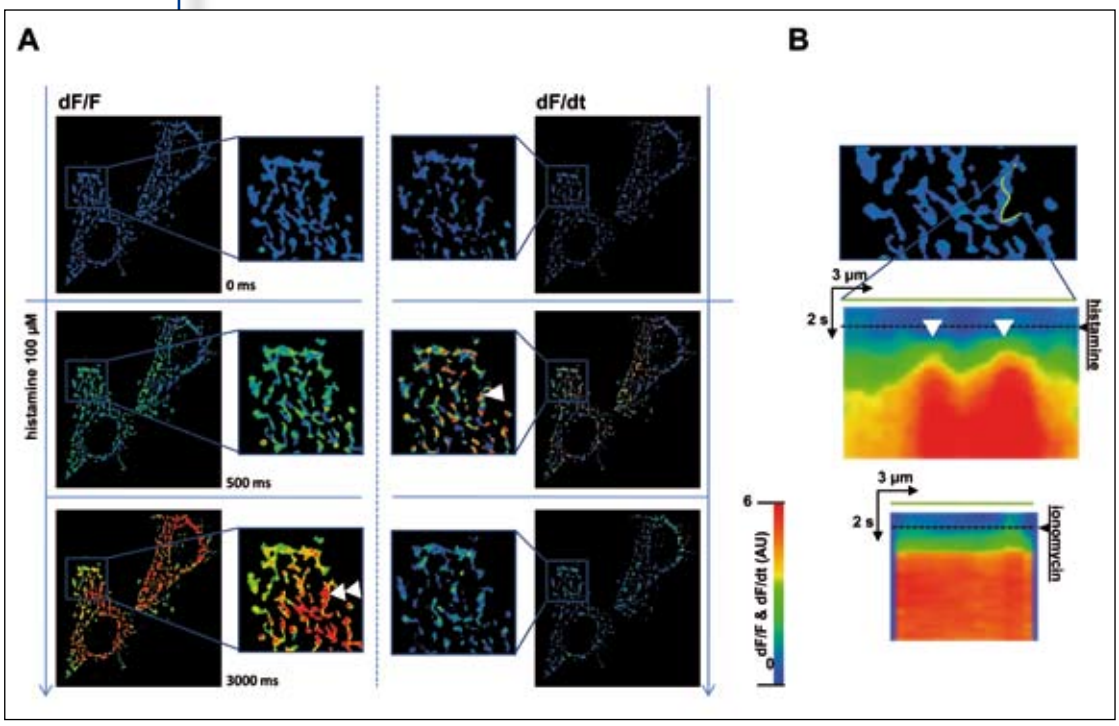

Fig. 7: Preferential Ca2+ uptake sites and intramitochondrial Ca2+ waves in the mitochondrial network of HeLa cells. Cells transfected with a mitochondrial targeted ratiometric pericam probe (2mtRP; Filippin et al., 2005), were stimulated with histamine which promotes IP3 mediated Ca2+ release from the ER. The probe was excited at 410 nm and images acquired using a back-illuminated CCD camera. A: pseudocolored time series shows changes in intensity (dF/F, left panel) and the velocity of changes (dF/dt). Ca2+ uptake sites are visible as red spots at the time of fast Ca2+ uptake into mitochondria (white arrowhead), followed by Ca2+ waves spreading through the mitochondrial network (double white arrowhead). B: Linescan analysis of 2mtRP fluorescence intensity along a long mitochondrial profile (upper panel). Preferential Ca2+ uptake sites are labeled with white arrowheads (middle panel). The propagation of the Ca2+ waves is represented by the spread of the high [Ca2+] area (shown as red). The Ca2+ ionophore ionomycin caused evenly distributed high Ca2+ throughout the mitochondrial pool (lower panel). Modified from Bianchi Szabadkai et al., 2005.

Monochlorobimane (MCB; Fig. 6) is a dye that allows us to obtain a measure of reduced glutathione (GSH) in cells as a one off snapshot (Keelan et al., 2001; Fig. 5). It is conjugated with glutathione through a reaction catalysed by glutathione-s-transferase, generating a fluorescent product. At a steady state, the fluorescence signal therefore reflects the GSH content of the cell. As in the process GSH is bound to the MCB, it can also be used to rapidly deplete GSH (Vesce et al., 2005) to explore the consequences of GSH depletion. The MCB signal seems to give a reliable indicator of oxidative stress and in our hands a decreased MCB signal correlates well with other measurements of increased free radical generation (see Abramov et al, 2003, 2007).

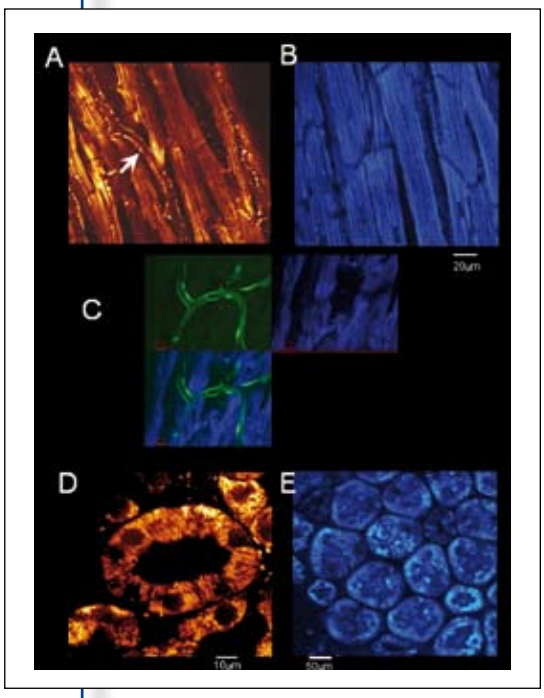

Fig. 8: Images obtained using multiphoton excitation in intact tissues. A and B show the signal from an isolated Langendorff perfused heart loaded with TMRM through the coronary arteries. A shows the distribution of mitochondria in the ventricular cardiomyocytes. Note the loading of mitochondria in endothelial cells lining a blood vessel (arrow). B shows the NADH fluorescence signal from a similar preparation. C. Calcein AM perfused into the coronary artery loaded first into endothelial cells lining the vasculature (green), seen against the blue NADH fluorescence. D and E: images of mitochondria in renal tubules in an acute slice preparation of rat kidney. D shows a high power image of the TMRM signal from proximal tubule. Mitochondria are enriched at the basal pole of the cells. E shows a lower power view of the distribution of NADH in the renal cortex. Mitochondrial structure, distribution and signal vary between different components of the tubule. (Courtesy of Sean Davidson and Andrew Hall)

Calcium

The electrogenic accumulation of calcium into mitochondria through the uniporter has been a source of great research interest for many years. By removing calcium from microdomains of cytosol, mitochondria act as spatial buffers and contribute to the subtle spatiotemporal patterning of calcium signals. Conversely, mitochondrial calcium accumulation plays a major role in regulation of mitochondrial metabolism and excess calcium accumulation is key as a trigger to cell death (for review, see Duchen, 2004). Measurements of calcium uptake remain more difficult. Key measurements were made using aequorin luminescence, but this requires populations of cells and so contains no spatial information (Rizzuto et al., 1992). Fluorescent dyes such as rhod-2 and x-rhod-1 have a positive charge in their membrane permeant form and so tend to accumulate in mitochondria, but this is variable and generally unreliable. Usually, enough dye remains in the cytosol that if cytosolic calcium becomes very high, it can be almost impossible to discern a specific mitochondrial component to the signal. The recent introduction of fluorescent protein based calcium sensors targeted to mitochondria has made such measurements much more reliable (Fillippin et al., 2005; Szabadkai et al., 2004; Fig 7). If these signals can be measured simultaneously with a cytosolic calcium indicator, it becomes possible to directly relate local calcium signals to local mitochondrial calcium uptake.

Into the Future?

Most imaging in cell physiology has required cells grown in culture. We have recently been exploring the use of tissue slices or intact isolated perfused organs. In tissue slices, the better tissue penetration of multiphoton imaging can be wonderful, although standard fluorescent dyes usually penetrate only a few cell diameters into the tissue. In an intact perfused organ system, dyes introduced through the vascular system reach the tissue more effectively (Figs. 8, 9), although tissues such as kidney and liver have anion pumps that remove the dyes efficiently, so that effective loading requires inhibition of the pumps with probenecid or sulphinpyrazole. Nevertheless, the potential power of such approaches is surely obvious, as it becomes possible to explore cell signalling pathways in an intact tissue. In the isolated perfused heart, movement is obviously a major problem, but it is possible to watch changes in mitochondria, redox state and calcium in ventricular cardiomyocytes and in the vasculature directly during ischaemia (Fig. 8, 9). Imaging kidney slices (Fig. 8) or the intact perfused kidney allows a direct exploration of the metabolic specialisations in different parts of the nephron. The beauty of such an approach is that it becomes possible to explore changes in physiology in multiple cell types within the tissue simultaneously.

The development of protein based fluorescent probes that can be targeted selectively to make measurements from discrete cell populations or compartments is perhaps the most exciting and important current advancing field. This approach also avoids the use of AM ester based reporters which are hard to load into tissues *in vivo*. The expression of such probes in intact tissues and animals, from nematode or drosophila to transgenic mice, promises to take us to new levels of understanding. Currently, both the range and quality of such probes and the availability of transgenic animals is limited, but it is an area which is growing so fast that in a few years time, it seems obvious that such experimental approaches will be commonplace.

Surely the ultimate goals of such imaging approaches must lie in translating the findings in isolated cells and tissues to intact organisms, and, ultimately, to people. For example, we have argued that mitochondrial state is critical in reperfusion injury in the heart, in the brain in glutamate toxicity or in the neurodegenerative diseases. Can we find ways to make such measurements in intact people so that we can track the development of such pathology in a human subject?

Acknowledgements: work in my lab is funded by grants from the Wellcome Trust, MRC, EU Marie Curie.

With thanks to Andrey Abramov, Andrew Hall, Remi Dumollard, Gyuri Szabadkai and Sean Davidson for providing images.

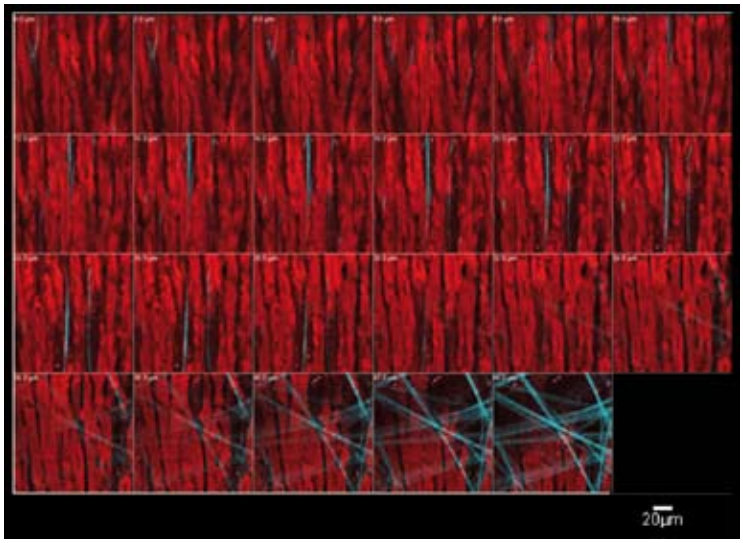

Fig. 9: An image series of a Z-stack of ventricular muscle of the isolated Langendorff perfused heart loaded with TMRM (ex 900 nm) by perfusion through the coronary artery. At the surface, collagen fibres are seen by second harmonic imaging at 450 nm. The collagen fibres are stretched and straight, but show tortuous patterns when cardiac filling is impaired. (Courtesy of Sean Davidson)

[1] Abramov AY, et al., J Neurosci., 23(12):5088-95. (2003)
[2] Blinova K, et al., . Biochemistry., 44(7):2585-94. (2005)
[3] Chance B, Baltscheffsky H. , J Biol Chem, 233(3):736-9. (1958)
[4] Duchen MR, Methods Enzymol, 361:353-89. (2003)
[5] Duchen MR. Mol Aspects Med. 25(4):365-451. (2004)
[6] Dumollard R, Development., 134(3):455-65. (2007)
[7] Filippin L, et al., Cell Calcium., 37(2):129-36. (2005)
[8] Keelan J et al., J Neurosci Res., 66(5):873-84. (2001)
[9] Rizzuto R, et al., Nature, 358(6384):325-7, (1992)
[10] Szabadkai G, et al., Mol Cell., 16(1):59-68. (2004)

Author Biography

Michael Duchen studied medicine and practiced as a physician for some years before moving to UCL where he did a PhD with Tim Biscoe. Starting out with electrophysiological studies, he became interested in cellular responses to hypoxia which led to an interest in mitochondrial biology and the impact of mitochondria on other aspects of cell signaling. The lack of available methodology to study mitochondria within cells led to adventures in fluorimetry and later to fluorescence imaging. He is a Professor of Physiology at University College London where he is now coordinator of a mitochondrial biology consortium, and retains a broad interest in comparative cell physiology, cell signalling and imaging technologies.

Contact:

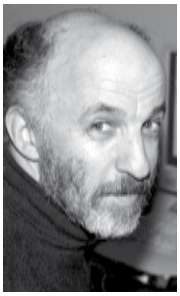

Michael Duchen, PhD
Professor of Physiology
University College London
Tel.: 44 207 679 3207
Fax: 44 207 813 5007
m.duchen@ucl.ac.uk
www.physiol.ucl.ac.uk/research/duchen_m

Bringing to Light

Form and Function in Animal Development

Our view of development has come to life. Developmental biologists used to rely solely on static images of fixed preparations taken at different stages to infer information about dynamic events during morphogenesis. Now, new developments in microscopy are providing a real-time view of dynamic processes of animal development and new answers to old questions are emerging. The explosion of tools available for live cell imaging is having a tremendous impact on what can be studied and quantified, leading to a huge refinement in our knowledge of how complex developmental processes are orchestrated at the tissue, cell and molecular level. In this review, I will describe some of the advances in microscope technology that have impacted our understanding of both morphological and physiological changes in living embryos.

「発生」を知ることは、生命そのものを知ることにつながっている。かつて発生生物学は、もっぱら異なる発生段階での固定サンプルに頼り、形態形成の過程でのダイナミックな変化を推論してきた。今日、顕微鏡技術の進歩は動物発生におけるダイナミックな変化をリアルタイムで明らかにし、古くからの疑問に対する答えを明らかにしてきている。ライブセルイメージングのためのツール（機器）の急増は、「何を調べて、そして定量化すべきなのか？」ということに関して、素晴らしいインパクトを与えてきており、組織、細胞そして分子レベルにおいてどんなに複雑な発生過程が統制されているのか？そのことに関する莫大な、洗練された知識に我々を導いてくれる。このレビューでは、生きた胚における形態的変化、生理的変化の両方の理解のために重要な、先端的な顕微鏡技術について述べてみたい。

Keywords:
cardiovascular development, cell tracking, morphogenesis, multiphoton microscopy

Introduction

Advances in microscopy technology and fluorescent reporters are providing fascinating new insights into dynamic developmental mechanisms. Microscopy has been used to answer fundamental questions about embryonic development since the days of Leeuwenhoek, Malpighi and Swammerdam in the 17th century (see (1)), but until recent years, microscopes have mostly been tools to observe changes in anatomy in either live or fixed embryos. Today's microscopy offers a dynamic, real-time perspective of developmental physiology, offering ways to not only reveal molecular and physical events but to quantify and correlate these processes. A fundamental question in developmental biology relates to how morphogenetic movements and cell differentiation are controlled by cell signaling events. Our knowledge of the interconnections between different signaling pathways continually increases and we now know that the genetic control of morphogenesis has complex feedback loops that involve mechanical as well as biochemical signals (2). Integrating information about physical forces and developmental signaling cascades has been a challenging pursuit in developmental biology, but the development of more sophisticated methods to probe these interactions is clearly providing new tools for researches. For instance, significant advances using optical microscopy have been recently made, which have greatly aided in understanding morphogenesis by providing better tools to quantify dynamic events and visualize cell signaling pathways in real time, bringing both anatomy and physiology into focus. This review will discuss some of the recent works where advancements in vital, optical microscopy have provided insights into the causal relationships between form and function.

Quantitative Imaging of Functional Changes in Cardiovascular Function

The cardiovascular system is the first organ system to become functional during vertebrate development. The heart and vessels are formed soon after gastrulation, and continual changes in heart structure and the circulatory network are made as new organs are formed and sources of nutritive support change as the embryo matures. There is great interest in understanding how the heart functions as its three-dimensional form changes, and how cardiac function is integrated with the

cell signaling cascades necessary for morphogenesis (3). The difficulty in answering these types of questions, in part, has been due to the lack of complete, real-time, 4-d models of the embryonic heart during development and the means to make quantitative measurements of functional changes. Since the embryonic heart beats 2–3 times/sec. and moves blood at mm/second rates, high resolution optical imaging methods such as confocal microscopy have traditionally lacked sufficient speed to capture 3-d optical sections fast enough to render interpretable 4-d models.

Recently, new developments in optical microscopy have provided a number of ways to image the beating heart and these studies have revealed some exciting insights into embryonic cardiovascular function. Traditional single point scanning confocal systems offer excellent optical sectioning capability but have slow image acquisition rates (~5 frames/second for 512 x 512 pixels). Multipoint scanning confocals, such as Nipkow spinning disk systems (4, 5) or slit scanning systems that scan an entire line of pixels at once (6–8), can image at faster speeds for studying rapid dynamic processes, but with reduced resolution at depth compared to single point-scanning systems. Recently, a slit-scanning system capable of imaging at 120 frames/sec (512 x 512pixels) has been developed that also offers excellent rejection of out-of-focus light (9–11). Using this microscope system (Zeiss LSM 5 LIVE) in conjunction with non-gated slice-sequence synchronization, we have been able to generate 4-d reconstructions of the beating, embryonic zebrafish heart (9, 10, 12). By imaging transgenic embryos expressing GFP in the blood cells, the endocardium or in the cardiomyocytes, it was possible to use these images to quantify blood flow and volume changes and to track the motion of contracting cardiomyocytes (Fig. 2) in the heart at several stages. These studies have revealed the following: that the embryonic zebrafish heart tube functions as a dynamic suction pump (12), that there is significant regurgitation of blood between chambers once they begin to form (10), and that functional valves do not form in the zebrafish embryonic heart until 111 hours post fertilization (10). Thus, the introduction of rapid confocal microscopy has revealed new information about early heart development in normal embryos and is a promising new way to assess embryonic heart function in mutant embryos. In addition, this system is ideal for studying other fast processes like calcium signaling and the mobility of intracellular molecules (11), providing an ideal tool for studying both dynamic changes in morphology and physiology.

Rapid confocal imaging with the LSM 5 LIVE has also enabled our group to track the trajectories of individual blood cells moving through the circulatory system in both zebrafish and mouse embryos (12); Lucitti, Vadakkan and Dickinson, unpublished, (Fig 1). Mouse embryos can be removed from the uterine environment and can undergo normal development while on the microscope stage permitting dynamic imaging using confocal microsopy (13). Previous measurements of the shear stress exerted by blood flow in early mouse embryos have been made using a point-scanning confocal system by scanning rapidly along a single line across the vessels to both record the velocity of moving blood cells and measure the hematocrit (14). This improvement in speed afforded by the slit-scanning system makes it possible to collect a series of full images, providing information about the number of flowing erythroblasts, their speed and the individual trajectories of moving cells (Fig. 1). Recently, we have also shown that the remodeling of yolk sac vessels in the mouse and the expression of eNOS in embryonic vessels is dependent on hemodynamic force (15), allowing us to begin to understand how endothelial cell signaling is regulated by blood flow in living embryos.

In addition to rapid confocal microscopy, another method – Selective Plane Illumination Microscopy (SPIM) – has also emerged as a way to image cardiac function in zebrafish embryos (16). In SPIM, a tomographic projection is made by illuminating the sample with a sheet of light and collecting fluorescence data orthogonal to the illumination plane (17). The living sample is embedded in transparent media and rotated during collection, allowing it to be imaged from many angles to produce a 3-d volume rendering. High resolution images, comparable to those obtained with confocal microscopy, can be obtained without the speed restrictions imposed by point-scanning systems. Recently, a second generation SPIM system – multidirectional SPIM (mSPIM) – has been reported that corrects some of the artifacts created by absorption and scatter encountered in the original SPIM configuration (18). SPIM has been used to create high resolution 3-d images from fluorescently labeled, live Medaka fish larva (17), Drosophila embryos (17) and microtubule asters in living yeast cells (19) and has recently been used to analyze cardiac conduction waves in kcnh2 mutants, a zebrafish model for long QT syndrome, providing insights into human arrythmias (16).

Although it is possible to image through the entire heart of developing zebrafish embryos with high spatial and temporal resolution, limits to the depth penetration of confocal microscopes make it difficult to obtain complete 4-d reconstructions of the embryonic heart in other species that more closely resemble human development, such as avians or mammals. The answer to this problem may be Optical Coherence Tomography (OCT). OCT has been shown to be an effective tool for imaging through highly scattering embryos with 5–15 µm axial resolution over a depth of several millimeters (20–22). In OCT, the image is formed by measuring backscattered infrared light from a tissue of interest within the coherence length of the source using an interferometer. Since IR light is used, OCT imaging is not damaging to cells and does not

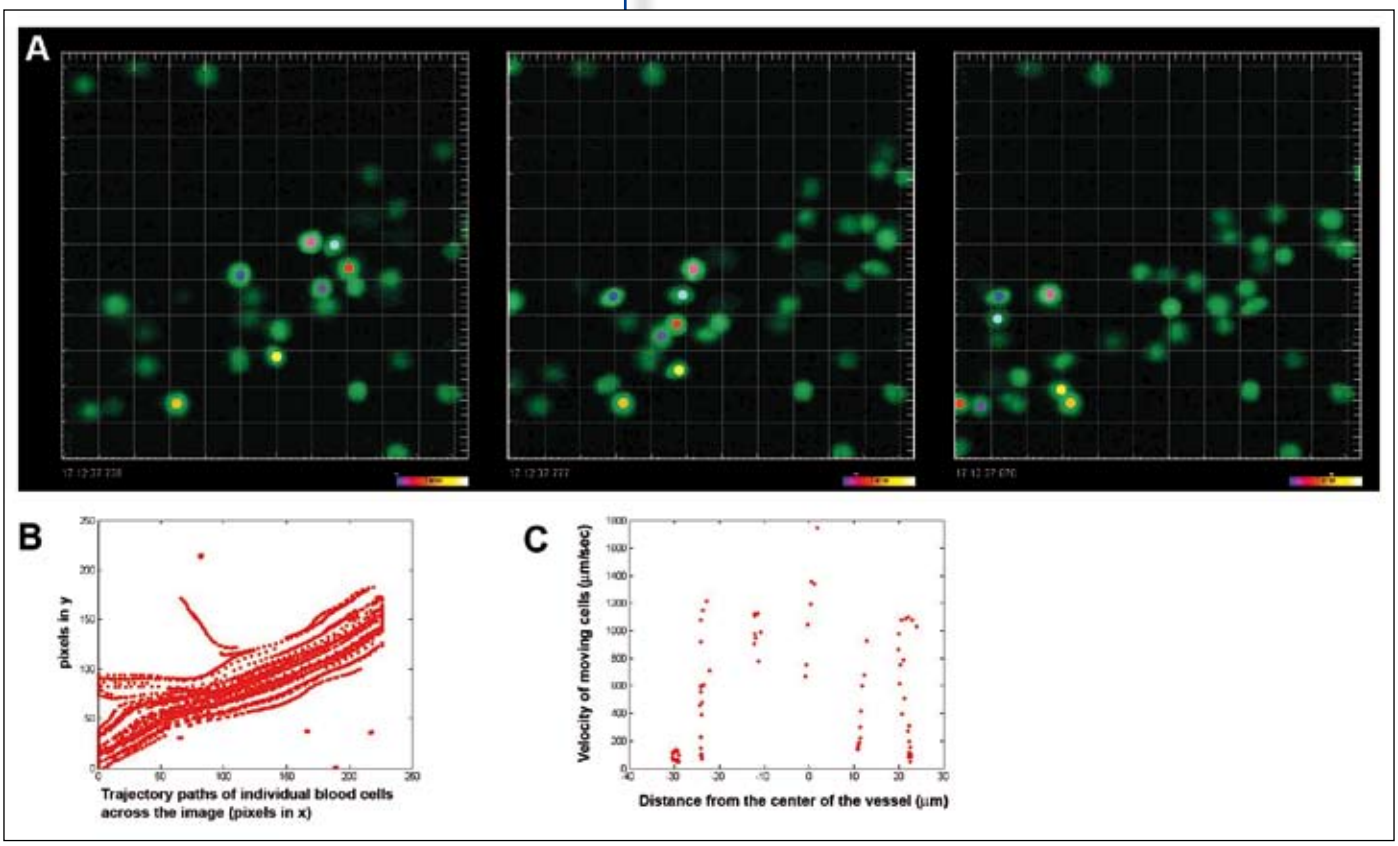

Fig. 1: LSM 5 LIVE imaging of blood flow in an 9.5 dpc Tg(epsilon-globin-GFP) mouse embryo. (A) Three images extracted from a 232 ms time sequence where images were taken every 4.5 ms. The three panels are 10 images apart in the sequence. Colored dots show that individual blood cells can be easily followed from frame to frame. Each blood cell is roughly 10 µm in diameter and the grid spacing in the image is 20 µm for the major gridlines. The trajectories of all the blood cells passing through this vessel during the course of the movie are shown in (B). In (C), maximum blood cell velocity (µm/sec) was plotted vs the distance from the center of the vessel to show that a laminar-like flow profile is observed. Cell tracking was performed using Imaris 5.0.1 (Bitplane A.G.) and velocity analysis was performed using MatLab R2006a (MathWorks, Natick, MA).

require additional contrast agents to resolve structures at cellular resolution. Rollins and colleagues have recently used OCT to produce 4-d reconstructions of the beating, embryonic quail heart (23). By gating the image collection with a laser Doppler velocimeter, 4-d images of the looping heart tube of an embryonic quail heart were made from 8 distinct phases of the cardiac cycle (23). Even without the addition of contrast agents, it is clearly possible to identify the myocardial and endocardial layers and the blood cells in these images, providing enough information to make estimates of volume and output changes. OCT imaging continues to improve in speed and resolution (24–26), and with continued emphasis on the development of appropriate contrast agents (27, 28), OCT holds much promise as a tool for imaging many different aspects of embryonic development.

Quantitative and Functional Analyses of Gradients that Specify Positional Information using Multiphoton Microscopy

Vital, time-lapse analysis using multiphoton or two-photon laser scanning microscopy (MPLSM or TPLSM) has become a commonly used tool for studying embryonic development (29, 30). With this method, one can achieve spatial resolutions within the image plane of about a micron, but with greater depth penetration and less specimen damage than confocal microscopy. These properties make it possible to make repeated measurements in live tissue with consistent results. Although MPLSM has been used for a number of different applications in developmental biology, two recent reports have used quantitative MPLSM to quantify the Bicoid (Bcd) morphogen gradient in early Drosophila embryos (31, 32). It has long been known that immunostaining for Bcd, a homedomain transcription factor, reveals a graded pattern of protein in the recently fertilized embryo and that Bcd establishes positional information in a concentration dependant manner (31–35). What has remained a mystery is how the Bcd gradient is established so quickly after fertilization and how the gradient is established with such tremendous reproducibility, despite change in cell division and variation in embryo size. Using a Bicoid-GFP fusion protein that recapitulates the properties of endogenous Bcd, the authors directly measure the amount of Bcd protein within each nucleus of living embryos with MPLSM. They show that the Bcd gradient is initially established very rapidly, despite slow diffusion rates, and levels of Bcd in the nucleus are modulated during the cell cycle, with Bcd moving out of the nucleus during mitosis. But after each division, the level of Bcd returns to a reproducible level, appropriate for the position of that nucleus in the gradient, showing only 10% variation from the level in the previous cell cycle (32). In a companion paper, the authors go on to show that Hunchback transcription, a Bcd target, also shows remarkable precision with the same level of accuracy of 10% (31). These groundbreaking studies have reported quantitative data, a morphogen in action and establish the methods

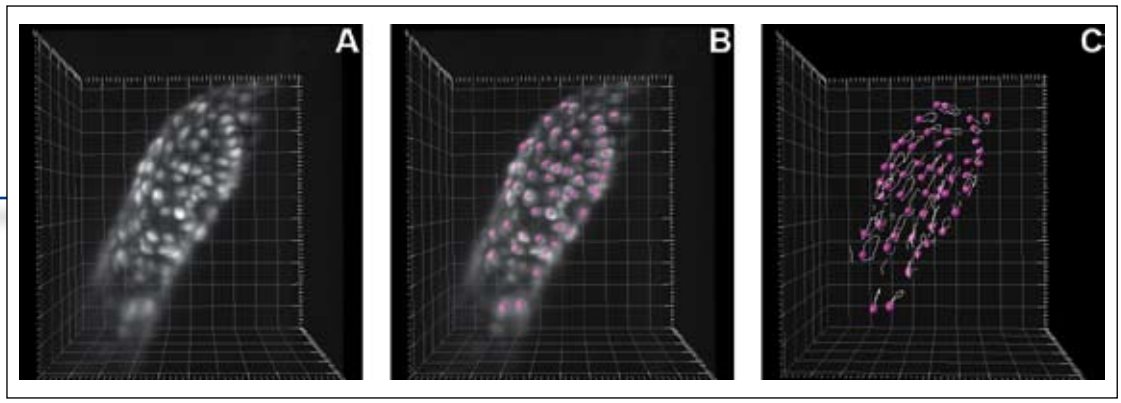

Fig. 2: Tracking muscle contraction in 4-d. (A) A single image from a 4-d reconstruction of a Tg(cmlc2:egfp) (52) embryo at 26 hpf. Each myocyte can be identified (B) and tracked over time (C). As in (12), data were acquired by A. Forouhar using a Zeiss LSM 5 LIVE fast confocal microscope at 151 frames per second, reconstructed into 3D volumes via programs written by M. Liebling, and rendered using Imaris (Bitplane A.G.).

needed to begin to understand how such morphogen gradients are established in living cells to control positional information and cell fate determination.

MPLSM first emerged as a point-scanning method (36), but as discussed above, point scanning can be very slow. Recently, a number of different design configurations for rapid multiphoton imaging have been developed (reviewed in (37)). Advances in this area have mostly been motivated by the need for higher speeds to address various aspects of neuronal signaling, but it is only a matter of time before these systems are used for imaging live embryos. Given the example above, where Bcd levels are so rapidly and precisely regulated to produce the proper gradient, one can easily see how increased frame rates may be very useful in elucidating the molecular mechanisms underlying the Bcd gradient.

Dissecting Morphogenetic Movements with Nonlinear Microscopy

MPLSM is one of several microscopy techniques that make use of the non-linear events that can be produced by pulsed, femtosecond IR lasers. Another type of non-linear microscopy is also gaining popularity for imaging developing embryos. Second and Third Harmonic Generation (SHG and THG) microscopy utilizes the frequency up-conversion that occurs in specific materials exposed to a high photon flux, producing light at half (SHG) or a third (TAG) the wavelength. This process, like multiphoton excitation, depends on the square (or cube) of the intensity of the incident light, only producing signal at the focal plane and providing optical sectioning without a pinhole. In biological tissues, SHG and THG signal is produced by structural molecules, like collagen and myosin (38). Because the process is non-absorptive utilizes infrared light and the contrast depends on distribution of endogenous molecules in the tissue, higher harmonic generation microscopy (HHGM) is a non-destructive method that does not require any added contrast agent.

HHGM is an effective method to image sub-cellular structures in live zebrafish embryos with over a millimeter of penetration, producing little damage to the embryo and permitting long term time-lapse imaging (39). THG has also recently been used to track the movements and trajectories of lipid droplets within Drosophila embryos and other tissues (40), improving on previous methods that compromised the normal development of the embryo (41). Lipid containing vesicles undergo dynein-driven transport prior to gastrulation and are thought to play an important role in the availability and delivery of signaling factors (42). The development of vital tracking methods is a necessary step to understand the role of lipid bodies in developmental signaling and the control of morphogenesis.

Another study has reported the combined use of two-photon excitation, third harmonic imaging and the use of high-repetition rate nanojoule pulses to perform laser ablations in Drosophila embryos to investigate the role of mechanical force during gastrulation (43). Previous studies have suggested that mechanical force during gastrulation plays a role in regulating gene hierarchies needed for the formation of mesoderm-derived tissues such as muscle (44). To further test this hypothesis, Supatto and colleagues disrupted gastrulation by ablating cells in the blastoderm using high-energy femtosecond pulses. Cell movements were tracked quantitatively using two-photon and THG microscopy, showing that morphogenesis was indeed disrupted. These perturbations led to a down regulation in a key transcription factor needed for mesoderm development in cells distant from the ablated region, but not adjacent to the ablated region, leading to the conclusion that transcription is dependent on local force interactions during gastrulation.

New Probes Bring Exciting Ways to Track Cells and Elucidate Lineage Relationships

It is probably close to impossible to find a developmental biologist that is not using a green fluorescent protein variant in his or her lab to answer some question about morphogenesis. Fluorescent proteins (FPs) have revolutionized live embryo imaging and have brought a wealth of new techniques to understand lineage relationships in the embryo. The advent of multiple fluorescent pro-

tein variants (45) combined with recent developments in microscopes that permit multispectral imaging analysis (see [29]) now make it possible to follow multiple cells at once in a time-lapse experiment, or to image different behaviors, like mitosis and membrane dynamics, by targeting different fluorescent proteins to distinct subcellular compartments. Some investigators have used 4 (46) and 5 (47) different fluorescent proteins in a single embryo preparation, using multispectral imaging to distinguish each individual FP variant.

In addition to using multiple colors in a single experiment, photoactivatable fluorescent proteins (PA-FPs) (48) provide an exciting opportunity to label whichever cell one chooses, and follow its fate. A comparison of different PA-FPs was recently carried out in avian embryos to determine the relative benefits of PAGFP, PSCFP2, KikGR and Kaede for vital time-lapse imaging (49). One drawback to the use of all the PA-FPs tested in this study was that photoconverted cells were not visible beyond 48h after conversion, limiting their use for any long-term analysis of cell fate. In contrast to this report, Wacker et al have recently shown that EosFP, a highly stable photoconvertable FP (50), is stable for 2 weeks after green to red photoconversion in Xenopus embryos (51). With efficient protocols in hand for tracing lineage relationships in the embryo with high-resolution, optical activation, there are countless new additions that can be made to current fate maps, furthering our knowledge of how cell diversity is achieved during embryogenesis.

Conclusion

It is truly an exciting time to be both a microscopist and a developmental biologist. The examples above clearly show that the developmental biology community is poised to employ new methods to study morphogenesis in living embryos. The ability to record functional changes in rapid processes, to quantify signaling events and to dissect the role of physical forces in living, developing animals are offering groundbreaking opportunities to unlock the mysteries that coordinately regulate form and function. And it is not just the embryologists that benefit. The lessons that are learned from embryos are offering profound insights into tissue engineering, stem cell therapies, growth control, cancer and even aging.

References:

[1] Gilbert, S.F. : Sinauer Associates, Inc. Publishers, Sunderland, Mass., 2006 (http://8e.devbio.com/article.php?ch=7&id=65).

[2] Ingber D.E., Faseb J. 20, 811 (2006).

[3] Schoenebeck J.J., Yelon D., Semin Cell Dev Biol 18, 27 (2007).

[4] Inoue, S., Inoue T., Cell Biological Applications of Confocal Microscopy 70, 87-93 (2002).

[5] Petran M., et al., Journal of the Optical Society of America 58, 661 (1968).

[6] Brakenhoff G.J., Kino G.S., J. Microsc. 165, 139 (1993).

[7] Corle T.R., Kino G.S.: Confocal scanning optical microscopy and related imaging systems, 1996, 97.

[8] Sheppard, C.J., Cogswell C.J.: Confocal Microscopy, Academic Press, London, 1990, 143-169.

[9] Liebling M., et al., J. Biomed. Opt. 10, 054001 (2005).

[10] Liebling M., et al., Dev. Dyn. 235, 2940 (2006).

The complete list of references is available within the online version.

Author Biography

Dr. Mary Dickinson began studying embryonic development as an undergraduate at Vanderbilt University, working with Dr. Brigid Hogan. Her work as a graduate student, mentored by Andrew McMahon, focused on understanding cell signaling events during central nervous system development using mouse and chick embryos. After extensive training in embryology, she joined Scott Fraser's group at Caltech to develop imaging strategies for studying dynamic events in vertebrate development and has developed many innovative strategies for using multiphoton, multispectral and rapid confocal microscopy to study mouse and zebrafish development. She has published over 50 primary research articles, reviews and book chapters in these areas and is a primary inventor on two patents.

Contact:

Mary E. Dickinson, PhD
Assistant Professor of Molecular Physiology and Biophysics
Baylor College of Medicine, Houston, USA
Adjunct Assistant Professor of Bioengineering
Rice University
Tel.: ++1 713 798 2104
Fax: ++1 603 804 8011
mdickins@bcm.tmc.edu

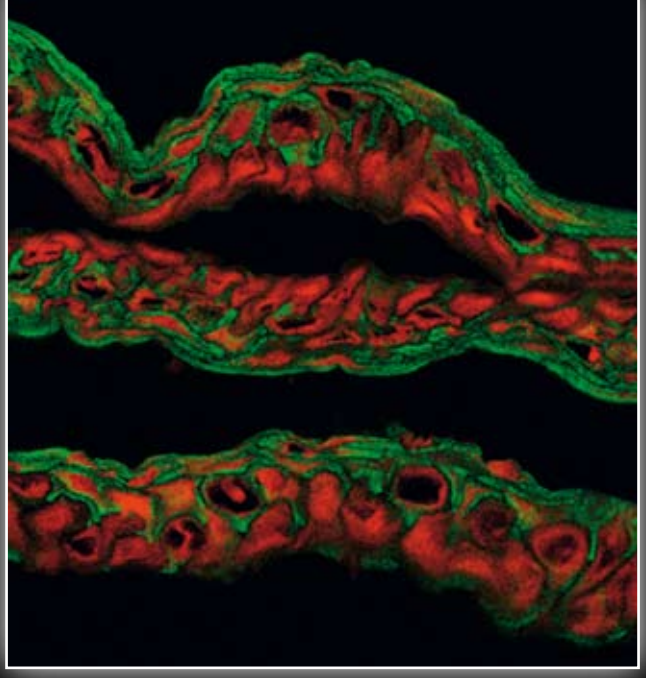

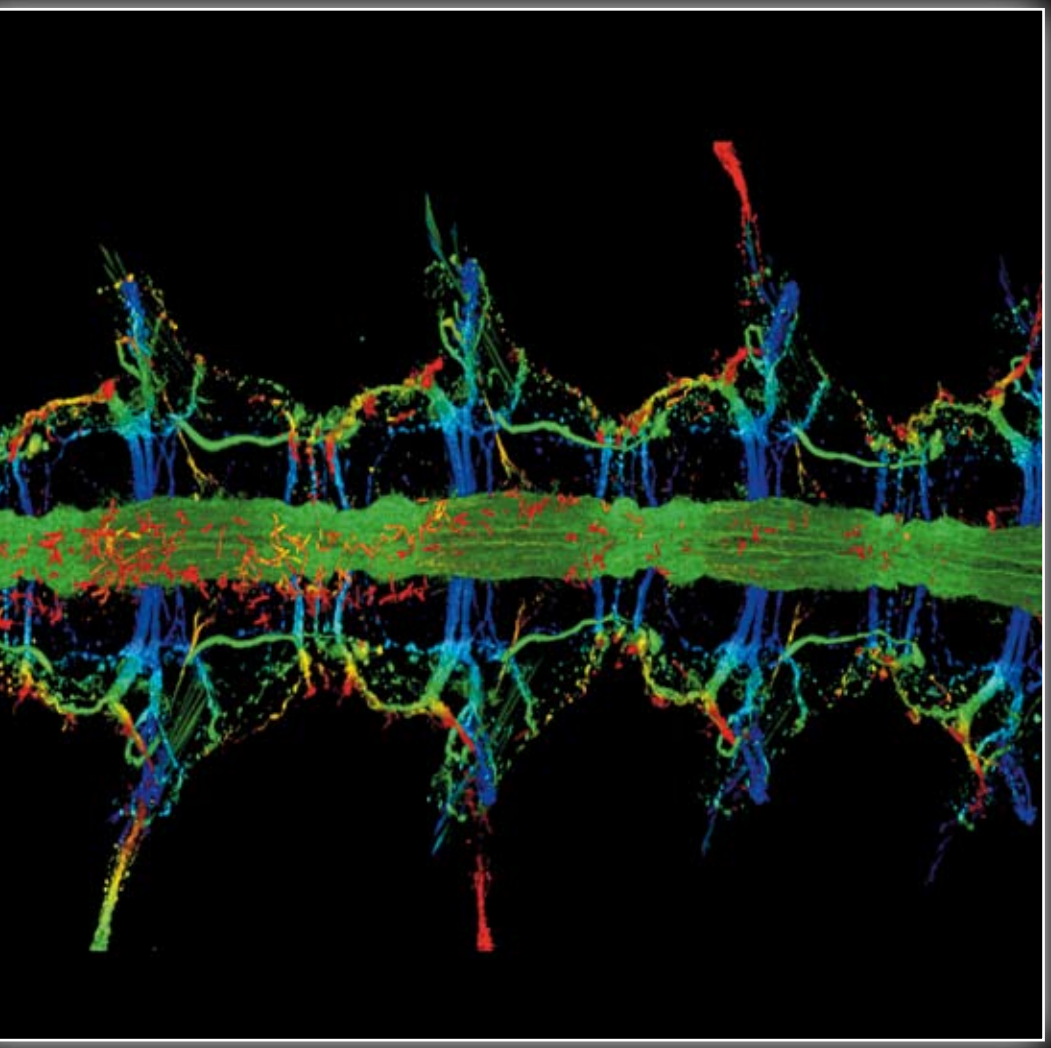

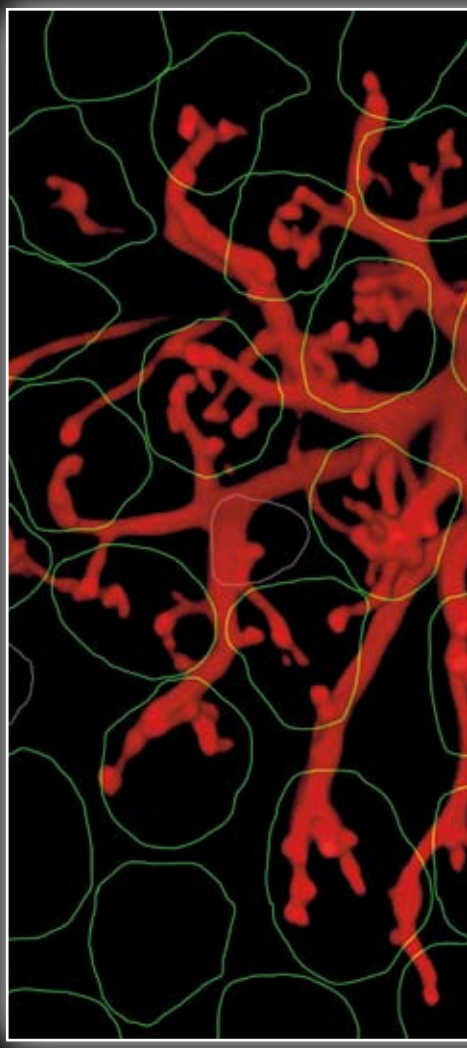

Value Unit Time Object Group Index